DOPAMINE SIGNALING ATTENUATES A RECURRENT NEURONAL NETWORK DURING *C. elegans* COPULATION

A Dissertation

by

PAOLA ALEJANDRA CORREA NUNEZ

Submitted to the Office of Graduate and Professional Studies of
Texas A&M University
in partial fulfillment of the requirements for the degree of

DOCTOR OF PHILOSOPHY

Chair of Committee,	Luis Rene Garcia
Committee Members,	Mark Harlow
	James Erickson
	Mendell Rimer
Head of Department,	Thomas McKnight

December 2015

Major Subject: Biology

ABSTRACT

Neuro-modulation of self-amplifying circuits drives the execution of behaviors to their appropriate context. These recursive networks are found throughout the *Caenorhabditis elegans* connectome, however the mechanism that fine-tunes reciprocal neural activity during complex behaviors is unknown. Here I dissect the cellular and molecular components involved in male copulation, a goal oriented behavior that entails initiation and termination under appropriate circumstances. The *C. elegans* mating circuit integrates sensory-motor cues resulting in copulatory spicule insertion into the hermaphrodite vulva. As the male tail presses against the hermaphrodite's genitalia, cholinergic and glutamatergic reciprocal innervations of post-cloaca sensilla (PCS) neurons (PCA, PCB and PCC), hook neurons (HOA, HOB) and their post-synaptic sex muscles execute rhythmic spicule thrusts. These repetitive spicule movements continue until the male shifts off the vulva or genital penetration. However, the signaling mechanism that temporally and spatially restricts intromission attempts to vulva cues was unclear.

My results suggest that dopamine (DA) neuromodulation delimits spicule insertion attempts to the hermaphrodite vulva by dampening stimulus-independent spicule circuit activity. I found that upon vulval contact, DA signaling from male specific sensory neurons stimulates D2-like receptors, DOP-2 and DOP-3, to decrease cholinergic induced sex muscle contractions. Through pharmacology and targeted optogenetics I demonstrate that D2-like pathways act coincidentally, and as a consequence of

cholinergic signaling, to reduce spicule intromission attempts with non-productive mating partners.

During spicule intromission attempts, DA up-regulates gap-junctions among PCB and a hook neuron to decrease self-amplifying PCS properties. Through forward genetics I isolated a missense mutation in an UNC-7L gap-junction isoform, which perturbs DOP-2 signaling in PCB and its electrical partner, HOA. Additional pharmacogenetic analysis suggests that the AVR-14 glutamate-gated channel partially introduces chloride ions into HOA to mediate DA downmodulation of the spicule circuit. Consistently, my analysis of the *unc-7(rg396)* allele indicates that when DOP-2 promotes UNC-7 electrical communication, AVR-14-mediated inhibitory signals pass from HOA to PCB. Consequently, the cholinergic PCB neuron is less receptive to stimulation by its recurrent glutamatergic synaptic partner, PCA. Furthermore, behavioral observations suggest that DA neuromodulation of UNC-7 ensures attenuation of recursive intromission attempts when the male disengages or is dislodged from the hermaphrodite genitalia.

ACKNOWLEDGEMENTS

I would like thank my supervisor Dr. García. His guidance was crucial to develop the work presented here. His creativity, hypothesis driven logic and relentless enthusiasm for science truly encourage me throughout my graduate-school experience. His dedicated mentorship has set an excellent example for my future scientific career. I would also like to thank my committee members, Dr. Erickson, Dr. Harlow and Dr. Rimer for their very helpful discussions during these years.

I really appreciated and enjoyed my time in the Garcia lab. All my lab mates here have made the long hours of work enjoyable and provided very useful advice: Dr. Daisy Gualberto; Dr. Yishi Liu, Dr. Brigitte LeBoeuf, Dr. Liusuo Zhang, Dr. Changhon Jee, Dr. Guo , Xin Chen, Jimmy Goncalves, Yu Fan and Michael Mohambdi. A special thanks goes to Dr. LeBoeuf and Dr. Guo for the exciting scientific discussions outside lab meetings and their help editing my manuscripts.

Thanks also go to several friends that in person or from far away have helped me deal with the stress, sleepless nights, and frustrating times. Chinita, Nikita Ojha, Alejandra Noemi González Rojos, Betty Alvarado, and Karen Triff, you all made me laugh when I needed it and made my College Station experience a great adventure. To my non-biological sister Sharlene Brown, who not only shares her great scientific ideas with me but has always been there just a dial up away. To Romina who has patiently helped me made it through the hardest last mile of this work.

Finally, thanks to the wonderful family I have. Even though they would like to be with me every day they understood my passion for science since the beginning and never doubted that all the years I have spent away from them are worth it. To my dad for all his riddles, and teaching me how to become *un pequeno-gran saltamonte*. To my mom, for her sweetest, toughest and unconditional love. To my younger sister, who makes me laugh, motivates me to become a better person, and makes my parents forget about my absence.

NOMENCLATURE

ACh	Acetylcholine
mAChR	Muscarinic Acetylcholine receptor
nAChR	Nicotinic Acetylcholine receptor
DA	Dopamine
ARE	Arecoline
LEV	Levamisole
NIC	Nicotine
EC_{90}	Effective concentration to cause response in 90% of the population
EC_{50}	Effective concentration to cause response in 50% of the population
RNN	Recurrent neuronal network
PCS	Postcloacal sensilla
UNC-103	*C. elegans* homologue of the ERG K+ channel
DOP-2	*C. elegans* homologue of the D2 receptor
DOP-3	*C. elegans* homologue of the D3 receptor
UNC-7	*C. elegans* UNC-7 innexin
CAT-2	*C. elegans* homologue of tyrosine hydroxylase
GCaMP	GFP calcium calmodulin permutated protein
YFP	Yellow Fluorescent Protein

TABLE OF CONTENTS

LIST OF FIGURES

Page

LIST OF TABLES

Page

CHAPTER I

INTRODUCTION

Intrinsic regulation of motivated behaviors

Motivated behaviors are characterized by the repetitive display of motor programs necessary to achieve certain actions that will satisfy a physiological need (i.e. reproduction and/or nutritional needs). Since these recursive motor routines might last even after removal of the initial incentive stimuli and/or activation of the cue detection system, a recurrent action continuation or termination is particularly dependent on intrinsic modulatory mechanisms. Part of this intrinsic regulation arises from neuromodulators secreted by the nervous system. Neuromodulators amplify or reduce hard-wired circuit activity to promote or weaken a motivational status. Altering motivational strength provides the necessary plasticity and adaptability to cope with constantly changing environmental context. However, how modulatory signals are interpreted by the nervous system to start, continue, modify and end specific behaviors, under the appropriate conditions is poorly understood.

The neuromodulator dopamine (DA) is involved in adjusting the level of motivation during several goal-oriented behaviors; thus DA neurotransmission is an excellent candidate for coupling actions to their proper situational context. DA modulates several behaviors including: reward, aversion, arousal, and voluntary motor patterns. DA has been widely studied for its effects reinforcing these goal-directed tasks, however the mechanisms by which DA signaling decreases and/or terminates certain motivated

routines is not well characterized. It is crucial that these motivated states are diminished at the appropriate time to provide animals with flexible strategies of achieving a goal. Since goal-directed tasks are displayed as repetitive actions, these behaviors are prone to become compulsions, resulting in compulsive emotional and/or motor pathologies (i.e addictions and motor choreas) seen in humans.

Neuroanatomical evidence for DA modulation of central nervous system circuits

DA modulation for specific goal-directed locomotor patterns (voluntary movements) has been described for vertebrate model organisms (Fienberg et al., 1998; Yan et al., 1999; Beaulieu et al., 2004; Beaulieu et al., 2005). Analysis of DA pathway connectivity suggest how DA midbrain neurons could regulate post-synaptic interneuronal activity involved in motor pattern regulation (Smith et al., 1998). In mammals, DA midbrain secretions from the substantia nigra (SN) or the ventral tegmental area (VTA) initiate this motor control. The SN and/or VTA adjust the cellular excitability of two main brain centers, which modify goal-oriented behaviors: the striatum and the cortex. A classical connectivity view suggests that SN restrictively synapse onto striatal neuronal populations, while the VTA only projects into cortical neurons. However, recent studies identify that both the SN and VTA innervate both the cortex and striatum (Puig et al., 2014). This indicates that the SN and VTA regulate either of these two post-synaptic centers and their roles might not be functionally exclusive. Nevertheless, mid-brain DA neurons innervate the striatum more prominently than other post-synaptic targets

(Bjorklund and Dunnett, 2007), explaining the abundant in-depth dissections of DA-striatal modulation.

How does DA modulation of the striatum direct voluntary actions? Neuroanatomical studies suggest that this occurs through striatum and thalamic interactions. Striatal neurons project onto the thalamus, a sensory-motor relay center, which communicates with the motor cortex. This part of the cortex sends projections onto the peripheral nervous system via cortico-spinal tracts to execute voluntary movements (Smith et al., 1998). Moreover, motor cortical centers receive input from the frontal cortex neurons; which are innervated by DA projections. Since the cortex feedbacks onto the thalamus, and the thalamus also projects back into the stritatum, a more indirect cortico-thalamic-striatal DA regulated feedback also takes place (Keeler et al., 2014). Thus, a context-dependent voluntary motion is orchestrated directly or indirectly by DA neurotransmission.

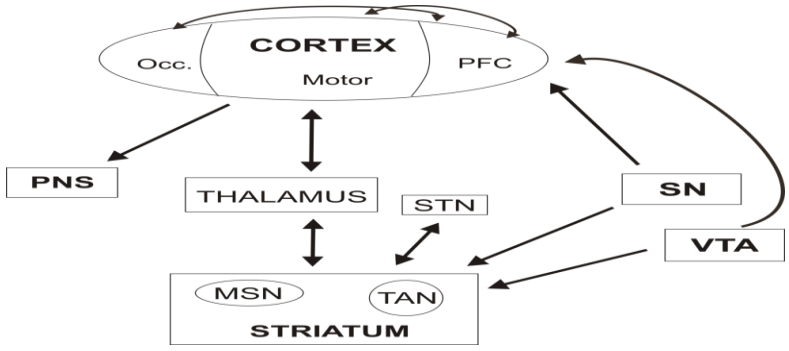

Figure 1. Schematic interactions of the DA circuit in the mammalian brain. This conceptual map indicates the direct and indirect DA post-synaptic targets. DA modulation of these neuronal clusters directs goal-oriented displays. Occ=occipital, PFC=prefrontal cortex, SN=substantia nigra, VTA=ventral-tegmental area, TAN=tonically active neurons, MSN=medium spiny neurons, STN=Sub-thalamic nucleus.

Functional studies indicate timing of DA neuron regulation during motor programs

In humans the DA circuitry is homologous to the above descriptions of mammalian models (Fig.1) (Puig et al., 2014). In corroboration of these anatomical dissections, functional magnetic resonance imagining (fMRI) analysis further implicate DA fine tuning of goal-oriented behaviors in humans. The VTA and SN are active during cognitive tasks that entailed context-dependent visual cue updates (D'Ardenne et al., 2012). During the same task, a functional dorso-lateral prefrontal cortex (PFC) region is necessary for optimal task performance (D'Ardenne et al., 2012). This finding indicates that DA neurons and PFC either co-regulate context-dependent behaviors in parallel, or as proposed by the neuroanatomy, DA neurotransmission up-regulates PFC activity. Additionally, during a voluntary motor behavior there is a sequential activation of direct and indirect DA post-synaptic targets. At the anticipation phase of grasping an object an increase in activity of the striatal cluster precedes the sub-thalamic nucleus (STN) activation (Fig1). The latter rise of activity in the STN region potentially regulates amplitude and rate of motor force generation (Pope et al., 2005; Vaillancourt et al., 2007). Accordingly, DA neuron deterioration results in perturbations of muscle-force movements observed during impulsive motor disorders, such as Parkinson's disease and other choreas (Raz et al., 2001; Calabresi et al., 2006; Ding et al., 2006; Pisani et al., 2007). These studies indicate that relevant DA inputs onto direct or indirect brain nuclei adjust motor programs. In order to unravel further details of complex motivational regulation, these human studies need to be complemented by DA neuron physiology dissections.

Phasic DA neuronal bursts encode motivational reinforcement in mammalian models

Mammalian model analysis pin-points the temporal and spatial attributes of DA neurotransmission during goal-directed behaviors. Through the use of electrophysiology, optogenetics, pharmacology and behavioral paradigms in non-human primates and rodents, these studies have resolved how environmental cues alter the activity of different DA neuron populations. One of the most prominent physiological changes in DA neuron activity in mammals occurs in response to rewarding stimuli (Salamone and Correa, 2012) to potentially reinforce a specific behavioral motor routine.

The switch of neuronal tonic activity into phasic DA bursts is correlated to presentation of rewarding stimuli, which acts as an internal reinforcement of motivation (Arsenault et al., 2014). Higher burst frequencies, and potentially higher DA discharge, is produced in response to appetitive stimuli (food) or stimuli that predicts rewards in non-human primates (visual cues associated with probabilistic food presentation) (Morris et al., 2004; Joshua et al., 2008). Additionally, the burst frequency magnitude is positively correlated with the probability of being presented with an incentive stimuli in the future, higher and lower probability resulting in more or less frequent DA neuron firing, respectively (Matsumoto and Hikosaka, 2009). The DA scaling response is observed in the VTA area prominently and more moderately in the SN (Matsumoto and Takada, 2013). This suggests that VTA bursts of activity promote a heightened motivational status.

Similarly, in rodents, prominent VTA firing occurs in response to rewards (Wise, 2004). Optogenetic VTA stimulation reinforces reward-seeking behaviors and even compulsive displays (Tsai et al., 2009; Hearing et al., 2013). The light induced VTA depolarization augments extra synaptic DA, similar to cocaine intake. During cocaine consumption, cocaine blocks the DA reuptake transporter (DAT-1), therefore inhibiting DA re-cycling and causing subsequent DA accumulation (Giros et al., 1996). Accordingly, cocaine self-administration motivates animals to further seek cocaine consumption (Choi et al., 2011). Taken together these observations indicate that augmented DA signaling in mammals, as a result of natural (food) or artificially induced rewards (psycostimulants), reinforces goal-oriented actions.

DA promotes goal-directed tasks through D1-like signaling

DA adjusts goal-directed behaviors by selective synergy or antagonism of tiered neuronal population's activities (Graybiel et al., 1994; Fienberg et al., 1998). DA signaling enhances circuitry outputs by triggering G-protein coupled receptor (GPCR) cascades. The five mammalian GPCR DA receptors are classified into two sub-categories D1-like (D1 and D5) or D2-like (D2, D3, and D4), which stimulate or down-modulate cellular excitability, respectively. Even though both receptor types are expressed in downstream cellular populations of mid-brain DA circuitry (Beaulieu and Gainetdinov, 2011), only the role of D1-like signaling enhancing goal-oriented behaviors in mammalian models has been well-characterized.

D1-like cascades promote motivated behavioral executions through ventral striatum neuron modulation. In rodents, D1-like signaling mediates the association of natural or artificial incentives with an environmental context to further promote reward-seeking actions. In the conditioned place preference (CPP) behavioral paradigm, after a training phase, mice or rats preferentially enter a space that is previously paired with cocaine *versus* vehicle injections. This association is abolished when an animal's striatum is infused with a D1-like antagonist (Cervo and Samanin, 1995; Baker et al., 1998; Baik, 2013). Moreover, when a striatal neuron sub-population that expresses D1-like receptors is inhibited via optogenetics, the cocaine CPP effects are lessened (Lobo et al., 2010). This indicates that D1-like signaling mediates the reinforcing effects of cocaine. Accordingly, exclusive D1 receptor (D1R) over-expression in ventral *versus* dorsal striatum of D1R KO mice (Gore and Zweifel, 2013), restores food-reward CPP associations. This striatal D1R expression also increases a mice's ability to press a lever for food administration. However, when the food delivery paradigm becomes more challenging, requiring more lever presses for a similar food pellet administration; D1R striatal expression is insufficient to restore the behavioral response needed for this exigent task (Gore and Zweifel, 2013). Thus, D1-like receptors might contribute to more complex goal-oriented processing in other brain areas supplementary to the striatum.

In addition to striatal D1-like signaling, several studies suggest that these pathways promote goal-oriented actions in cortical brain regions. Short- and long-range D1-like signaling mediates cognitive task-oriented behaviors in the cortex through regulation of recurrent-neuronal networks (RNNs), networks where neurons send feedback signals to

each other (Brozoski et al., 1979; Goldman-Rakic et al., 1989; Arnsten et al., 2012). In long-range RNNs of the prefrontal and occipital cortices, D1-like receptors mediate network amplification, improving the accuracy of purposeful eye movements according to visual targets in primates (Noudoost and Moore, 2011; Zaldivar et al., 2014). The D1-like dependent strengthening between visual and pre-frontal cortex allows coupling of the reward-related visual cue in subsequent trained target trails. Similarly, in rodents D1-like receptors enhance short-range RNNs in different layers of the auditory and somato-sensory cortex (Shao et al., 2013; Happel et al., 2014) to improve stimuli detection. In this example, the accurate environmental perceptions promoted by D1-like signaling could aid in action selection to best match a goal-directed routine, similar to the role in primates.

Conflicting evidence on how D2-like signaling modulates motivational states

In contrast to the reinforcing role of D1-like signaling during goal-directed tasks, the *in vivo* implications of D2-like receptors are less straight forward. Part of the challenge is because these DA receptors are less abundant than D1-like receptors in the brain (Andersson et al., 2012). Additionally, the D2 receptor has two isoforms, one as a pre-synaptic autoreceptor, and another expressed in post-synaptic subsets (Ford, 2014). Pharmacological and genetic manipulations are non-specific for the two isoforms, making it is difficult to interpret how D2-like receptors shape behaviors. Nonetheless, a growing number of targeted genetic and optogenetic studies has allowed some dissection of how D2-like receptors mediate goal-oriented displays.

D1-like and D2-like receptors are expressed in non-overlapping medium spiny neurons (MSN) of the striatum, allowing selective optogenetic manipulations of these cellular sub-types. These optogenetic behavioral dissections indicate that D2-like cascades increase reward seeking actions. When the D2-like MSN neurons are inhibited, mimicking a D2-like regulation, the motivational output increases, as evidenced by the augmented cocaine self administration and high conditioned-place-preference (CPP) cocaine index (Bock et al., 2013). Accordingly, when these D2-like MSN neurons are stimulated the reinforcing associative properties of cocaine are reduced (Lobo et al., 2010). Since D1-like signaling promotes motivation, the opposing D2-like cascade would suggests an opposite behavioral outcome; however these paradoxical results indicate that D2-like cascades increase reward seeking actions.

Additional experiments suggest that D2-like signaling dampens a motivational state through DA mediated antagonism of cholinergic signaling. Increased cholinergic signaling mediates attention and promotes task-oriented behaviors (St Peters et al., 2011; Martinowich et al., 2012). In the primate striatum the peak of DA bursts during rewarding stimuli overlaps with a decrease in the activity of post-synaptic cholinergic tonically active neurons (TANS) (Morris et al., 2004; Joshua et al., 2008). In the TAN, D2-like signaling dampens their excitability *in* vitro, indicating that DA midbrain release coupled with D2-like signaling might reduce the cholinergic output during a goal oriented task (Pisani et al., 2000; Wang et al., 2006; Deng et al., 2007). However, how these TANs pauses are utilized to restrict goal-oriented displays remains unknown.

The complex cortical connectivity poses an additional challenge for elucidating how D2-like receptors alter RNNs to potentially mediate aspects of the task-oriented eye movement response (Wang et al., 2004). Compulsive behaviors such as human schizophrenic pathologies suggests that disrupted cortical D2-like signaling results in mismatched spatio-temporal perceptions, which are typical symptoms of these disorders (Creese et al., 1976; Spencer et al., 2004; Wang and Goldman-Rakic, 2004). Although this behavioral evidence suggests that DA signaling might fine-tune RNNs, the limited molecular/genetic characterization of the mammalian cortex presents a challenge for further in depth behavioral studies. In this regard, the complete neuronal wiring connectome, genetic screens and sophisticated molecular tools (White et al., 1986; Allen et al., 2011; Jarrell et al., 2012; Wei et al., 2012; Flavell et al., 2013), make *Caenorhabditis elegans* a tractable model to dissect how D2-like signaling within neural circuits regulate purposeful behaviors.

C. elegans **as a model for DA signaling dissections**

The adult *C. elegans* nervous system contains 302 neurons in the hermaphrodite and an additional 81 neurons in the male (Sulston et al., 1980). It has several analogous components to the vertebrate DA system. Similar to DA neurotransmission in mammals, where only few central nervous system neurons are dopaminergic (~<1%) (Bjorklund and Dunnett, 2007), DA is synthesized by 8 cells in the hermaphrodite and 6 extra male-specific neurons. The largest neuronal cluster collection in *C. elegans* is localized in the head nerve ring, where some of the DA neurons reside. These include, the anterior most

four cephalic CEPs (CEPv and CEPd), and the anterior derid neurons (ADE). The processes of the final sex-shared DA neuron pair, the posterior derid neurons (PDEs), run in parallel to the ventral chord, which projects horizontally down the worm length. The additional 6 male specific DA neurons are the ray neurons 5A, 7A and 9A (anterior to posterior) located in the male tail, where a large array of male specific ganglia are situated. As in vertebrates, all of these DA cells synthesize DA in a two step reaction, where tyrosine hydroxylase (C. *elegans* CAT-2) converts tyrosine into L-DOPA, and AAA-decarboxylase coverts L-DOPA into dopamine (Lints and Emmons, 1999). The D1 and D2- like receptors share 40-50% homology with human DA receptors (Jayanthi et al., 1998; Suo et al., 2003; Chase et al., 2004), and signal through common downstream effector mechanisms as those found in mammalian models.

DA receptors modulate cellular excitability in *C. elegans* through canonical and non-canonical pathways. The classically characterized D1-like and D2-like signal transduction increases or decreases intracellular cAMP levels, respectively (Greengard, 2001; Beaulieu and Gainetdinov, 2011). The four *C. elegans* DA GPCRs (DOP-1 through DOP-4) are classified as D1-like (DOP-1 and DOP-4) and D2-like (DOP-2 and DOP-3) based on their *in vitro* ability to alter cAMP levels. Accordingly, DOP-2 and DOP-3 attenuate forskolin cAMP accumulation, and DOP-1 and DOP-4 increase cAMP levels (Suo et al., 2002, 2003; Sugiura et al., 2005). This suggests that similar to canonical signaling, the enzyme catalyzing cAMP production, adenelyl cyclase (AC), might be downstream of these opposing cascades (Fig. 2). In the canonical signaling, opposing effects on cAMP levels result in the corresponding altered PKA activity. This

kinase then changes the phosphorylation of several targets, such as ion channels, ionotropic receptors, ion pumps, and gap-junction sub-units (Greengard, 2001; Bloomfield and Volgyi, 2009; Beaulieu and Gainetdinov, 2011). Altering the phosphorylation state of these membrane proteins changes their ion transport properties, resulting in upregulation or downmodulation of cellular excitability. However, *in vivo C. elegans* DA signaling analyses have never found PKA as a downstream effector, indicating that non-canonical DA cascades might transduce DA signaling in the nematode. As I discuss below, several *C. elegans* experiments suggest that most of the vertebrate and invertebrate conserved DA modulation occurs through non-canonical pathways (Fig. 2).

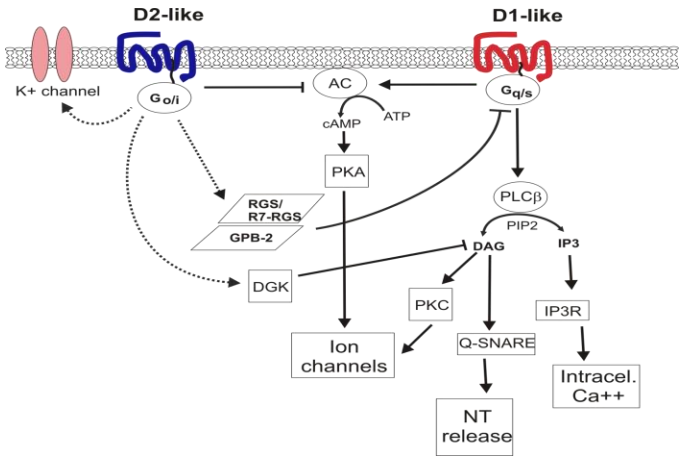

Figure 2. DA signaling cascades modulate cellular excitability. D1-like and D2-like signaling cascades discussed throughout the introduction. Dotted lines indicate hypothetical interactions amongst signaling effectors. AC=adenylate cyclase, PKA=protein kinase A, PKC=protein kinase C, DGK=diacyl-glycerol kinase, RGS=regulator of G- protein, GPB-2=G-protein-beta-2, PLC=phospholipase C, DAG=diacyl glycerol, PIP2=phospholipid phosphatidylinositol bisphosphate, IP3= inositol triphosphate, IP3R=IP3 receptor, NT=neurotransmitter

D1-like and D2-like signaling modulate the general locomotor circuit

The sinusoidal *C. elegans* locomotion occurs through propagating dorsoventral body bends from head to tail at 0.5Hz (Vidal-Gadea et al., 2011). However, D2-like signaling attenuates this body bend frequency once the animal reaches a bacterial food source. This decrease in locomotion, or 'basal slowing response', is dependent on mechanical redundant stimulation of CEPs, ADEs, and PDEs DA neurons (Sulston et al., 1975; Sawin et al., 2000; Kindt et al., 2007; Vidal-Gadea et al., 2011). DA secretion from these neurons triggers extra synaptic DOP-3 signaling. Rescue experiments indicate that one of the extra-synaptic sites for DOP-3 signaling are the cholinergic ventral chord (VC) neurons, which mediate DA induced basal slowing response (Chase et al., 2004; Allen et al., 2011) (Fig. 3). Accordingly, soaking worms in DA or increasing endogenous DA levels, through mutations in the C. *elegans* dopamine re-uptake transporter (DAT-1) induces paralysis (Schafer and Kenyon, 1995; Chase et al., 2004; McDonald et al., 2007; Allen et al., 2011). The paralyzing effects of exogenous DA are also dependent on DOP-3 signaling. Through this simple pharmacological assay the heterotrimeric G-alpha subunit Gαo-GOA-1 was identified as a main downstream effector of DOP-3 signaling (Fig. 3). Similarly, vertebrate studies suggest that D2-like receptors couple to Gαo in addition to Gαi subunits (Beaulieu and Gainetdinov, 2011). Thus, D2-like signaling through Gαo represents a conserved mechanism of down-modulation of neuronal responses in vertebrates and invertebrates.

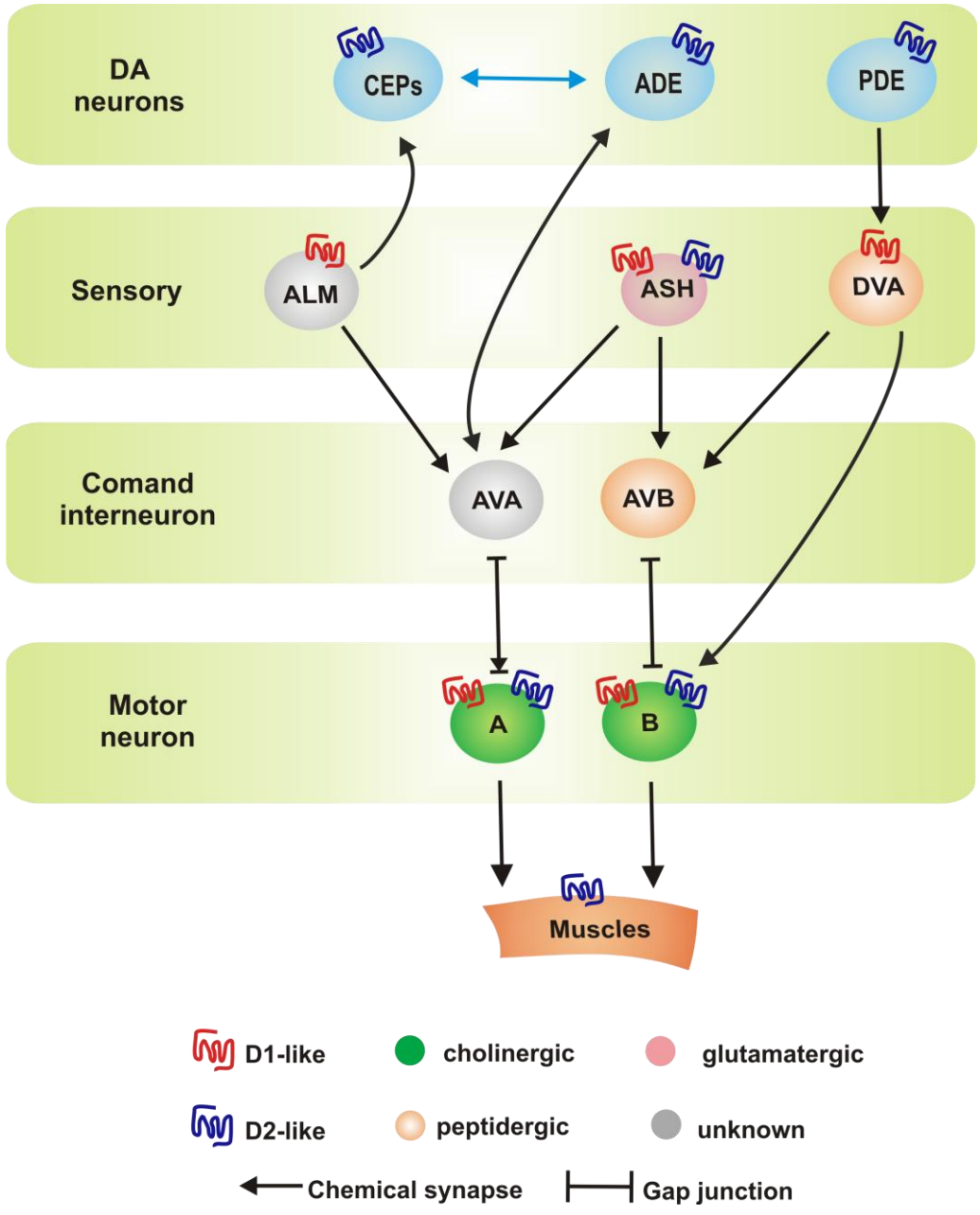

Figure 3. Abridged diagram of DA neuron interactions with downstream circuits. Color labels of cells suggest the type of neurotransmitter or peptide secreted. The muscles represent the body-wall muscles. Arrows indicate the chemical or electrical synapses.

Interestingly DOP-3 is not the only DA receptor that regulates cholinergic VC neuron activity. DOP-1 is also expressed in VC cells, and increases their excitability potentially through enhancing ACh release. When *dop-1* and *dop-3* are mutated DA can induce paralysis similar to wild type levels (Chase et al., 2004), suggesting antagonistic receptor functions. In these double mutants DOP-1 expression in VC neurons renders animals less sensitive to paralysis, suggesting that DOP-1 stimulates excitability. Additionally, endogenously increasing ACh signaling, through inhibition of an acetylcholine hydrolyzing enzyme, acetylcholinesterase, causes paralysis of *dop-1;dop-3* double mutants at a similar rate to wild type (Allen et al., 2011). However, VC DOP-1 overexpression in *dop-1;dop-3* animals results in a faster paralysis than wild-type, indicating that DOP-1 potentiates VC ACh release. This increment in ACh neurotransmission could result from DOP-1 coupling to $G\alpha_q$ (Chase et al., 2004; Kindt et al., 2007; Allen et al., 2011). The $G\alpha_q$ cascade triggers the phospholipase C (PLC) pathway, raising IP_3 to increase intracellular Ca^{++} levels, and DAG production to potentiate the synaptic vesicle release machinery (Kindt et al., 2007; Hu et al., 2015). Moreover, in mammalian cell lines DOP-1 increases intracellular Ca^{++} levels, thus indicating similar DOP-1 $G\alpha_q$ -PLC signaling in vertebrates (Liu et al., 2009; Lee et al., 2014). However, since several mammalian *in vivo* analyses indicate that D1-receptors couple to a $G\alpha_s$-AC pathway (Vijayraghavan et al., 2007; Beaulieu and Gainetdinov, 2011), further elucidation is required to postulate whether the D1-$G\alpha_q$ cascade is potentially conserved. Nevertheless, in *C. elegans* DOP-1 $G\alpha_q$ signaling upregulates ACh release to increase locomotor activity.

If both D1-like and D2-like signaling antagonistically adjusts the excitability of the same cholinergic cell, how can a decrease in locomotion supersede enhancement during the basal slowing response? The answer entails a mechanism where D2-like signaling antagonizes D1-like signal transduction. Additional DOP-3 effectors are part of a downstream G-protein regulatory system that terminates DOP-1 signaling. These molecules include: *eat-16* (a regulator of G-protein signaling-RGS), *gpb-2* (Gγ protein), and *rsbp-1* (RGS binding protein) (Chase et al., 2004; Allen et al., 2011; Wani et al., 2012). The GPB-2/EAT-16 and RSBP-1/EAT-16 complexes are hypothesized to terminate DOP-1 signal through enhancing hydrolysis of the GTP that is bound to an active Gαq- subunit. Thus, potential D2-like GTPase induced activity of these complexes would diminish DOP-1 signaling (Fig 2). Moreover, the diacyl-glycerol kinase (DGK-1) is another molecule that might be downstream of DOP-3, and antagonizes DOP-1 signaling (Nurrish et al., 1999; Chase et al., 2004). This kinase inactivates DAG, which is downstream of the EGL-30 cascade, thus potentially reducing cholinergic release (Fig 2). Taken together, these observations suggest that DA induces intricate G-protein coupled signaling networks to modulate a behavioral response.

D1-like signaling enhances area-restricted search locomotion

Even though most of the discussed DA modulation suggests that DA signaling alters locomotory rates under the context of food, DA also adapts C. *elegans* movement in the absence of bacteria. One of these examples is the DA-mediated increment of high angle turns frequency at the beginning period of food depletion (0-5min). This alternative

locomotion is adopted to forage for nutrients in an area restricted manner, since bacteria patches might be found in nearby areas where the animals originally located them (Hills et al., 2004). DOP-1 signaling mediates this area restricted search through enhancing NLP-12 peptide release from the DVA mechanosensory neuron (Hills et al., 2004; Bhattacharya et al., 2014). The DOP-1 downstream effectors that enhance NLP-12 release are unknown. It is unlikely that Gαq signaling acts downstream of this cascade, since as mentioned DOP-1-Gαq signaling enhances neurotransmitter vesicle release machinery, which is potentially different from proteins used for peptide release. Moreover, DVA receives inputs from PDE, the sex-shared posterior DA neuron, thus synaptic rather than humoral DA triggers D1-like signaling in this case. Interestingly, since DVA is a stretch sensory neuron directly stimulated through body wall muscles contractions during deep-body bends (Li et al., 2006), mechanosensory and D1-like signals might potentiate DVA activity. The DVA dependent change in locomotion is then produced through signaling onto VC neurons, since prominent NLP-12 release was found throughout the long DVA process that extends parallel to the VC (Fig 3). Taken together, these observations suggest that D1-like induces humoral peptide release, which stimulates several VC neurons to produce a lasting area restricted search response for several minutes.

DA up-regulates and down-modulates repellant chemo-sensory responses

DA signaling directly regulates the *C. elegans* navigation system to alter different body bend features; however DA can also modulate how sensory systems respond to

indirectly adjust locomotory gaits. When *C. elegans* encounter noxious stimuli, D1-like signaling up-regulates the noxious stimuli detection response, and therefore promotes the switch of predominant forward movement into reversals. The polymodal ASH sensory neuron detects chemical repellents and nose pressure to induce an avoidance response (Kaplan and Horvitz, 1993). The D1-like receptor DOP-4, enhances the ASH excitability to soluble repellants (cooper and glycerol), only under the presence of food, indicating that this sensitization is dependent on nutrient availability (Ezcurra et al., 2011). In the absence of food or in a *dop-4* background ASH still responds to repellants, however the magnitude and duration of ASH activity is decreased under these conditions. This indicates that DOP-4 does not alter ASH sensory properties *per see*, rather potentiates the sensory response. Since ASH synapses onto command interneurons (AVA and AVB) (Fig. 3), DA mediated ASH potentiation could lead to enhanced communication with AVA, the command interneuron that mediates backwards locomotion. In accordance with this idea, ASH artificial photo-stimulation induces AVA activity (Guo et al., 2009). Therefore, DOP-4 signaling would ultimately affect the locomotor responses through enhancing ASH interactions with the AVA backward circuitry.

D2-like signaling also modulates ASH sensitivity during the detection of 1-octanol, a volatile repellent. At lower 1-octanol concentrations, worms take longer to start the escape response, due to DOP-3 potentially diminishes ASH excitability (Ezak and Ferkey, 2010). A regulator of G-protein signaling (RGS-3) also mediates ASH sensitivity to odorants (Ferkey et al., 2007), thus RGS signaling interactions might

occurs in this neuron, similar to those in the ventral chord. This mechanism might then mediate the preference of either D1- versus D2-like signaling in ASH, to intricately regulate repellent versus non-repellent responses.

DOP-1 cascade enhances recurrent neuronal signaling within a mechanosensory circuitry

Similar to the repellant escape response, upon a generalized tap on the culture plate, *C. elegans* change their forward locomotion into reversals, however, repeated non-localized stimulation causes habituation and consequently a decrease in the reversal response (Rose and Rankin, 2001; Sanyal et al., 2004). Nonetheless, animals sustain their response to plate taps for at least 1min, due to DOP-1 potentiating ALM mechanosensory activity. Localized and non-localized mechanosensory stimuli detection is mediated by the ALM neuron (Kindt et al., 2007), which induces a rapid reversal response, potentially through synapses with AVA (Fig. 3). However, during non-localized stimuli DOP-1 signaling in ALM perpetuates an ALM-CEP loop to increase the plate-tap response duration. ALM and CEPs reciprocally communicate with each other through humoral and non-humoral signaling (Fig. 3). Thus, CEPs DA release is triggered when ALM senses mechanical cues; CEPs then feedback onto ALM via DOP-1 signaling. In this circuitry, DOP-1 results in $G\alpha_q$ signaling, subsequent phospholipase C (PLC) activation, and DAG and IP3 increment. However, unlike the potential DAG role increasing synaptic vesicle release, as observed in VC neurons, DAG induces protein-kinase C activity in ALM (Kindt et al., 2007). Interestingly, this is one of the few

examples in *C. elegans* where DA enhances a recurrent loop to actively regulate a behavioral response.

D2-like signaling regulates muscle excitability during egg-laying

Thus far I have discussed how DA signaling modulates neuronal responses; however DA might also alter muscle excitability in *C. elegans* in order to mediate behavioral outputs. For instance, the rate of egg-laying is decreased when hermaphrodites are exposed to exogenous DA (Schafer and Kenyon, 1995). Eggs are propelled out of the hermaphrodite body into the external environment through vulva muscle contractions. This occurs via enhancement of the voltage gated- like K+ channel EGL-2, potentially via D2-like signaling. The *egl-2(n693)* gain-of-function mutation causes an inhibition of vulva muscle contractions, and therefore egg retention. Though, the constitutively hypopolarized vulva muscles recover excitability back to wild type levels by D2-like antagonists exposure, such as chlorpromazine and haloperidol (Weinshenker et al., 1995; Weinshenker et al., 1999). This suggests that D2-like signaling can potentially enhance potassium channel activation and therefore regulate muscle contraction frequency. Even though DOP-3 is the only reported receptor expressed in muscles; its expression only extends to body-wall muscles (Chase et al., 2004), suggesting that other D2-like receptors might mediate vulva muscle excitability. Alternatively, the DOP-3 expression pattern might need further examination. These studies indicate that DA signaling not only alters neuronal excitability, but also modulates muscles.

The *C. elegans* copulatory spicule circuit as a model for goal-oriented behaviors

The DA modulation of the *C. elegans* general locomotor circuits discussed above suggests parallels with vertebrate DA signaling; however most of these invertebrate neuronal interactions are not reciprocal, nor mediate a step-wise goal-oriented behavior. Therefore, dissections of *C. elegans* male mating, which comprise an intricate routine with stereotyped steps directed by a heavily interconnected network is better suited for the study of context-dependent behaviors. Since the molecular and cellular components of the mating circuit are well-characterized, studying how DA signaling mediates behavioral flexibility during copulation would provide excellent resolution to complex motivational-reward computations.

Male mating behavioral sub-routines

Male copulation requires monitoring mechanisms to initiate and terminate multiple sub-steps under the proper context. Mating begins when the male presses his tail against the hermaphrodite and moves backwards, scanning for the vulva (Loer and Kenyon, 1993; Garcia et al., 2001). After the male locates the vulva, he initiates repetitive 7-11 Hz copulatory spicule thrusts to breach the vulval slit. During this sub-behavior, the male progressively adopts an arched body posture, which persists throughout spicule insertion and sperm transfer (Fig. 4). In rare events, the arched posture is adopted during scanning. Successful ejaculation occurs after repeated attempts of these motor sub-behaviors (Liu and Sternberg, 1995; Liu et al., 2007b). Molecules that promote mating execution have been identified, but few modulators that regulate and refine the behavior

have been described (Schindelman et al., 2006; Liu et al., 2007a; White et al., 2007; Barrios et al., 2008; Srinivasan et al., 2008; Whittaker and Sternberg, 2009; Koo et al., 2011; LeBoeuf et al., 2011; Liu et al., 2011; O'Hagan et al., 2011). DA signaling adjusts several *C. elegans* sensory-motor behaviors; thus this neuromodulator might also mediate aspects of the male mating routine.

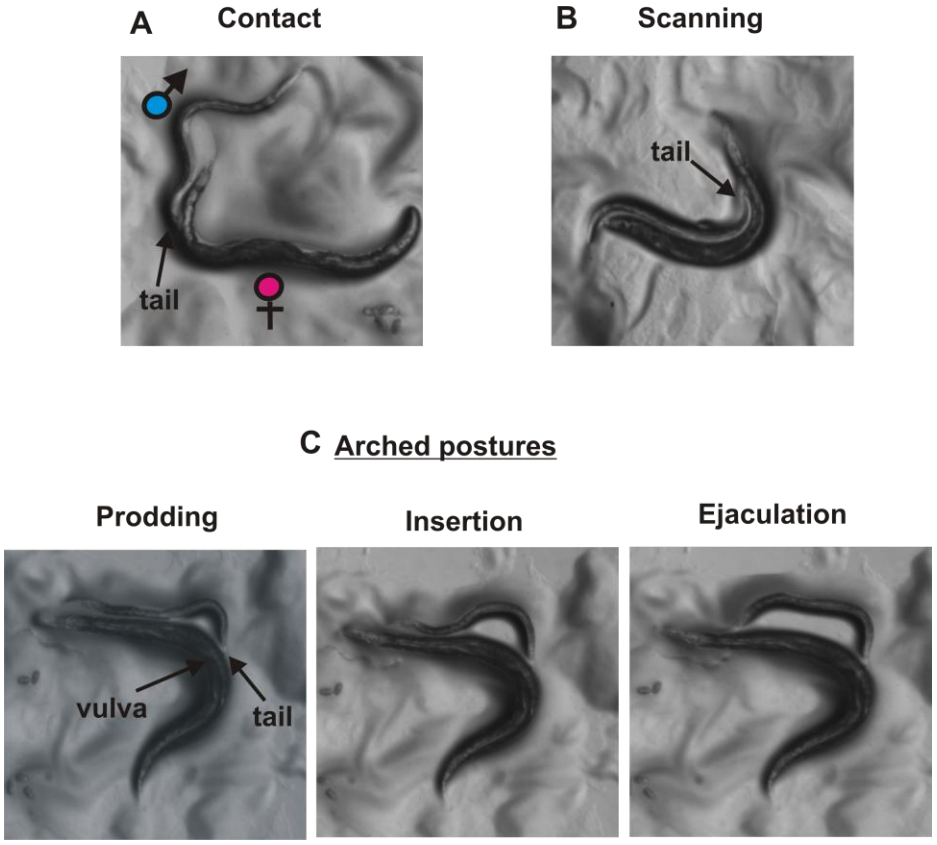

Figure 4. Stereotyped mating sub-steps. (A&B) Non-arched postures. (A) The contact response: a male apposing the ventral side of his tail against the hermaphrodite cuticle. (B) Scanning: a male moving backwards along the hermaphrodite outline. (C) Arched postures: depicting a progressively growing arch during spicule intromission attempts (prodding), insertion and ejaculation

The mating circuit components

The recurrently connected sensory-motor neurons in *C. elegans'* male tail regulate mating sub-behaviors to accomplish copulatory spicule intromission into his mate (Jarrell et al., 2012). The 18 sensory ray neuron pairs (termed R1A/B through R9A/B) induce ventral male tail contact with the hermaphrodite's cuticle (Koo et al., 2011). As the male approaches the general genital region, anterior-cloacal sensory neuron processes (HOA and HOB) sense long-range chemical and/or mechanical vulva characteristics (Liu and Sternberg, 1995; Barr and Sternberg, 1999). These neurons reduce the male's backward velocity, allowing the post-cloacal-sensilla (PCS) to detect short-range vulva features and initiate the copulatory spicule intromission sub-routine (Garcia et al., 2001).

Upon vulval contact, scanning behavior ceases and the PCS network promotes repetitive spicule insertion attempts at the vulval slit. The three reciprocally connected pairs (PCA, PCB and PCC**)** (Fig. 5) maintain the male's position over the vulva while simultaneously inducing spicule thrusts (Garcia et al., 2001). The cholinergic pairs, PCB and PCC (Garcia et al., 2001), and glutamatergic PCA pair (LeBoeuf et al., 2014), stimulate posterior sex muscles contractions. Electrical coupling of these sex muscles with spicule-attached protractor muscles causes simultaneous muscle group contraction, leading to rhythmic spicule thrusts against the vulva (Liu et al., 2011). This repetitive spicule ‘prodding’ lasts until the spicules penetrate the hermaphrodite vulva, or when the male shifts off the vulva and resumes backward locomotion (Liu et al., 2011).

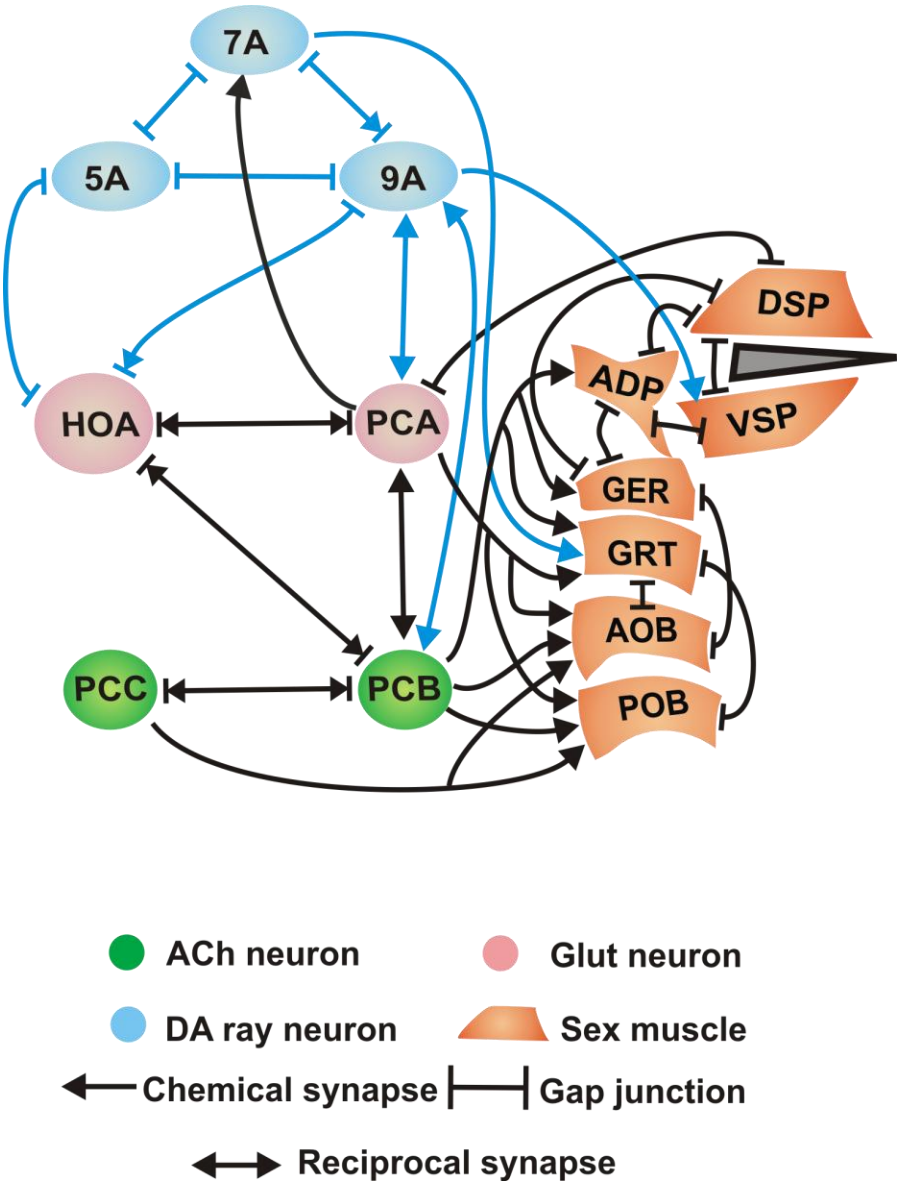

Figure 5. Abridged spicule intromission circuit connectome. Chemical, reciprocal and electrical synapses amongst abridged neurons and/or muscles of the male mating circuit, depicted by connector arrows. Neurons: post cloacal sensilla (PCA, PCB and PCC), hook sensillum (HOA), and dopaminergic ray neurons (R5A, R7A and R9A). Sex-muscles: Gubernaculum erector (GER), gubernaculum retractor (GRT), anterior oblique (AOB), posterior oblique (POB), dorsal spicule protractor (DSP), ventral spicule protractor (VSP) and anal depressor (ADP). The arrows represent bilateral connections. The copulatory spicule is depicted in gray (Jarrell et al., 2012).

Cholinergic signaling induces spicule movements

Ionotropic and metabotropic ACh receptors located on multiple genital muscles induce the male to press his tail against the vulva and stimulate rhythmic movements of the attached copulatory spicules. The lab of Dr. Garcia has found that signaling from specific nicotinic ACh receptors (ACR-16 and UNC-29), as well as the muscarinic ACh receptor GAR-3 are required to maintain the male tail positioned over the vulva (Liu et al., 2007b; Liu et al., 2011). Moreover, ACh secretions from the putative proprioceptive SPC motor neurons and simultaneous PCS stimulation results in a tonic muscle contraction, and subsequent spicule protrusion from the male tail (Garcia et al., 2001; Liu et al., 2007b; Liu et al., 2011). Accordingly, exogenous specific and non-specific ACh agonists artificially induce spicule protraction in the absence of hermaphrodite cues (Garcia et al., 2001).

Intrinsic and extrinsic factors likely modify the cholinergic circuit's activity prior to and during mating (Garcia and Sternberg, 2003; Gruninger et al., 2006; LeBoeuf et al., 2007; Gruninger et al., 2008; LeBoeuf et al., 2011). Since the DA rays chemically synapse onto HOA, PCA, PCB and sex muscles (Fig. 5), DA might adjust circuit component excitability and therefore modulate male mating. Moreover, a previous observation from my lab suggested that exogenous DA down-modulates ACh induced protraction. Therefore, I hypothesize that DA might restrict, rather than enhance, spicule circuit outputs.

Dissertation objectives

The *C. elegans* male mating circuit integrates sensory-motor cues that result in successful spicule insertion into the hermaphrodite vulva (Garcia et al., 2001; Liu et al., 2011). The positioning of the male tail over the vulva lips is a stepwise process monitored by reciprocally interconnected neurons (Liu and Sternberg, 1995; Koo et al., 2011). The main objective of this dissertation is to identify how the spatio-temporal regulation of this recurrent sensory-motor circuit delimits repetitive spicule thrusts to vulva cues context.

Chapter II describes in detail the experimental procedures used to elucidate this dissertation objective. In this study, I use pharmacology, genetics, mating behavioral observations, calcium imaging and targeted optogenetics to determine how circuit components restrict mating attempts to the vulva.

In Chapter III I determined that DA delimits spicule motor impulses during male mating via down-modulation of ACh signaling. Through behavioral assays, I show that DA is required for successful spicule insertion by promoting sex muscle contractile rhythmicity after the male positions his tail over the vulva. Pharamacogenetics indicated that simultaneous DA and ACh signaling antagonize the spicule circuit excitability through D2-like DOP2- and DOP-3, redundantly coupling to Gα proteins GOA-1 and GPA-7. Additionally, further behavioral paradigms indicate that a DA-ACh balance becomes essential to restrict non-productive mating attempts at non-vulva hermaphrodite areas and with inappropriate mates, such as other males.

In Chapter IV I described in detail the complex computations between DA ray neurons and the PCS sensilla. Live calcium imaging of dopaminergic ray 5A,7A,9A neurons and cholinergic PCS suggest that these two neurotransmitter's signaling coincide during rhythmic muscle contractions. Targeted light-stimulation combined with calcium measurements indicated that the PCS up-regulates Rn7A activity. This DA feedback is used to potentially terminate prodding after prolonged insertions attempts, or if the male shifts off the vulva. In accordance with this result, I found that DOP-2 expression in PCB diminishes PCA onto PCB stimulation to adjust the robustness of PCS recurrency.

In Chapter V I identified that D2-like modulation of gap-junctions restricts repetitive spicule thrusts to the vulva slit. Using forward genetics I identified an *unc-7* gap-junction mutation that disrupts DA signaling in PCB and a hook sensillum neuron (HOA), suggesting that this gap-junction sub-unit is a neuronal DOP-2 signaling effector. Drug tests indicate that DOP-2 promotes UNC-7 electrical communication to increase the relay of inhibitory glutamate-induced signals from HOA into PCB. This mechanism diminishes the PCS inter-neuronal stimulation to ensure termination of spicule intromission attempts, when the male moves off the vulva.

CHAPTER II

EXPERIMENTAL PROCEDURES

Strains

Strains were maintained at 20°C on NGM agar plates and fed with *E. coli* OP50. The *avr-14(ad1302)* LGI, *avr-15(ad1051)* LGV (Dent et al., 1997), and *avr-14(ad1302)(Dent et al., 2000); avr-15(ad1051)* L4 hermaphrodites were heat shocked at 30°C to obtain males carrying these alleles. Assays performed with these heat-shocked mutant males were conducted in parallel with N2 heat-shocked males. Otherwise all *C. elegans* males contain the *him-5(e1490)* allele LGV(Hodgkin et al., 1979). Additional alleles used were: *unc-7(e5)* LGX (Brenner, 1974), *pha-1 (e2123)* LGIII (Schnabel and Schnabel, 1990), *lite-1(ce314)* LGX (Edwards et al., 2008) and *glc-1(pk54)* LGV (Vassilatis et al., 1997). *cat-2(e1112)* LGV (Sulston et al., 1975) , *dop-1(vs100)* LGX, *dop-2(vs105)* LGV, *dop-3 (vs106)* LGX (Chase et al., 2004), *dop-4(tm1392)* LGX, *goa-1(n363)* LGI (Segalat et al., 1995), *gpa-7(pk610)* LGIV, *gpa-14(pk347)* LGI, *gpa-16(it143)* LGI (Jansen et al., 1999), *pha-1 (e2123)* LGIII (Schnabel and Schnabel, 1990), *unc-64(e246)* LGIII (Brenner, 1974), *fog-2(q71)* LGV , *unc-29(e193)* LGI (Lewis et al., 1980), *gar-3(gk305)* LGV and *acr-16(ok789)* LGV.

The *rg396* allele described in this study was isolated from an EMS screen that selected for males, which constitutively protracted their spicules (Prc phenotype). In brief, a mutation in *lev-11* suppresses the Prc phenotype of the *unc-103(sy557)* allele (Gruninger et al., 2008). The *unc-103; lev-11* strain was used for the EMS mutagenesis to identify

mutations that restored the Prc phenotype. The pseudo-revertants were then pharmacologically tested for their DA+ARE response. The *rg396* strain was identified and outcrossed five times to repulse *unc-103* and *lev-11*. The allele was mapped to LGX. Whole genome sequencing was conducted by BGI Americas Corporation (http://www.genomics.cn/en) and the *rg396* allele was found to be located in the *unc-7* locus. The *rg396* mutation changed the wild type sequence AAACT**G**CGCTCAG to the mutant sequence AAACT**A**CGCTCAG.

Transgenic strains include: *pha-1(lf) lite-1(lf) rg*Ex197[P*unc-103E*:*G-CaMP1.3*, P*unc-103E*:*mDsRed*, *pha-1*(+)]; *pha-1(lf) lite-1(lf) rg*Ex317[P*dop-2*:*ChR2*::*YFP*; *pha-1*(+)]; *pha-1(lf) lite-1(lf) rg*Ex326[P*tph-1*:*CFP*; *pha-1*(+)]; *pha-1(lf) lite-1(lf) rg*Ex431[P*hsp-16*:*egl-2(n693gf)*cDNA; P*unc-103E*:mDsRed; *pha-1(+)*]; *dop-2(lf) rg*Ex462 [P*aex-3*:*dop-2*::*CFP*]; *dop-2 rg*EX467 [P*unc103E*:*dop-2*::*CFP*]; *dop-3 rg*Ex482 [P*unc103E*:*dop-3*::*YFP*]; *dop-3 rg*Ex490 [P*aex3*:*dop-3*::*YFP*]; *pha-1(lf) lite-1(lf) rg*Ex491[P*gpa-7*:*YFP*; *pha-1*(+)]; *pha-1(lf) lite-1(lf) rg*Ex512[P*gar-3*B:*GCaMP3*::*SL2*:::*mDsRed*; *pha-1*(+)]; *dop-2(lf) dop-3(lf) rg*Ex515[P*tph-1*:*YFP*]; *pha-1(lf) lite-1(lf) rg*Ex517[P*dat-1*:*GCaMP3*::*SL2*:::*mDsRed*; *pha-1*]; *pha-1(lf) lite-1(lf) rg*Ex519[P*gpa-16*: *gpa-16* exon1::*YFP*; *pha-1*(+)]; *pha-1(lf) lite-1(lf) rg*Ex523[P*dat-1*:*G-CaMP3*::SL2:::*mDsRed*, P*gar-3*B:*ChR2*::*YFP*, *pha-1(+)*];*pha-1(lf) lite-1(lf) rg*Ex549[P*dat-1*:*G-CaMP3*::SL2:::*mDsRed*, P*dat-1:unc-103(gf)* , *pha-1(+)*], *dop-2(lf) dop-3(lf) pha-1(lf) rg*Ex550[P*dat-1*:*ChR2*::*YFP*, *pha-1(+)*], *pha-1(lf), lite-1(lf), rg*Ex625[P*unc-17*:*ChR2::YFP*, P*eat-4*: *GCaMP6*::*SL2*:::*mDsRed*, *pha-1*(+)]; *pha-1(lf), lite-1(lf), rg*Ex601[P*unc-17*: *GCaMP6*::*SL2*:::*mDsRed*, P*eat-4*: *ChR2::YFP, pha-1*(+)]; *pha-1(lf),*

*lite-1(lf) dop-2(lf), rg*Ex601[P*unc-17*:*GCaMP6*::*SL2*:::*mDsRed*, P*eat-4*:*ChR2::YFP, pha-1*(+)]; *pha-1(lf), unc-7(rg396), rg*Ex601[P*unc-17*: *GCaMP6*::*SL2*:::*mDsRed*, P*eat-4*:*ChR2::YFP, pha-1*(+)]; *pha-1(lf), lite-1(lf), rg*Ex431[P*hsp-16*:*egl-2(n693gf)*cDNA; P*unc-103E*:mDsRed; *pha-1(+)*]; *pha-1(lf), unc-7(e5), rgEx*653 [*Punc-7(5kb):unc-7*::YFP + co-injected SL2::GFP fragment ; *pha-1(+)*]; *pha-1(lf), rgEx*652[*Punc-7: unc-7*(A59T)::YFP + co-injected SL2::GFP fragment; *pha-1(+)*]; *pha-1(lf), rgEx*653[*Punc-7(5kb): unc-7*::YFP + co-injected SL2::GFP fragment; *pha-1(+)*]; *pha-1(lf), rgEx*668 [*Punc-7: unc-7* (A59T)::YFP; + co-injected SL2::GFP fragment ; *pha-1(+)*]; *pha-1(lf), unc-7 (rg396), rgEx*644 [*Punc-7: unc-7*::YFP; *pha-1(+)*]; *pha-1(lf), rgEx*672 [*Plev-11:unc-7(*A59T)::YFP; *pha-1(+)*]; *pha-1(lf), rgEx*673 [*Paex-3:unc-7* (A59T)::YFP; *pha-1(+)*]; *pha-1(lf), rgEx*671 [*Punc-103E: unc-7* (A59T)::YFP; *pha-1(+)*]; *pha-1(lf) rgEx*674 [*Pdop-2: unc-7* (A59T)::YFP; *pha-1(+)*]; *pha-1(lf) rgEx*649 [*Pdop-2: unc-7*::YFP; *pha-1(+)*]; *pha-1(lf) rgEx*[*Punc-7(7kb): unc-7*::YFP co-injected SL2::GFP fragment; *pha-1(+)*]

Mating behavior assays

For behavioral assays, virgin males were isolated from non-crowded plates, either at the late L4 stage (when cells in the male tail spike have completely migrated anteriorly) or after they newly crawled out of their L4 cuticle. They were kept solitary or in groups of 10-20 for 18-24hrs. When a mating assay was scored with individual or a group of potential mates, the virgin males were placed on10µl of a saturated *E. coli* culture spotted onto a NGM agar plate, to make a 3.5mm lawn (referred as mating plate). The

paralyzed hermaphrodites were obtained two ways: through an *unc-64* mutation, which broadly perturbs synaptic transmission rendering animals immobile, or through heat shock. The *pha-1*, *lite-1 rg*Ex431[P*hsp-16*:*egl-2(n693gf)*cDNA; P*unc-103E*:mDsRed; *pha-1(+)*] (referred to as *HS-egl-2)* hermaphrodites were incubated for 30min at 30^{o}C. After 3hrs, the heat shocked-expressed EGL-2(gf) K+ channels caused complete paralysis.

Graphpad Prism 5 software was used to perform all statistics. Fisher's exact test was used when comparing categorical variables (protracted vs. non-protracted, potent vs. non-potent). Mann-Whitney nonparametric test was used to compare the metrics of an experimental group with a control group. 1-way ANOVA and Tukey's post-test were used to compare the means and standard deviations of more than two groups.

Mating behavior metrics

To score multiple mating behavioral parameters for individual males, I digitally recorded every mating event from the time a male contacted a hermaphrodite with the ventral side of its tail, until spicule insertion or 5 min. To ensure consistent behavioral measurements, I digitally recorded and watched mating movies for mutants or transgenic males and control groups on the same date. For mating behavioral assays, 10-15 heat-shocked paralyzed *HS-egl-2* or *unc-64(lf)* hermaphrodites were evenly spaced on the lawn of a mating plate. A virgin 1-day old male was then placed in the middle of the hermaphrodite array. A Hamamatsu ImagEM CCD camera (Hamamatsu, USA) mounted on a compound microscope or a stereomicroscope recorded movies. From observations

of these recordings I scored the following mating metrics: number of times a male contacted the vulva, total duration of vulval contact and the time a male spent scanning a hermaphrodite in between vulva stops. The same group of males was used to obtain these data sets for each behavioral metric. A similar number of control and mutant males were tested in parallel on the same day for statistical comparisons. Through direct observation and using a hand-held timer, I measured the time it took wild type and *cat-2(lf)* males to contact and start scanning a hermaphrodite. Moving hermaphrodites were used to measure the duration over the vulval slit after the 1st contact for wild type and *dop-2(lf); dop-3(lf)* males.

The spicule movements of wild type or mutant males copulating with *HS-egl-2* hermaphrodites were digitally recorded with Hamamatsu ImagEM camera at a rate of ~15-20 frames per second. The recordings were reviewed to find an interval where the male repetitively prods the vulva with his spicules for an uninterrupted duration of 6 seconds or higher. Those frames of the recording were later analyzed using the SimplePCI software. A rectangular ROI was drawn over the male spicule region, and another over the vulva of a heat-shock hermaphrodite, to normalize the spicule movement against any slight hermaphrodite displacement. In each frame, both ROIs were used to obtain the standard deviation (STDEV) of the mean pixel intensity. The mean STDEV of the hermaphrodite ROI was used to correct the STDEV for each spicule ROI frame measurement. The oscillation amplitudes were then plotted against time for *unc-7(rg396) vs.* control strain. For statistical comparison the mean pixel fluxes per second during 5 seconds for *unc-7* and wild type were calculated for individual

males from each group. In the case of *dop-2; dop-3* comparisons oscillation amplitudes greater than 5% were considered to be due to a spicule deflection and the duration between these oscillations were graphed.

Efficiency of spicule insertion

Because the mating behavioral steps that lead up to sperm transfer can be highly variable, it required a metric to score/rank a spectrum of behavioral responses that result in successful spicule insertion. The metric had to differentiate a male that instantly found the vulva and inserted within a second or two of contact, from a male that meandered around the hermaphrodite for 110 secs, but eventually contacts the vulva, and inserts. However, this metric must be able to rank the spectrum of males that immediately undergo spicule insertion attempts and are persistent, but are unsuccessful in penetration, with males that were erratic in prodding behavior (and other steps of mating behavior), but fully inserted their spicules. To achieve this, the metric had to measure the period between vulval contact and full insertion, but it also had to incorporate a penalty for not being diligent at immediately initiating vulval spicule insertion behavior after contacting with a mate, and a bonus if successful penetration occurred, even after erratic performance of other mating behavioral steps. The efficiency of spicule insertion, E_{SI}, was calculated from recordings made during the first 120 seconds of contact between the male and a paralyzed 2-day-old *unc-64* hermaphrodite. If the male successfully inserted his spicules before the 120 seconds were over, then the observation was stopped. E_{SI} = (time (sec) spent at spicule insertion attempts / total time (sec) in contact with

hermaphrodite, up to 120 sec) X (1/time (sec) in contact with the hermaphrodite, such scanning, but not attempting insertion (penalty)) X (1+ (0 if no penetration, otherwise time (sec) remaining after a successful penetration, / 120 sec)(bonus)). A hypothetical E_{SI} of 1.99 would mean that the male located the vulva and inserted his spicules approximately 1 sec after contact with the hermaphrodite; whereas a hypothetical E_{SI} of 0.0 meant that the males spent their first 120 seconds of contact not attempting spicule insertion at the vulva (Guo et al., 2012).

Vulva index of prodding

The vulva index of prodding (VIP) was calculated for mutant, transgenic and control groups. After placing the paralyzed hermaphrodites on the small OP50 lawn, a 2 cm square chunk from the NGM plate was placed on a microscope slide. Prodding attempts were visualized using the 20X objective on an Olympus BX51 microscope (Olympus, USA), and digitally recorded using the Hamamatsu ImagEM camera at ~20 frames per second for ~3min or until insertion was achieved. These movies were pre-screened to find a consecutive interval where animals preferentially placed their tail over the vulva lips area without inserting for 60 secs. These intervals were more difficult to find for UNC-7 defective animals, since these males move off the vulva more often than wild type. Nonetheless, I still found a small group of *rg396* and P*dop-2*:UNC7(A59T) males where the total time in contact with the vulva was not significantly different when compared to their respective controls (5 wild type vs. 6 *rg396* animals, average=59 *vs.* 52 sec. respectively, *p=0.23;* 5 control (P*dop-2*:UNC7) 7 P*dop-2*:UNC7(A59T)

animals, average=58 *vs.* 50 sec, *p=0.63;* Mann-Whitney non parametric test). Thus, I observed these 'at vulva' mating intervals frame by frame to account for the time that the spicule tip contacted the hermaphrodite vulva slit or adjacent vulva slit areas. The interval where the spicule prodded at adjacent vulva slit areas was then subtracted from the interval of spicule thrusts at the slit, and subsequently divided by the total time that the male tail was in contact with the vulva. A score of +1 indicates exclusive spicule thrusts at the vulva slit, and a score of -1 indicates only adjacent vulva slit spicule thrusts for the time a male attempts prodding during the 60 seconds interval.

Mating potency assays

For mating potency tests, a single male and a single adult virgin *pha-1(lf)* hermaphrodite were put on a mating plate and incubated at 20°C for ~20 hrs. A male was considered potent if the plate contained cross-progeny.

For mating assays with multiple mates, a one-day-old wild type or *dop-2; dop-3(lf)* male was paired with 1, 5, or 20 two-day-old *fog-2(lf)* females in a mating plate. After 4hrs, the male was removed. The number of females laying eggs were determined 4 and 18 hours later. In experiments were wild type or *dop-2; dop-3* males must discriminate between *C. elegans* or *C. briggsae*, L4 *fog-2(lf)* females were grown to adulthood on OP50-seeded NGM agar plates containing 50µM red fluorescent dye SYTO-17 (Invitrogen, Eugene OR); the dye allowed the *fog-2(lf)* females to be identified from *C. briggsae* animals. One stained virgin 18-24hrs adult *fog-2(lf)* female was placed with ten 18-24hrs adult *C. briggsae* hermaphrodites on a mating plate. The animals were allowed

to acclimate to the lawn for one to two hours before a single virgin wild type or *dop-2; dop-3* male was introduced. Males were kept continuously with their mates for 18 hours. Four and 18 hours later after the male was first introduced with his mates, using an epi-fluorescence-equipped stereomicroscope, I analyzed SYTO-17 stained *fog-2(lf)* females for containing eggs in the uterus or sperm in the spermatheca.

For the mating competition tests, transgenic males contained expressed YFP or CFP from the *tph-1* promoter. One CFP-expressing wild type and one YFP-expressing mutant male were simultaneously placed in the middle of the mating plate containing a *fog-2* female. The first male to insert was determined via observations and subsequently identified using fluorescent microscopy. When mating competition tests were assayed with paralyzed males, the *HS-egl-2* strain was used to obtain immobile males similarly to heat-shock induced paralyzed hermaphrodites.

To determine if *dop-2; dop-3(lf)* males differ from wild type in their chemotactic or locomoter behaviors toward paralyzed *HS-egl-2* hermaphrodites or males, 6 paralyzed hermaphrodites and 6 paralyzed males were alternately and equally positioned at the periphery of a 1.5cm diameter OP50 lawn. One wild type or *dop-2; dop-3(lf)* male was placed at the center of the lawn and allowed to crawl around for up to 5 minutes. The males were timed when they first placed the ventral side of their tail against the cuticle of a paralyzed worm (either male or hermaphrodite) for greater than 1 second.

To observed how post-cloacal sensilla-ablated wild type and *dop-2; dop-3(lf)* males behave with paralyzed males, the cells PCA, PCB and PCC were laser-ablated in L4

males. Eighteen to 24hrs later, 3-4 laser-ablated or mock-ablated adult males were added to a mating plate that contained 40-50 paralyzed *HS-egl-2* males. The animals were digitally recorded at 1 frame per second for 10 minutes. The recordings were then reviewed, and time and duration that the moving male placed the ventral side of his tail against the cuticle of a paralyzed worm or another moving worm for greater than 1 second was determined for the 10 min recording. Cumulative time was calculated by adding up the total time a male was in ventral contact with other males. The average time was calculated by dividing the total time in contact by the number of mating contacts.

Pharmacology

For pharmacology assays virgin males were isolated at the L4 stage and tested on the following day. To assay agonist-induced spicule protraction, I dissolved levamisole (LEV) (ICN Biomedicals, OH), arecoline (ARE) (Acrose organics, NJ) , nicotine (NIC) (EM, NJ), oxotremorine M (OXOM) (Sigma, MO) and dopamine (DA) (Sigma) in water to make a stock solution of 10mM, 10mM, 100mM , 50mM and 30mM, respectively. Abamectin (ABA), and ivermectin (IVR) were dissolved in DMSO to make stock solutions of both drugs at 10 mg/mL. I added between 400- 1000µL of the drug to a three well round-bottom Pyrex titer dish. Five to ten males were then transferred to the drug bath and observed for five minutes at 20° C. Males were considered drug responsive if their spicules remained protracted for ≥ 10sec. For simultaneous exposure, DA and ACh-agonists were pre-mixed. For sequential exposure, worms were bathed in

DA for 1min and then ACh-agonists were added. Since ABA and IVR slowly induce detectable behavioral responses, such as locomotor paralysis, worms were bathed in avermectins for 7min and then ARE was added. In both of these sequential drug exposures the ACh agonists was added at a small volume, such that the final DA, ABA or IVR concentration was not significantly changed. In any of these drug mixtures the ACh agonist concentration was set at the EC90 concentration.

Plasmid construction

Reporters of *dop-2*, *gpa-7*, *gpa-16*, *unc-7* and *avr-14* expression

Primer sequences are provided in the Appendix. A 9.2 kb region upstream of the *dop-2* ATG was PCR-amplified using the primers: ATTB1Dop2pr and ATTB2Dop2pr. A 3.1 kb region upstream of the *gpa-7* ATG and the first four codons was PCR-amplified with the primers: ATTB1gpa-7F and ATTB2gpa-7R. A 2.6 kb region upstream of the *gpa-16* ATG, exon1 and 34 codons of exon2 was PCR-amplified with the primers: Pgpa-16Fv2 and Pgpa-16Rv2. These primers contained Gateway ATTB sites, which allowed the *dop-2, gpa-7*and *gpa-16* PCR products to be recombined using BP clonase (Invitrogen, CA), into the low copy number Gateway entry vector pDG15 (Reiner et al., 2006b), to generate pPC1, pPC24 and pPC40, respectively. To place the dopamine receptor and G-protein sequences upstream of YFP, these vectors were recombined with YFP destination vectors. pPC1 was recombined with pLR167 (a plasmid containing the gateway destination AttR Reading frame Cassette C.1 upstream of the channel rhodopsin fusion protein ChR2:YFP) (Liu et al., 2011); pPC24 and pPC40 were individually

recombined with pGW322YFP (a low-copy plasmid containing the gateway destination AttR Reading frame Cassette C.1 upstream of YFP) (Reiner et al., 2006b) using LR clonase (Invitrogen) to make plasmids pPC2, pPC39, pPC41, respectively.

Primer sequences are provided in the Appendix. A 5 kb region upstream of the *avr-14* ATG and the first 7 codons was PCR-amplified using the primers: ATTB1Pavr-14F and ATTB2Pavr14R. A 5.7 kb and a 7.7 kb region upstream of the *unc-7* ATG was PCR-amplified using the primers: attb1Punc7F, Punc7(8kb)F, and Punc7(8/9)R. All these primers contained Gateway ATTB sites, which allowed one *avr-14* and two *unc-7* PCR products to be recombined using BP clonase (Invitrogen, CA), into the low copy number Gateway entry vector pDG15(Reiner et al., 2006b), to generate pPC112, pPC76 and pPC103, respectively. To place the *avr-14* and *unc-7* promoter sequences upstream of YFP, the pPC112, pPC76 and pPC103 vectors were individually recombined with the YFP destination vector pGW322YFP (Reiner et al., 2006b)(a plasmid containing the gateway destination AttR Reading frame Cassette C.1 upstream of YFP) using LR clonase (Invitrogen) to make plasmids pPC111, pPC78, pPC101, respectively.

Cell specific expression of dop-2, dop-3 and unc-7 genomic DNA.

A 5.2 kb genomic *dop*-2-containing sequence from the ATG to last valine codon was PCR-amplified via primers Attb1DOP2F and Attb1DOP2R (see the Appendix). Since these PCR primers contained Gateway ATTB sites, *dop-2(*genomic DNA) was recombined using BP clonase, into pDG15, to generate pPC9. To make pPC11 [*dop-2::CFP*], pPC9 was recombined with pGW77C (a high-copy plasmid containing the

gateway destination AttR cassette upstream of CFP (Gruninger et al., 2006) using LR clonase. The LR sites flanking DOP-2 were removed using single site mutagenesis to obtain the pPC15 plasmid. To drive *dop-2::CFP* expression from different promoters, pPC15 was cut with *Afe*III and Gateway Vector Conversion Reading frame Cassette B(Invitrogen) ligation generated the destination vector pPC16. To drive *dop-2::CFP* expression from the *dop-2* endogenous promoter (*Pdop-2),* a sex-muscle expressing promoter (P*unc-103E)* and a pan-neuronal promoter (P*aex-3*), the plasmids pPC1, pLR21(Reiner et al., 2006b) and pLR35 (LeBoeuf et al., 2007) were individually recombined into pPC16 using LR clonase, to make pPC21 [P*dop-2* :*dop-2*::*CFP*] and pPC18 [P*aex-3*:*dop-2*::*CFP*] and pPC19 [*Punc103E*:*dop-2*::*CFP*], respectively. A 5.2 kb genomic *dop*-3-containing sequence from the ATG to last cysteine codon was PCR-amplified via primers DOP3geneF and DOP3geneR (Appendix). To fuse DOP-3 C-terminal end to YFP, the PCR product was cut with *BamH*I and *Age*I, and then cloned into the YFP-containing plasmid pSX322 *BamHI* site (Reiner et al., 2006b) to generate pPC23. To drive *dop-3::YFP* expression, pPC23 was cut with *BamH*I and ligated with the Gateway Vector Conversion Reading frame Cassette C.1(Invitrogen) to generate the destination vector pPC33. To make sex-muscle specific and pan-neuronal *dop-3::YFP* expression vectors, the plasmids pLR21 and pLR35 containing *Punc-103E* and *Paex-3*, respectively, were recombined into pPC23 using LR clonase, to generate pPC36 [P*unc-103E* :*dop-3*::*YFP*] and pPC37 [P*aex-3*:*dop-3*::*YFP*].

A 5.7 kb genomic *unc-7*-containing sequence from the ATG to the penultimate codon was PCR-amplified via primers UNC7(gene)Attb1and UNC7(gene)Attb2 (Appendix).

Since these PCR primers contained Gateway ATTB sites, *unc-7(*genomic DNA) was recombined using BP clonase into pDG15, to generate pPC86. To make pPC87 [*unc-7::YFP*], pPC86 was recombined with pGW322YFP using LR clonase. To drive *unc-7::YFP* expression from different promoters, pPC87 was cut with *Afe*III and ligated with the Gateway Vector Conversion Reading frame Cassette B (Invitrogen) to generate the destination vector pPC89. The LR sites flanking *unc-7* were removed using single site mutagenesis to obtain the pPC89R plasmid. To drive *unc-7 (genomic):YFP* expression from *unc-7*(5kb) *and unc-7*(7.7) endogenous promoters, the plasmids pPC86 and pPC103 were individually recombined into pPC89R using LR clonase to obtain pPC90 and pPC102. Moreover, the A59T mutation in the first *unc-7* exon was introduced into pPC89R via single site mutagenesis to generate pPC99. To drive *unc-7 (A59T):YFP* expression from the *unc-7(5kb)*promoter, the pPC86 plasmid was recombined into pPC99 to obtain pPC100.

To generate the minigine *unc-7* (A59T) version, the following changes were made using single site mutagenesis: two large intronic regions (intron 2 and 5) were removed from the pPC89R plasmid to generate pPC93 and pPC94, respectively. Subsequently the A59T mutation was introduced into pPC94 to generate pPC104. To drive *unc-7 (A59Tminigene)::YFP* expression from the *dop-2* endogenous promoter (*Pdop-2)*, a sex-muscle expressing promoter (P*unc-103E)*, a pan-muscular promoter (P*lev-11*) and the pan-neuronal promoter (P*aex-3*), the plasmids pPC1(Correa et al., 2012), pLR21 (Reiner et al., 2006a) , pLR22 (Kagawa et al., 1995) and pLR35(LeBoeuf et al., 2007) were individually recombined into pPC104 using LR clonase, to make pPC108 [P*dop-2:unc-*

7(A59T)::*YFP*], pPC105 [*Punc103E*: *unc-7(A59T)*::*YFP*], pPC106[P*lev11*: *unc-7(A59T)*::*YFP*] and pPC107 [*Paex-3*: *unc-7(A59T)*::*YFP*].

G-CaMP3, G-CaMP6 and ChR2 plasmids

I inserted an SL2-accepting *trans*-splice site followed by the mDsRed gene and an *unc-54* 3'UTR immediately downstream of Gateway AttR Reading frame Cassette C.1and G-CaMP3 (Tian et al., 2009) to create the vector pLR279. To introduce promoters upstream of the G-CaMP and DsRed sequences, the plasmids containing the promoters: P*gar-3B*(pLR57) (Liu et al., 2007b) and P*dat-1*(pZL15) (Koo et al., 2011) were recombined with pLR279 to generate the plasmids pLR283 and pLR286,respectively.

I inserted an SL2-accepting *trans*-splice site followed by the mDsRed gene and an *unc-54* 3'UTR immediately downstream of Gateway AttR Reading frame Cassette C.1and GCaMP6(M) to create the vector pLR305. In the pLR167(Liu et al., 2011) plasmid containing the ChR2:YFP (no introns) downstream of Gateway AttR Reading frame Cassette C.1, the YFP was swapped for the YFP containing all introns from the pGWYFP plasmid to create pBL248 for better fluorescence expression. This was done through In-fusion (Clonetech). To introduce promoters upstream of the GCaMP6 and DsRed sequences or ChR2:YFP, the plasmids containing the promoters: P*unc-17*(pBL228) and *Peat-4*(pPC52) (LeBoeuf et al., 2014)were individually recombined with pLR305 and pBL248 to generate the plasmids: pPC64 [P*unc-17*:GCaMP6::SL2:::mDsRed], pBL250 [P*unc-17*:ChR2::YFP], pPC68[P*eat4*: GCaMP6::SL2:::mDsRed], and pPC54[*Peat-4*:ChR2::YFP].

Plasmids used for hyper-polarization and stimulation of DA neurons

I introduced the *Pdat-1* upstream of the *unc-103(gf)* and ChR2 sequences to hyper-polarized and stimulate DA neurons respectively. The plasmid containing the *dat-1* promoter (pZL15) was recombined with pLR279 and pLR167 (Gruninger et al., 2008)to generate the plasmids pPC47 and pPC48.

Length measurements

The in-contact-length (ICL) was calculated by using the SimplePCI imaging software skeletonized tool to measure the length of the male outline that contacted the hermaphrodite cuticle of a representative frame. This measurement was then divided by the total male body length and converted to percentage values.

RNAi

To monitor *gpa-16* RNAi effectiveness, pPC41[P*gpa-16*:*gpa-16*::YFP] was injected into *goa-1(lf);gpa-7(lf)* strain. RNAi was induced by feeding worms bacteria producing double stranded RNA to the target *gpa-16* ORF. Bacteria with the L4440 double-T7 vector including *gpa-16* fourth and fifth exons were grown and induced by IPTG using a standard protocol (Kamath et al., 2001). The target gene sequences in the bacteria were verified by regular enzyme digestion. L4 males expressing the pPC41 transgene were transferred to plates spotted with the dsRNA bacteria or OP50, as a control, and incubated for 20 hours. Fluorescence of these males was checked before and after

feeding to address intensity changes induced by RNAi . The adult males then were assayed for their response to DA+ARE drug baths.

In copula Ca^{2+} imaging and optogenetics

The genetically encoded Ca^{2+} indicator G-CaMP1.3 was used to visualize calcium transients in the sex muscles, and G-CaMP3 was used to visualize Ca^{2+} transients in neurons. A mating plate was set up similarly to the mating behavioral assays. In brief, a chunk from an NGM plate containing OP50 lawn with HS hermaphrodites was placed on a microscope slide. One 18-20hrs adult virgin transgenic male was placed on the lawn without a microscope coverslip and immediately placed on an epifluorescence–equipped Olympus BX51 microscope (Olympus, USA). Mating was visualized using a 10X, 20X or 40X long working distance objective. Males were not exposed to high intensity filtered blue and green light until they initiated mating behavior. Exposure to the high intensity blue light, even though the males contain the *lite-1* mutation, interferes with the contact response step of mating. As the males were being recorded, the stage position and focusing were actively manually manipulated to keep the fluorescent cells in focus and in the center of the viewing field.

The G-CaMP and DsRed fluorescence signals at the male tail were recorded simultaneously using a Dual View Simultaneous Image splitter (Photometrics, AZ) and a Hamamatsu ImagEM Electron multiplier (EM) CCD camera, at the speed of ~30 frames per second. The Ca^{2+} data was analyzed using the Hamamatsu SimplePCI (version

6.6.0.0) software and Microsoft Excel, as described previously (LeBoeuf et al., 2011; Liu et al., 2011).

The recordings were reviewed to find the first instance of an uninterrupted behavioral step (either moving forwards or backwards along the hermaphrodite cuticle, or attempting spicule insertion at the vulva) with a duration of 6 seconds or greater. Region-of-interests (ROIs), of equal areas, were generated in the Simple PCI software. The individual ray 5,7,9A neurons were too close to one another to separate at 10X or 20x magnification with different ROIs, and thus their composite fluorescence was measured with a single ROI. The male gubernacular erector muscle, anal depressor and ventral protractor muscles were far enough so that separate ROIs could be generated for each muscle. ROIs were used to measure the background and cellular fluorescence signals in both the green and red excitation channels. The positions of the ROIs were manually adjusted for every frame in the movies. The mean pixel intensity (MPI) was measured for every ROI in every frame, in each recording. The data was then transferred from Simple PCI to Microsoft Excel. For each recording frame, background ROIs values were then subtracted from their respective ROIs that quantified neuronal or muscular fluorescence.

Focusing /gross movement/muscle contraction/mercury arc lamp flicking and photobleaching artifacts caused non-interesting fluorescence changes in both channels and in every frame. A higher rate of mDsRed photobleaching, relative to the minimal G-CaMP photobleaching, made a simple green-to-red fluorescence ratio-metric analysis

not appropriate to use. To correct this, the red channel was used as a reference to analyze the green channel. In each frame, the red channel background-subtracted MPI for each ROI was plotted with respect to time, and a one-phase decay curve (to correct for mDsRed specific photobleaching) was fitted over the data points using GraphPad Prism (version 4.03). The fitted curve serves as an arbitrary reference to quantify the magnitude of non-interesting fluorescence changes that occurred in each frame. For each frame, the measured background subtracted red channel MPI value was divided by the interpolated value to give a correction value. The corrected inverse value for each frame was then multiplied to the subtracted green channel MPI of the respective frame. This corrects the values for the green channel, so that the fluorescence changes reflect calcium transients rather than experimental artifacts. The values for each recorded frame was then calculated as $\Delta F/F0$ = (((corrected MPI (frame n)-corrected MPI (frame 0(initial frame)))/corrected MPI (frame 0(initial frame))) X 100). The values were then plotted with respect to time.

Target illumination experiments

For the optogenetic analyses entailing the PCS and ray neurons, *rg*Ex523[P*dat-1*:G-CaMP3::SL2:::mDsRed, P*gar-3*B:ChR2::YFP, *pha-1*(+)] males, incubated +/- with all-*trans*-retinal, were immobilized between a microscope coverslip and a 8-9% Noble agar pad containing Polybead polystyrene 0.1μm microspheres (Polysciences, Inc., WA). The males were then put on an Olympus IX81microscope scope fitted with the Mosaic illumination targeting system (Andor Technology, USA). Using the Metamorph

microscopy automation and imaging analysis software (Molecular Devices, PA), illumination regions were specified over the areas of the cloacal ganglia and dopaminergic rays. The software then controlled the Mosaic targeted illumination system mirrors to reflect the filtered blue and green excitation light to the G-CaMP-3 or G-CaMP-6/mDsRed expressing dopaminergic rays for ~4.2sec, followed by directing the illumination to both the ChR2-expressing cloacal ganglia and G-CaMP3-expressing dopaminergic rays for ~5.7sec, and then redirect the illumination to only the dopaminergic rays for ~4.2sec. The time between illumination protocols varied between 0.1 to 0.5sec.

For optogenetic analyses of the PCS, the *rg*Ex625[P*unc-17*:*ChR2::YFP*, P*eat-4*: *GCaMP6*::*SL2*:::*mDsRed, pha-1*(+)] and *rg*Ex601[P*unc-17*: *GCaMP6*::*SL2*:::*mDsRed*, P*eat-4*: *ChR2::YFP, pha-1*(+)] L4 males were used. Using Metamorph software a 5X5 square illumination region was specified nearby the PCA or PCB areas. To distinguish between PCA and PCB, I first observed the mounted males under DIC. To determine sufficient *GCaMP6*::*SL2*:::*mDsRed* transgenic expression, I briefly observed these cells under filtered green light. To increase mDsRed signal detection, I fitted an additional epi-flourescent light source to our microscope that provided whole field green-light illumination. I image GCaMP6/mDsRed expressing neuron for ~15secs, followed by directing the illumination to both ChR2-expressing and G-CaMP6 expressing neurons for ~30secs. Similar to experiments done with ray neurons, the G-CaMP and mDsRed fluorescence signals were recorded simultaneously using an Optosplit II simultaneous image splitter (Cairn Research, UK) and an Andor iXon EM CCD camera. After the

males were recorded, the coverslip of the immobilized male was removed. If the male did not immediately crawl around the slide, the data was discarded. The fluorescence data was analyzed using the SimplePCI software and Microsoft Excel, as described earlier.

Cellular ablations

To address the HOA sensilla contribution to either the DA+ARE drug sensitivity or to the PCA to PCB target illumination response I laser ablated HOA in paralyzed wild type males. I used a Spectra-Physics VSL-337ND-S nitrogen laser attached to an Olympus BX51 microscope via the MicroPoint laser focusing system to ablate the P10pppa cell (HOA) in early-to-mid L4 males. Both the laser-ablated and mock-ablated males were immobilized between a microscope coverslip and 4% noble agar pad containing 2 mM of sodium azide. Males that were used in the optogenetic experiments were placed on NGM plates for 1-2 hrs and then transferred to an all-trans-retinol plate for 2 more hours. The ablated males used for drug tests were placed on NGM plates for 18-24 hrs.

CHAPTER III

DA SIGNALING IS ESSENTIAL DURING COPULATION*

DA is required for efficient spicule insertion during mating

Male copulation requires monitoring mechanisms to initiate and terminate multiple repetitive sub-steps under the proper context. Mating begins when the male presses his tail against the hermaphrodite and moves backwards, scanning for the vulva (Loer and Kenyon, 1993; Garcia et al., 2001). After he locates the vulva, he initiates repetitive 7-11 Hz spicule thrusts to breach the vulval slit. During this sub-behavior, the male progressively adopts an arched body posture, which persists throughout spicule insertion and sperm transfer (Fig. 4). In rare events, this arched posture is adopted during scanning. Successful ejaculation occurs after repeated attempts of these motor sub-behaviors (Liu and Sternberg, 1995; Liu et al., 2007b). Molecules that promote mating execution have been identified mainly in cholinergic and/or peptidergic signaling (Schindelman et al., 2006; Liu et al., 2007a; White et al., 2007; Barrios et al., 2008; Srinivasan et al., 2008; Whittaker and Sternberg, 2009; Koo et al., 2011; LeBoeuf et al., 2011; Liu et al., 2011; O'Hagan et al., 2011). However, few signaling molecules that regulate and refine the behavior have been described. DA signaling is known to modulate general *C. elegans* locomotor behaviors.

---

* Portions of this chapter reprinted from Paola Correa, Brigitte Leboeuf and L. René García (2012) *C. elegans* dopaminergic D2-like receptors delimit recurrent cholinergic mediated motor programs during a goal-oriented behavior. *Plos Genetics* 8(11): 1-18 Copyright 2012 by PLOS

Since 3 pairs of sex-specific sensory ray neurons secrete the neurotransmitter (Rn5A, Rn7A, and Rn9A) DA is a candidate for modulating mating (Sulston et al., 1975; Sawin et al., 2000). Tyrosine hydroxylase is a key enzyme in the biosynthesis of DA. I first asked how well tyrosine hydroxylase deficient *cat-2(lf)* males mate (Sulston et al., 1975; Sawin et al., 2000). Initially I noticed that in *cat-2* male populations, a higher percentage displayed spontaneously protracted spicules (44%; n=67) relative to wild type (9.6%; n=62) *(p*=0.0018, Fisher's exact test). This suggested that DA might down-modulate the spicule protraction circuit. When I paired a non-protracted virgin mutant or wild-type 1-day-old adult male with a 1-day-old moving hermaphrodite for 24hrs, I found that 56% of *cat-2* males could sire progeny compared to the 88% of wild type (Fig. 6). To confirm that *cat-2* mating deficits were caused by DA depletion and not due to unknown background mutations, dopaminergic neurons were artificially hyperpolarized by expressing a hyperpolarizing UNC-103 ERG-like K+ channel (*unc-103(gf)*) (Petersen et al., 2004) from the *dat-1* dopamine transporter promoter (McDonald et al., 2007). Similar to *cat-2* mutants, males containing the *unc-103(gf)* transgene had increased number of spontaneously protracted spicules (28%; n=46 vs. 4%; n=27) (*p*-value=0.04, Fisher's exact test), and had decreased ability to sire progeny (40%; n=49 vs. 69%; n=50) when compared to the transgenic control strain (Fig. 6). Therefore, indicating that DA is necessary for efficient mating.

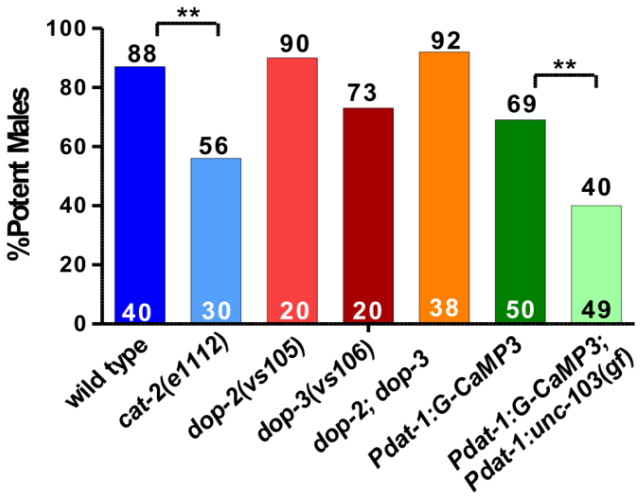

Figure 6. DA is necessary during copulation. Percentage of potent males (vertical axis) with different genetic and/or transgenic backgrounds (horizontal axis) mated into moving hermaphrodites. The number of males tested and the percentage of potent males is listed at the bottom and top of the bars, respectively. The brackets indicate the *p*-values calculated according to a Fisher's exact T-test.

To ask how the *cat-2* mutation compromised mating, I observed copulations between *cat-2* males and 2-day-old paralyzed *unc-64* hermaphrodites for 2min. I assayed mating initiation time, vulva contact duration and the number of vulva contacts, and found no difference between wild type and *cat-2* males. However, when I measured the average duration a male spent between vulval insertions attempts, I found that *cat-2* males had longer intervals than wild type (Fig. 7A). This was because *cat-2* males displayed abnormal arched postures and precocious spicule thrusts at random areas on the hermaphrodite (i.e. ectopic spicule thrusts) (Fig. 7B). This defect also accounted for the mutant's reduced spicule penetration ability compared to wild type (36% vs. 73%, respectively, Fig. 7B). To quantify the variability of spicule insertion behavior, I calculated the efficiency of spicule insertion (E_{SI}) in both groups. This metric combines

how fast males initiate, sustain, re-attempt and complete spicule insertion. I found that *cat-2* males on average had a lower E_{SI} than wild type (0.19 vs. 0.075, Fig. 7C). Thus, DA signaling promotes spicule insertion by lowering the probability of displaying non-productive ectopic spicule thrusts.

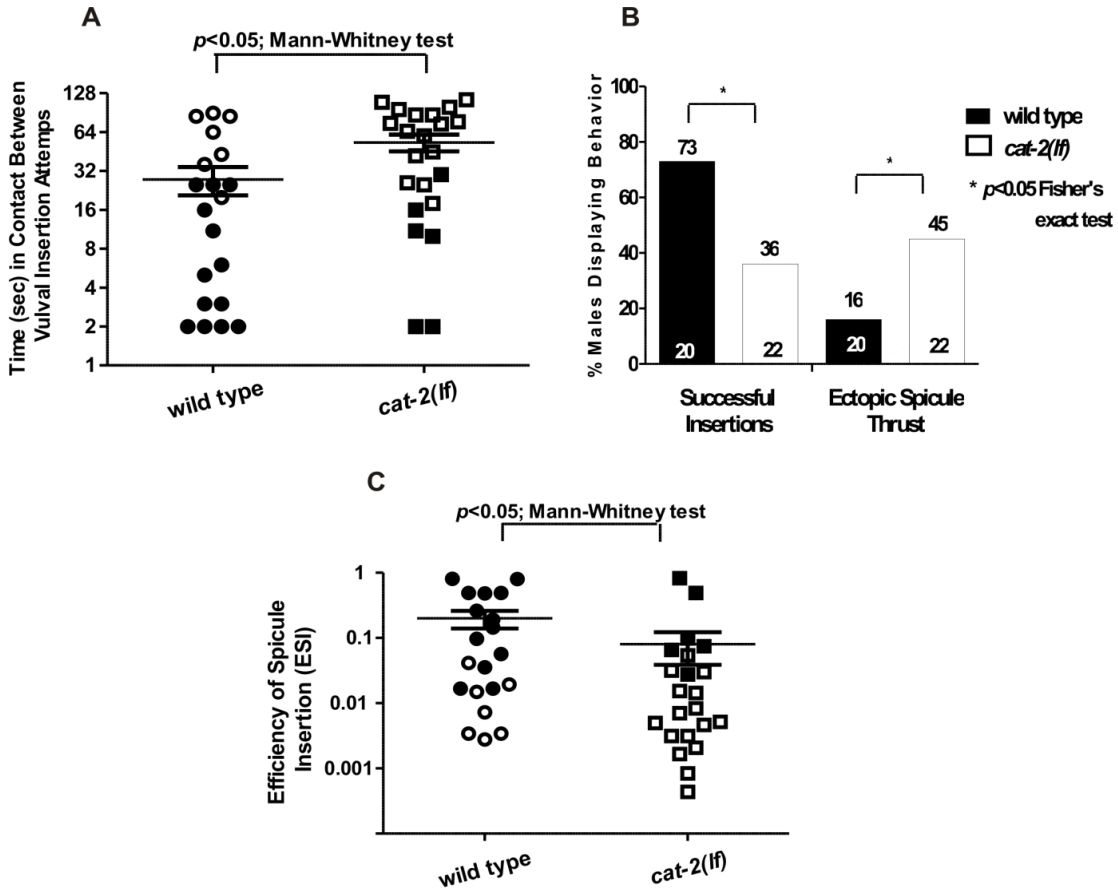

Figure 7. DA decreases non-productive repetitive spicule displays. (A-C) Score of different behavioral metrics for wild type and *cat-2(lf)* males mating with paralyzed mates. (A) The duration in contact with a mate between insertion attempts. (B) Percent of males displaying spicule related behaviors. The number of tested males and the percentage of males that successfully inserted their spicules or display ectopic spicule thrusts indicated at the bottom and top of the bars, respectively. (C) The spicule efficiency index. Symbols represent an individual male's performance, where open symbols represent unsuccessful insertions.

Exposure to DA inhibits ACh-induced spicule protraction

Next, I used pharmacology to address whether DA modulates the cholinergic spicule circuit by pre- or co-regulating the ACh response. ACh agonists artificially stimulate receptors on the spicule neurons and muscles to induce spicule protraction. These agonists include levamisole (LEV) and nicotine (NIC), which activate ionotropic ACh receptors (AChR), and oxotremorine-M (OXOM), which activates $G_{\alpha q}$ -coupled muscarinic AChRs (mAChR) (Garcia et al., 2001; Liu et al., 2007b). Arecoline (ARE) has been reported to stimulate mAChRs in the pharynx (Steger and Avery, 2004); however, I found that in the spicule circuit, ARE is a non-selective agonist. For the spicule protraction circuit to be ARE-insensitive, a male must contain mutations in the NIC receptor (*acr-16 (ok789)*), LEV receptor (*unc-29(e193)*) and the OXOM receptor (*gar-3(gk305)*) (see Appendix). Therefore, suggesting that out of the tested ACh agonists ARE mimics naive ACh signaling the most in the spciule circuit.

Since the behavioral data with *cat-2(lf)* suggested that endogenous DA down-modulates the cholinergic and glutamatergic driven spicule circuit, I address whether exogenous DA can attenuate the spicule protraction response induced by different ACh agonists. I exposed males to DA and ACh agonists simultaneously for 5min and assayed males with protracted spicules. The effective concentrations inducing spicule protraction for 90% of the males (EC90) were 5µM for LEV, 1mM for both NIC and ARE and 50mM for OXOM. The EC90 concentration for DA, inducing paralysis in 90% of hermaphrodites, was previously reported to be between 20-30mM (Chase et al., 2004). I confirmed this

observation by exposing males to 20mM of DA or water. This DA exposure was sufficient to paralyzed ~90% of males in 1min (Fig. 8A). Additionally, I quantified spicule protraction in this drug bath, and found that neither DA nor water induced spicule protraction in any male during a 150sec. observation (Fig. 8A). Therefore, I exposed one-day-old virgin males to 30mM of DA combined with individual AChR agonists at their respective EC90 concentration (Fig. 8B). I found that DA reduced ACh-agonist induced protraction (Fig8. B), supporting my hypothesis that DA antagonizes ACh signaling.

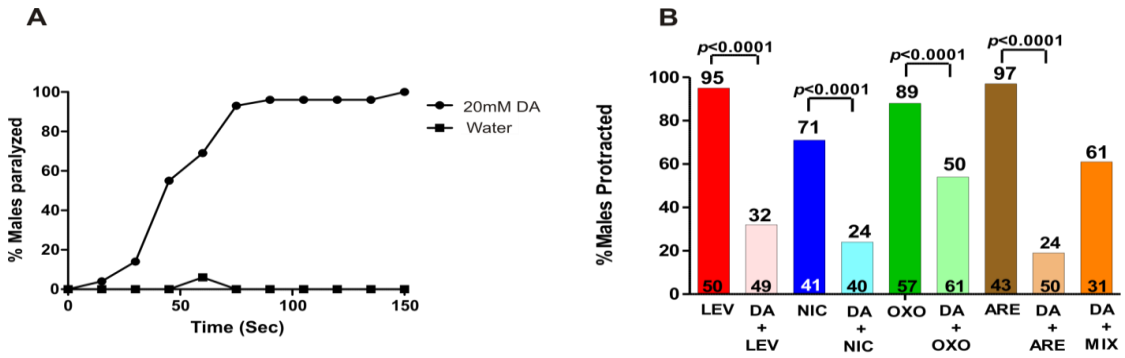

Figure 8. DA down-modulates ACh-induced protraction. (A) DA at 20mM induces paralysis in 90% one-day-old virgin males (n=20). No spicule protraction was observed for either DA or water (n=20) exposure. (B) One-day-old virgin males were exposed to 30mM DA and either LEV, NIC, OXOM or ARE at EC90 concentrations and ACh-agonist mixture (MIX). The number of males tested and the percentage of spicule protracted males is listed at the bottom and top of the bars, respectively. *p*-values determined with Fisher's exact test comparing groups indicated by the brackets.

To address if DA also preconditions the spicule protraction circuit to be less responsive to ACh stimulation, I bathed males in 30mM of DA or water for 1min, followed by *(f.b)* exposure to the EC90 ACh-agonist concentration. I found that DA pre-application still inhibited LEV- and NIC- and to a lesser extent OXOM-induced protraction (Fig. 9).

Interestingly, DA pre-exposure didn't inhibit ARE-induced spicule protraction. To rule out the possibility that after DA exposure ARE induces protraction independently of AChR stimulation, males were exposed to DA followed by an ACh-agonists mixture (MIX). This MIX contained LEV, NIC and OXOM at the EC90 concentrations. Similar to the ARE responses, I found that pre-exposure to DA did not inhibit the MIX-induced protraction and when treating males with the MIX and DA simultaneously, spicule protraction was down-regulated (Fig. 8B and Fig. 9). These results suggest that DA down-modulation occurs simultaneously with ionotropic and muscarinic ACh signaling.

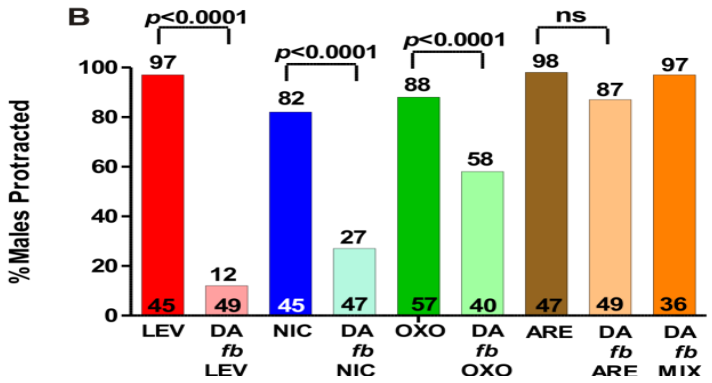

Figure 9. DA pre-exposure down-modulates LEV, NIC, and OXO and does not affect ARE-induced protraction. One-day-old virgin males were exposed to 30mM DA for 1min *followed by* (*fb*) either LEV, NIC, OXOM , ARE or ACh-agonist mixture (MIX). The number of males tested and the percentage of spicule protracted males is listed at the bottom and top of the bars, respectively. *p*-values determined with Fisher's exact test comparing groups indicated by the brackets.

Since ARE's non- selectivity approximates more native ACh signaling (Table 1), DA+ARE co-treatment was used to characterize the mechanism of DA down-modulation. First, I tested males containing the G-protein coupled receptor loss-of-function (*lf*) mutations *dop-1(vs100), dop-2(vs105), dop-3(vs106)* or *dop-4(tm1392)*

(Chase et al., 2004; Vidal-Gadea et al., 2011). In the *dop-1* and *dop-4* mutants DA suppressed ARE-induced protraction to wild type levels, in accordance with previous studies where these receptors are found to enhance cellular excitability via $G\alpha_q$ pathways (Chase et al., 2004; Ezcurra et al., 2011). However, in the *dop-2(lf)* or *dop-3(lf)* single mutants and *dop-2*; *dop-3* double mutants DA did not decrease ARE-induced protraction to wild type levels (Table1). Therefore, my results indicate that the DOP-2 and DOP-3 receptors partially mediate DA response.

Table1. DA down-modulates ARE-induced protraction via DOP-2 and DOP-3

Genotype	**% Males protracted(n)**			**P-value**
	ARE (1mM)	DA(30mM) +ARE(1mM)	DA(20M) +ARE(1mM)	**Fisher's exact test**
Wild type	94 (61)	14 (117)	ND	
dop-1 (vs100)	75 (24)	20 (25)	ND	NS
dop-2 (vs105)	92 (50)	58 (101)	ND	P<0.0001
dop-3 (vs106)	90 (30)	59 (32)	ND	P=0.0006
dop-4 (tm1392)	93 (31)	26 (26)	ND	NS
dop-2 ; dop-3	95 (76)	54 (85)	63 (40)	P=0.005

The GOA-1 and GPA-7 Gα-proteins transduce D2-like signaling in the spicule circuit

The *C. elegans* D2-like receptors signal via $G\alpha_{o/i}$ –pathways. There are 16 Gα proteins identified in *C. elegans* (Jansen et al., 1999); however there are few studies that categorizes them into $G\alpha_{o/i}$ sub-family. Out of the 16 genes GPA-7, GPA-14 and GPA-16 have the best BLAST matching sequences with GOA-1, the *C. elegans* $G\alpha_{o/I}$ homolog. The third intracellular loop of the DOP-2 receptor has been shown to interact with GPA-14 *in vitro* (Pandey and Harbinder, 2012). Moreover, pharmacological and behavioral studies suggest that GOA-1 transduces the DOP-3 receptor signal (Chase et al., 2004; Allen et al., 2011). Therefore, the alleles *goa-1(n363), gpa-7(pk610), gpa-14(pk347)* and *gpa-16(it143)* were tested for DA+ARE responses. None of the single mutants for these G-proteins were insensitive to exogenous DA down-modulation. However, the double mutant *goa-1(lf); gpa-7(lf)* males had increased spicule protraction in DA+ARE (Table 2), suggesting that DOP-2 and DOP-3 are coupled to GOA-1 and/or GPA-7.

Table 2. Effect of mutant Gα alleles on DA inhibition of ARE-induced protraction

Genotype	**% Males protracted(n)**		**P -value Fisher's**
	ARE (1mM)	DA(20mM)+ ARE(1mM)	**exact test**
Wild type	99(51)	21(112)	
goa-1(n363)	97(20)	12 (41)	NS
gpa-7(pk610)	90(20)	5(20)	NS
gpa-16 (it143)	90(30)	11 (30)	NS
gpa-14 (pk347)	90(21)	10(48)	NS
goa-1 (n363); gpa-7(pk610)	98(20)	62 (50)	P<0.001*
gpa-7 (pk610); gpa14(pk347)	93 (20)	25 (30)	NS
goa-1; gpa-7; (RNAi gpa-16)	91 (19)	60(31)	NS**

*compared to wild type, ** compared to *goa-1; gpa-7*

DOP-2, DOP-3 and GPA-7 down-modulate ARE-induced protraction in sex-muscles

Next I addressed in which tissues of the spicule circuit the D2-like components might trasnduce the DA signal. Since GOA-1 is expressed throughout the *C. elegans* nervous system (Mendel et al., 1995), I assumed that GOA-1 broad expression would include neurons and/or muscles that are regulated by D2-like pathways. Thus, I assessed YFP and/or GFP promoter fusion expressions of the *dop-2*, *dop-3* and *gpa-7* genes. I found

that DOP-2, DOP-3, and GPA-7 expression coincides in the sex-muscles (Fig. 10) and that DOP-2 is expressed in spicule circuit neurons such as PCB (Fig. 10).

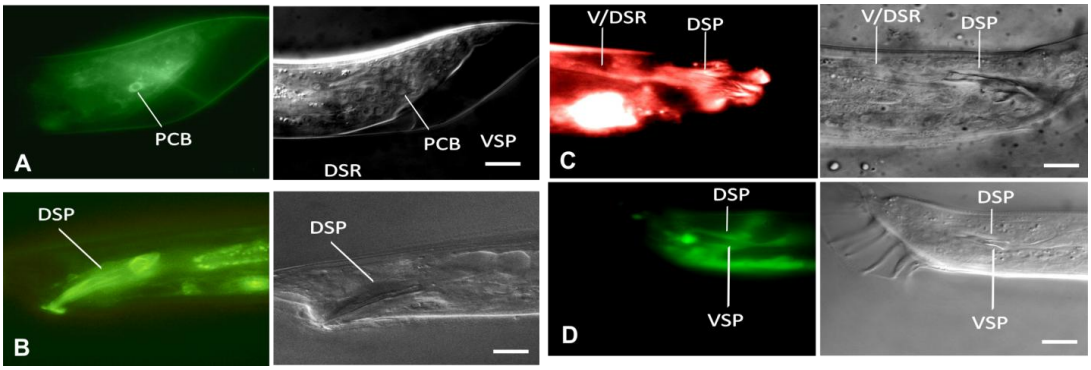

Figure 10. Expression pattern of DOP-2, DOP-3 and GPA-7. (A&B) *Pdop*-2:YFP expression in (A) post-cloacal sensilla B (PCB) at the L4 stage and (B) dorsal spicule protractor (DSP). (C) *Pdop*-3:RFP expression in DSP and dorsal spicule retractor (DSR). (D) P*gpa-7*:YFP expression in V/DSR and D/VSP. DIC (right) and fluorescence (left) images of adult male tail regions unless indicated. Scale bar 10 µM.

Since D2-like signaling components are expressed in sex-muscles and the PCB neuron, these molecules might regulate cellular excitability of the spicule circuit in either of these tissues. Therefore, I attempted to ameliorate the resistance to DA+ARE in the *dop-2* and *dop-3* males by tissue specific expression of these GPCRs. I observed that DA down-modulation was restored in *dop-2* and *dop-3* males when DOP-2 and DOP-3 was expressed in sex muscles from the *unc-103E* promoter, respectively (Table 3). These data suggest that DA antagonizes ACh signaling via DOP-2 and DOP-3 in the sex muscles.

Table3. DOP-2 and DOP-3 down-modulate ARE-induced protraction in sex muscles

Genotype	Tissue expression	%Males protracted in 20mM DA+ 1mM ARE	P-value(Fisher's exact test)
dop-2(vs105)		52(48)	
*dop-2, rg*Ex462 [P*aex-3:dop-2*:CFP]	All neurons	43 (48)	NS
*dop-2, rg*Ex467 [P*unc-103E:dop-2*:CFP]	Sex-muscles	15 (51)	0.0002
dop-3 (vs106)		40(76)	
*dop-3, rg*Ex490 [P*aex-3:dop-3*:YFP]	All neurons	24 (37)	NS
*dop-3,rg*Ex482[P*unc-103E:dop-3*:YFP]	Sex-muscles	7(39)	0.001

D2-like receptors promote spicule muscle contractile rhythmicity

To ask how DOP-2 and DOP-3 regulate mating, I determined the mating potency of *dop-2; dop-3* mutant males with moving hermaphrodites. The mutant and wild-type potencies were similar, 92% (n=38) vs. 88% (n=40), respectively (Fig. 6). Thus, the functions of DOP-2 and DOP-3 are subtle. I then quantified *dop-2; dop-3* males' mating

performance with *unc-64(lf)* paralyzed hermaphrodites and found that wild type, the double and single mutants behaved similarly during various mating steps. However, the double mutants can insert their spicules faster, into the paralyzed and easy to penetrate hermaphrodites, than wild type (Fig. 11A). This paradoxical result suggests that having a wild type version of D2-like receptors reduces reproductive fitness. However, males that lack D2-like receptors might not be at a behavioral advantage when paired with a more challenging mate. Therefore, I coupled *dop-2; dop-3* or a wild-type male with a moving hermaphrodite and directly measured the first vulval contact duration. I found that *dop-2; dop-3* males are displaced from the vulva faster than wild type (Fig. 11B). Unlike wild-type mating events, most hermaphrodites coupled with mutant males would abruptly move during spicule insertion attempts, causing the males to move off the vulva and thrust their spicules at areas adjacent to the vulva.

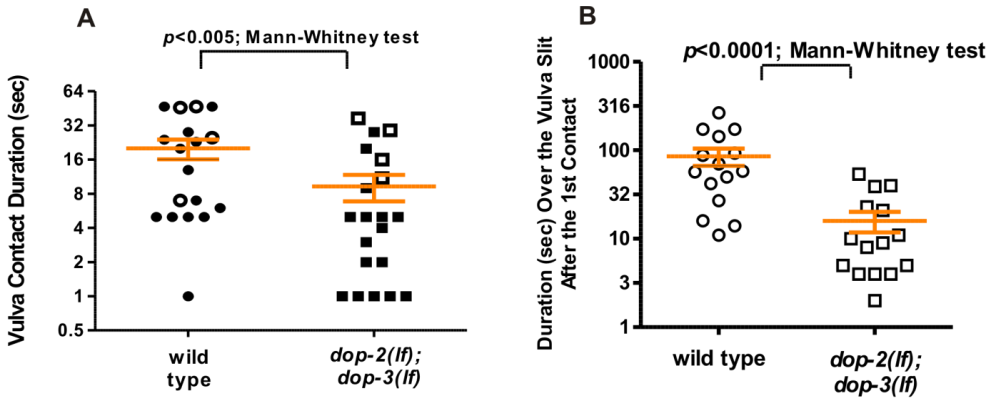

Figure 11. D2-like receptors maintain the male tail position over the vulva (A) Duration of vulval contact until spicule insertion or 120sec with paralyzed hermpahrodites. Symbols represent individual male performance. Open symbols represent unsuccessful insertions. (B) Duration over the vulval slit during the 1st spicule insertion attempt with a moving hermaphrodite.

We previously showed that a K+ channel mutation disrupts the frequency and amplitude of sex muscle contractions during spicule insertion attempts; the arrhythmic spicule thrusts will startle the hermaphrodite and increase the probability of the male losing contact (Garcia and Sternberg, 2003). I reasoned that a similar phenomenon is occurring with *dop-2; dop-3* males. Thus, I measured spicule movement frequency when a male attempted insertion at a paralyzed hermaphrodite vulval slit. I found that relative to wild type, *dop-2;dop-3* spicule insertion attempts were less rhythmic. Among the assayed *dop-2; dop-3* males, the variability of durations between spicule thrusts was greater than compared to wild type males, indicating that the mutant males displayed more random sustained thrusts in runs of rapid shallow thrusts (Fig 12). Therefore, suggesting that DOP-2 and DOP-3 decrease arrhythmic spicule thrusts.

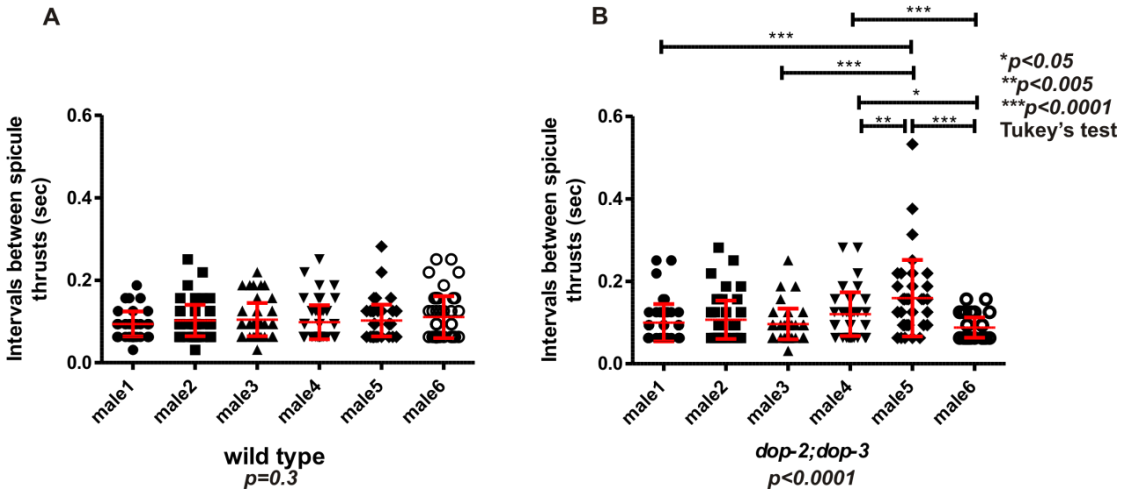

<u>Figure 12.</u> D2-like signaling promotes spicule thrusts rythmicity. Intervals between spicule thrusts for (A) wild type and (B) *dop-2; dop-3* males assayed for six consecutive seconds of spicule insertion attempts. The *p-values* on the bottom of each strain were obtained with 1-way ANOVA analysis.

Restriction of non-productive mating behaviors requires D2-like signaling

Since *dop-2; dop-3* males behave differently during copulation with moving mates, I identified conditions where that difference would result in reduced mating fitness for these mutants. I paired either one wild type or one mutant male for 4hrs with increasing numbers of moving *fog-2(lf)* virgin females (which contain a mutation disrupting self-sperm generation), and counted the number of impregnated females. I reasoned that since mates with variable mating receptiveness exist in a population, the subtle defects of *dop-2; dop-3* males might be more evident in a competition to impregnate the most partners. I found that when the female numbers increased, wild type impregnated more females than *dop-2; dop-3* males (Fig. 13A). This difference was obvious when *dop-2; dop-3* males were exposed to 20 females. The lower serial mating potency is likely attributed to behavioral differences prior to insertion. However, DA signaling is also involved in maintaining a refractory period between insertions (LeBoeuf et al., 2014); thus these serial mating differences could also result from post-ejaculatory behavioral variations. To rule out this possibility, I measured the amount of time between ejaculations and found that wild type and mutant males' refractory periods are similar (Fig. 13B).

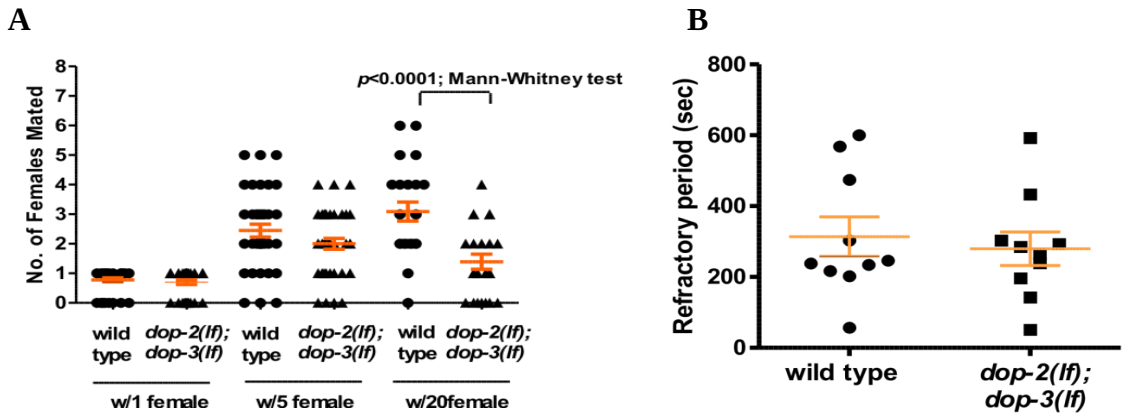

Figure 13. D2-like signaling promotes mating fitness. Serial mating potency (A) and refractory periods (B) for wild type and *dop-2; dop-3* males mating with moving *fog-2* females.

To address if behavioral differences caused the double mutants to impregnate fewer females, I simultaneously paired a mutant and a wild-type male with a single 1-day-old *fog-2* female and asked which male mated first. I found that *dop-2; dop-3* and wild type males impregnated a similar percentage of females (56% vs. 44%) (Fig. 14A). Similar to Fig 7A data, this indicates that with a single mate, mutant males are similar to wild type in copulation. However, when I challenged the double mutant and a wild type male with a single *fog-2* female and 10 paralyzed males, as unproductive mating distractions, I found that wild type impregnated 80% of the females versus 20% that of wild type (Fig. 14A). Furthermore, in this mating competition with a distraction set-up I observed that wild type and mutant males contacted both sexes with equivalent frequency (Fig. 14B), and in a male-female mate choice assay, I did not find any indication that the mutant males had a greater chemotaxic preference to males (Fig. 14C). However wild-type males immediately terminated mating attempts with paralyzed males, whereas mutant

males would abnormally scan and attempt spicule insertion into these inappropriate mates (Fig. 14D). Therefore, taken together these observations indicate that during mating, D2-like signaling dampens ACh-induced behaviors with uncooperative/inappropriate mates.

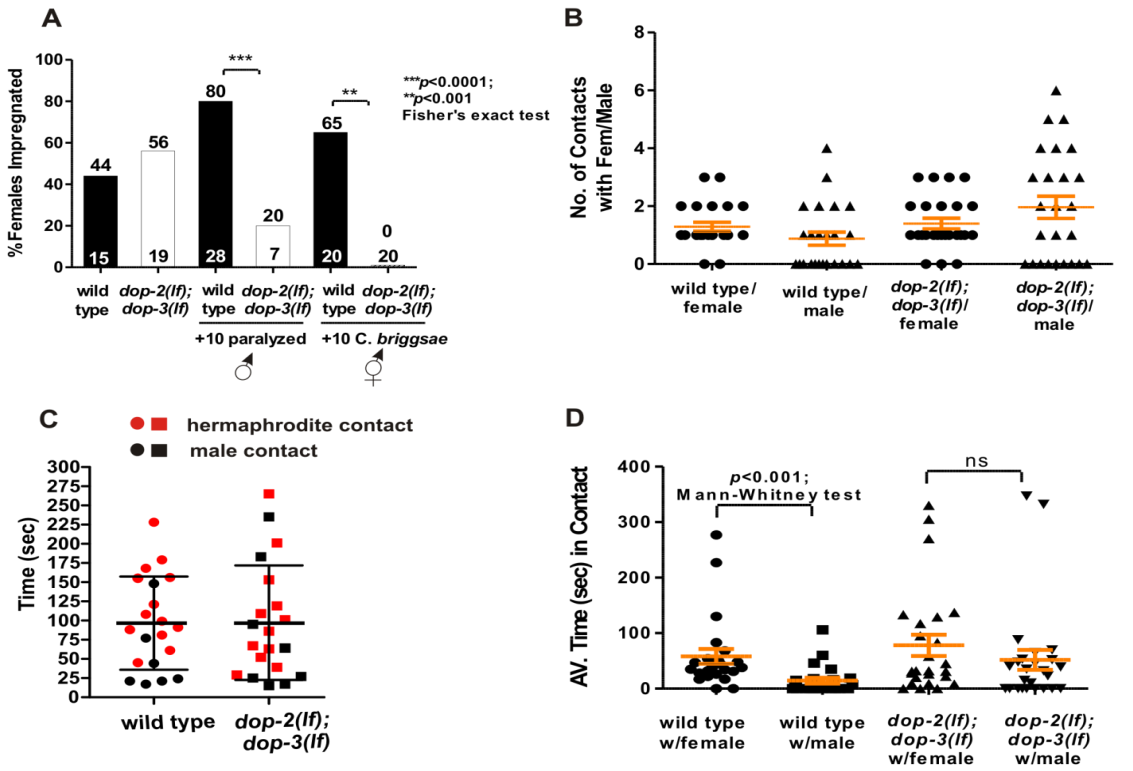

Figure 14. D2-like signaling restricts mating with inappropriate partners. (A) Mating competition with distraction partners pairing a wild type and a *dop-2; dop-3* male with one *fog-2* female +/-10 paralyzed males (first 4 columns), and individual pairings of wild type and mutant males with 10 C. briggsae hermaphrodites in addition to individual fog-2 females (last 2 columns). The top and bottom of each column indicates the % of pregnant females and the number of males that copulated or number of males assayed (last 2 columns). (B) Number of transient contacts with either a *fog-2(lf)* female or a paralyzed male calculated when pairing one wild type or *dop-2; dop-3(lf)* males with a single *fog-2(lf)* female and 10 paralyzed males. (C) The time required for a *dop-2; dop-3* or a wild type male to contact another worm containing 6 paralyzed males and 6 paralyzed hermaphrodites. (D) Average time males spent in contact with either a female or a paralyzed male, calculated when pairing one wild type or *dop-2; dop-3(lf)* males, singly with a *fog-2(lf)* female and 10 paralyzed males. *p*-values indicated by the brackets

Next, I addressed, in a more natural scenario, the importance of D2-like receptors in decreasing fruitless mating attempts with nematodes of other species. I paired one *fog-2* female and 10 *C. briggsae* hermaphrodites, with one wild type or a *dop-2; dop-3* male and counted how efficiently the *fog-2* female became impregnated. I found that after 4hrs, wild type impregnated 65% more females than mutant males, when challenged with 10 *C. briggsae* hermaphrodites (Fig. 14A). This indicates that D2-like signaling might limit unproductive mating attempts with other hermaphroditic nematode species.

Finally I addressed whether D2-like signals specifically dampened spicule circuit excitability or other mating circuits, to restrict aberrant mating attempts. The male's response to contacting a mate is primarily facilitated by the ray sensilla. However, published reports have demonstrated that other male sensilla, such as the post-cloacal sensilla (p.c.s), spicule tips and possibly the hook sensillum can feebly substitute for ray function; therefore the activity of these sensilla might be increased in the *dop-2; dop-3* males (Liu and Sternberg, 1995,{Koo, 2011 #6321; Koo et al., 2011)]. Since driving expression of DOP-2/DOP-3 exclusively in cells of the spicule circuit is not technically possible, I opted for an alternative approach of laser ablating the *dop-2*-expressing PCB neuron or all of the p.c.s neurons (PCA, PCB and PCC), and asking if mating with a non-hermaphrodite is reduced. First I quantified in wild-type males lacking PCB or all 3 PCS neurons, the cumulative and average duration in contact with another male during a 10min assay period, when surrounded by 40-50 paralyzed males. I found that the cumulative time that PCB or PCS ablated males spent with other males was reduced in comparison to mock-ablated males (Fig. 15A). This result is consistent with the idea that

the post-cloacal sensilla play a minor role in contact response and scanning behavior. However if an operated male does initiate scanning with another male, the average time was not significantly different amongst these groups (Fig. 15B). I then tested if PCB or p.c.s ablations in *dop-2; dop-3* males would reduce abnormal mating attempts. I found that *dop-2; dop-3* males on average spent longer amount of times scanning other males than wild type (Fig. 15B); however, neither PCB nor p.c.s ablations reduced this phenotype. In addition, the cumulative time in contact of mutant males with another male was similar between operated and intact males (Fig. 15A). This indicates that D2-like signaling must be modulating other circuits in addition to the post-cloacal sensilla to attenuate contact response and scanning behavior.

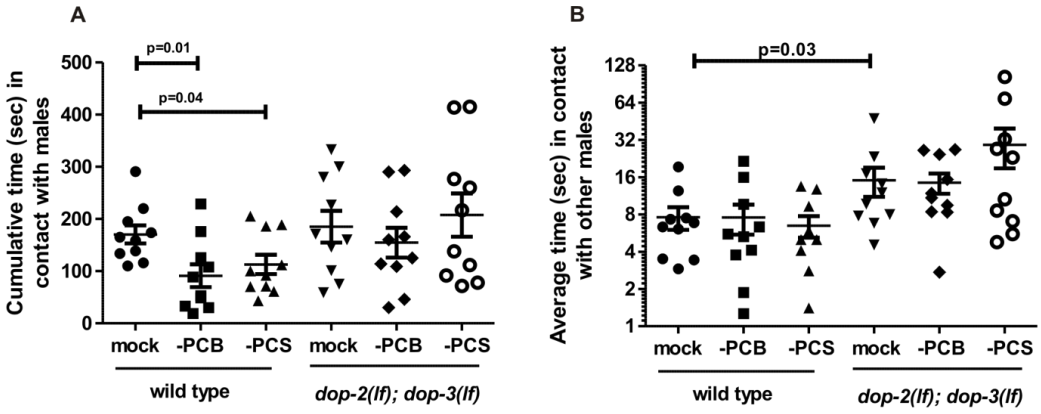

Figure 15. D2-like signaling regulates other circuit's excitability in addition to the PCS. (A&B) The cumulative time in contact with males (A) or the average time in contact with males (B) that a wild type or a *dop-2; dop-3* males spent, represented by each symbol, when surrounded by 40-50 paralyzed males. Each data subset represents non-ablated animals (mock), PCB or PCS ablated animals. *p-values* calculated using the Mann-Whitney test.

Chapter III summary

In chapter III, I have demonstrated that D2-like signaling directs copulatory spicule insertion attempts to the hermaphrodite vulva by dampening sex muscle contractions. The D2-like receptors, DOP-2 and DOP3, are coupled to $G\alpha_{o/i}$ proteins GOA-1 and GPA-7, to antagonize excitability of the spicule circuit. This D2-like signaling cascade down-modulates sex muscle excitability to promote spicule thrust rythmicity during insertion attempts. Moreover, I find that D2-like receptor signaling reduces the duration of mating attempts with unproductive and/or inappropriate mate partners.

CHAPTER IV

RAY NEURONS AND PCS BIDIRECTIONAL INTERACTIONS*

Heighthened DA ray neurons acitivity during arched spicule insertion attempts

In the hermaphrodite, broad D2-like receptor expression indicates that humoral DA secretions might activate these receptors (Sawin et al., 2000; Suo et al., 2003; Chase et al., 2004; Sugiura et al., 2005). The 3 sex-specific sensory dopaminergic ray neurons (left/ right Rn5A, Rn7A and Rn9A) located in the male tail might provide humoral or synaptic DA necessary to antagonize ACh signaling (Koo et al., 2011). These ray neurons synapse to other ray neurons, inter- and motor neurons, post-cloacal sensilla neurons (PCS) and sex muscles (Fig. 5) (Jarrell et al., 2012)

To measure the Ca^{+2} transients in DA ray neurons during mating, I compared the changes in fluorescence emissions of the G-CaMP Ca^{+2} sensor to a mDSred internal standard, both co-expressed from the DA reuptake transporter promoter (P*dat-1).* The G-CaMP transgene slightly reduces the mating potency of the males, but not statistically significant from wild type males (Fig. 6). This indicates that the calcium binding property of the sensor does not interfere too greatly with dopaminergic cell function.

---

* Portions of this chapter reprinted from Paola Correa, Brigitte Leboeuf and L. René García (2012) *C. elegans* dopaminergic D2-like receptors delimit recurrent cholinergic mediated motor programs during a goal-oriented behavior. *Plos Genetics* 8(11): 1-18, Copyright 2012 by PLOS

To distinguish fluorescent changes caused by focusing artifacts when the male is performing scanning behavior, from fluorescent changes caused by neural activity, I imaged males in which Rn5,7,9A were additionally hyper-polarized via a *dat-1* promoter-expressing *unc-103(gf)* transgene. The mutant K+ channel should attenuate the ability of neurons to depolarize, and thus allow one to determine the fluorescence ranges that can confidently be attributed to cell activity. I found that throughout matings of *unc-103(gf)*-containing males, measurements in Rn5,7,9A fluorescence can range between 0 to approximately 20% change (Fig. 16D). These results suggest that focusing/motion artifacts can affect G-CaMP fluorescence measurements within this range.

In contrast, I sometimes observed 30-80% Ca^{+2} transient changes in the DA neurons when the male located the vulva (Fig. 16A). Occasionally, I also noticed up to 30% Ca^{+2} transient changes in DA ray neurons during *arch scanning* postures (Fig. 16C). This observation led us to hypothesize that posture was correlated with DA ray neuron activity. To further correlate neuronal dynamics with copulatory postures, I measured In Contact Length percent (%ICL) between the male's body and the hermaphrodite, as a proxy for the adopted posture (arch vs. non-arch). The %ICL was higher when a male was engaged in non-arched vs. arched postures either during scanning or at the vulva. Lower %ICLs, indicating progressive arched postures, coincided with higher Ca^{+2} transient dynamics in DA ray neurons occurring while the male pressed his tail sternly against the vulva and with milder Ca^{+2} transient dynamics during scanning. However, if the male reached the vulva in a non-arched posture and proceeded to attempt spicule

insertion in this posture the observed Ca^{+2} changes were within baseline levels (10-20%) (Fig. 16B).This suggests that during arched postures, DA ray neurons might be more active to down-modulate possible spicule circuit cholinergic activity.

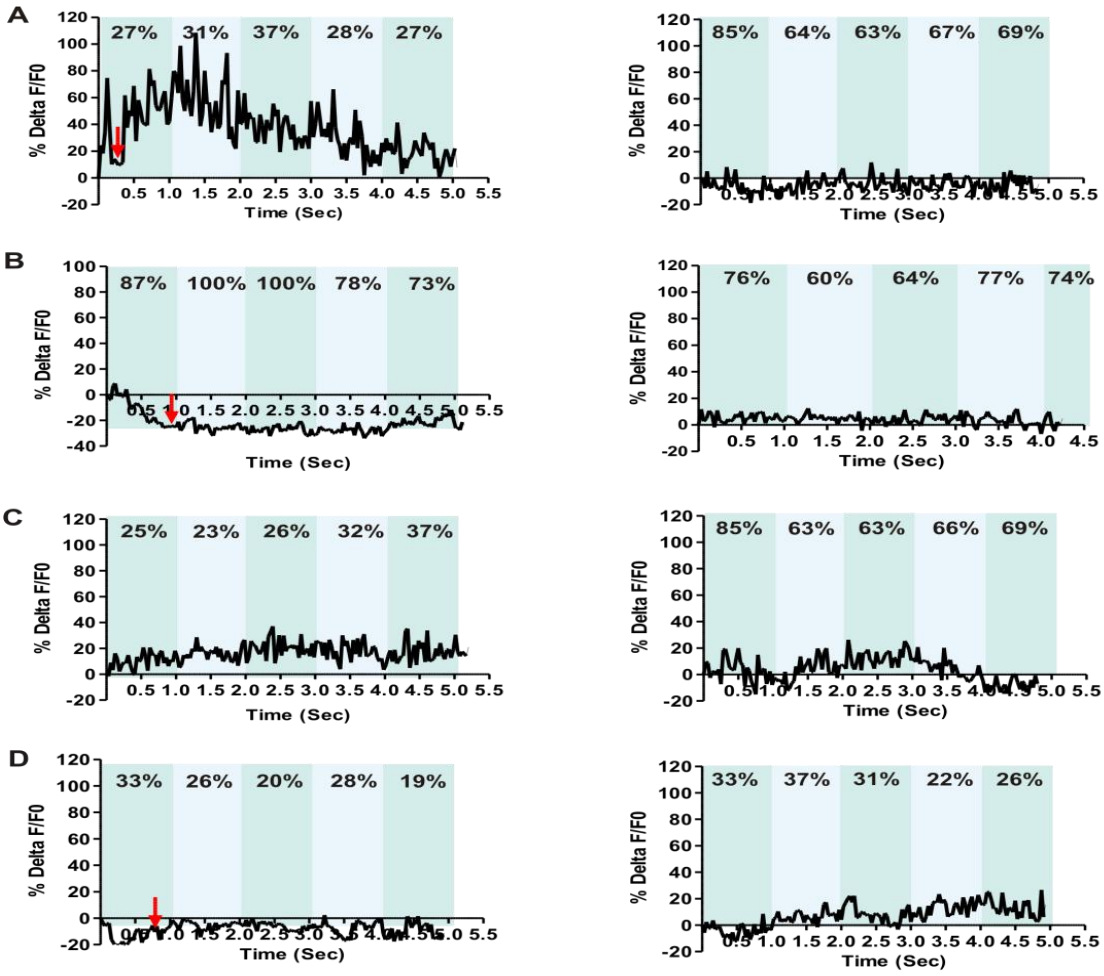

Figure 16. Ca^{+2} transients in DA ray neurons increase during arched postures. % ΔF/F0 trace for 5 seconds. Representative recordings for individual wild type males with (A) an arched posture during spicule insertion attempts (left), (B) with non-arched posture during spicule insertion attempts (left), and (C) arched scanning posture (left). Non-arched scanning recordings for each male are displayed on the right (A-C). A *Pdat-1:unc-103(gf)* transgenic male displaying an arched posture at the vulva (left) and during scanning (right) (D). The In-Contact Length % (ICL%) are the numbers located at the top of each bar taken from a representative frame for each 1sec intervals.

The PCB and sex mucles are active during spciule insertion attempts

To confirm that DA and ACh systems were active simultaneously when the male's cloacal region contacted the vulva, I measured Ca^{+2} transients in the male sex muscles (i.e. the gubernacular erector, the protractor and the anal depressor muscles), and two PCS neurons (PCA and PCB). The contractile activities of these sex muscle cells are responsive to the ACh secretions of the PCB PCC post-cloacal sensory neurons and the SPC motor neuron, and potentially to glutamatergic signals of PCA (LeBoeuf et al., 2014). Thus, I expressed GCaMP from the glutamatergic vesicular transporter (*eat-4),* the DOP-2 receptor (*dop-2)* and the K-channel (*unc-103)* promoters to independently measure Ca^{+2} transients in PCA, PCB and sex-muscles, respectively. I found that PCA and PCB increased their activity when these neurons presumably sensed the vulva (Fig. 17B&C). As a consequence, all of the sex muscles, Ca^{+2} transients also increased when the male tail contacted the vulva (Fig. 17A) (Garcia et al., 2001; Liu et al., 2011). Thus DA ray neurons likely down-modulate the simultaneously active cholinergic and glutamatergic spicule protraction circuit during insertion attempts.

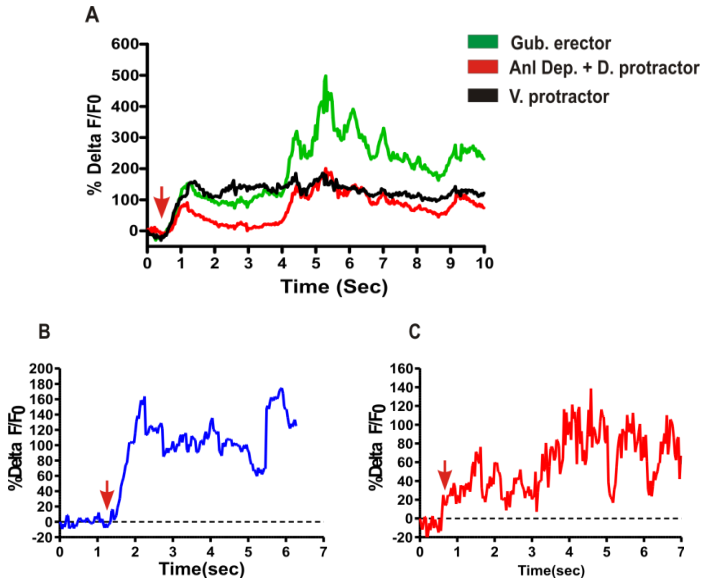

Figure 17. PCS and sex-muscle Ca^{+2} transients during spicule insertion attempts. (A) The Ca^{+2} transients determined by % ΔF/F0 (y-axis) when at the vulva trying to insert their spicules during 10secs (x-axis). For posterior sex-muscles: gubernaculum erector, anal depressor and ventral protractor measured at 20X. (B&C) The Ca^{+2} transients for PCB (B) and PCA (C) measured during attempts of insertion for 7secs at 20X. Red arrow indicates when the male tail is positioned over the vulva.

Cholinergic spicule neuron stimulation causes Ca^{+2} transients in Rn7A

DA sensory ray neuron activity might be increased at the vulva because of direct vulval chemosensory stimulation, mechanical stimulation from pressing against the vulva or from humoral or synaptic stimulation from other cells. Since the increased activities of DA ray neurons and the spicule protraction neurons coincide during the insertion step of mating (Fig. 16), I asked whether ray neuronal activity could change as a direct or indirect response to PCB and SPC stimulation (Fig. 18A). Therefore, I photo-stimulated PCB and SPC using channelrhodopsin-2 (ChR2), a light sensitive cation channel expressed from the *gar-3* mAChR promoter, while simultaneously recording DA ray

neurons G-CaMP fluorescence (Fig. 18B&C). The immobilized males were grown with or without all-*trans* retinol (ATR), a cofactor for ChR2. A microscope fitted with the Mosaic imaging and illumination targeting system localized the blue light to the area of the G-CaMP-expressing ray neurons and then concurrently to the ChR2-expressing PCB, SPC neurons. I noticed that in ATR-grown males, the Ca^{+2} transients in Rn7A exclusively increased after PCB, SPC stimulation (n=14 males) (Fig. 18B&C). However, no obvious dynamic Ca^{+2} changes were observed in Rn5A and Rn9A. Moreover, in males grown in the absence of ATR, there were no Ca^{+2} changes in Rn7A (Fig. 18D). These data suggest that Rn7A can respond, directly or indirectly to spicule circuit activity, whereas Rn5A and Rn9A likely respond to other signals.

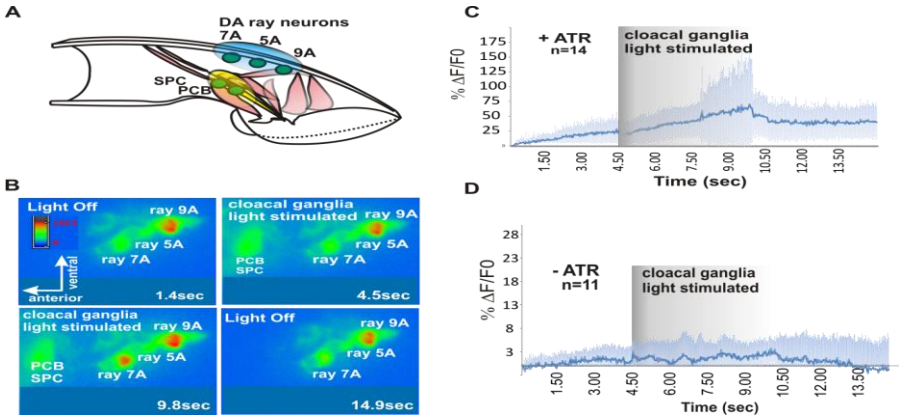

Figure 18. Activation of cloacal neurons increase Ca^{+2} transients in Rn7A. (A) Cartoon depicting the general area of illumination (blue ovals) of DA ray neurons expressing G-CaMP and SPC PCB cloacal ganglia neurons (yellow circles) expressing ChR2. (B) Video montage depicting changes in G-CaMP fluorescence in Rn7A. (C) The average %ΔF/F0 determined from all tested males used in samples with retinol (n=14) or (D) Without retinol (n=11). The C&D traces represent Rn7A neuron Ca^{+2} transients before, during and after PCB, SPC stimulation. The dark and light blue lines represent the average and standard deviation values, respectively.

Although the activity of the dopaminergic ray neurons are more dynamic when the male contacts the vulva, and D2-like receptors are expressed in the PCB neurons and sex-muscles (Fig. 10), these ray neurons might attenuate the excitability of the spicule protraction circuits, not through endogenous dopamine and D2-like receptors, but through circuitous electrical signaling or other secreted neuropeptides. To address this, I photo-stimulated DA neurons by expressing ChR2 from the *Pdat-1* promoter, while simultaneously exposing the males to agar pads soaked with ARE. I have previously noticed that a higher ARE concentration is needed to elicit spicule protraction when males are placed on agar pads. Thus, I determined the drug concentration that would cause ~80% of males to protract their spicules within 5 minutes (Fig. 19A) and concomitantly shined blue light over the DA rays. In a heterozygous *dop-2; dop-3/+; Pdat-1:*ChR2 background, 32% of the males protracted their spicules when photo-stimulated; however, in the homozygous *dop-2;dop-3(lf)* background, 71% of the photo-stimulated males protracted their spicules (Fig. 19B). This suggests that endogenously evoked DA can attenuate ACh signaling in the spicule circuit via D2-like receptors.

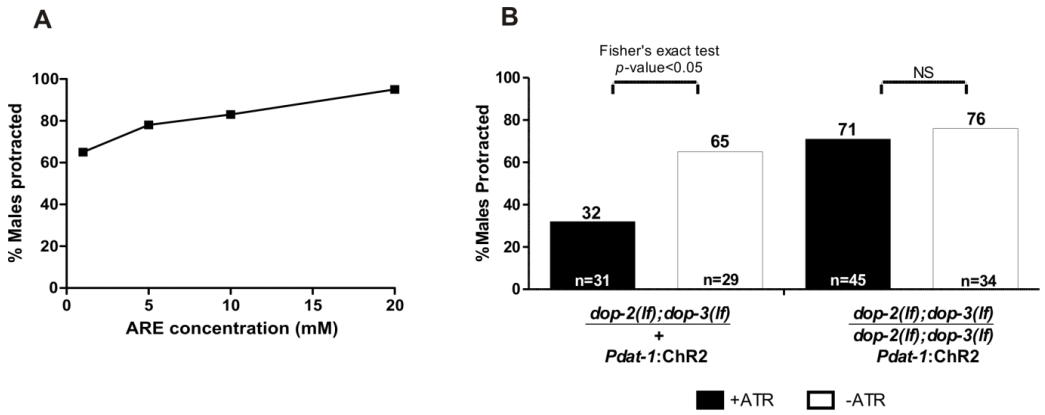

Figure 19. Activation of DA ray neurons attenuate ARE-induced muscle contraction via D2-like receptors. (A) Dose response curve for spicule protraction in 2% agarose ARE pads. Each data point represents the response of 20-30 males per concentration. (B) Males that protracted their spicules during simultaneous blue light stimulation of DA neurons and ARE exposure on pads. The genotypes are written below each bar. The number of males tested and the percentage of spicule protracted males are listed at the bottom and top of the bars, respectively. +/-ATR indicates groups of males grown with or without retinol.

D2-like signaling reduces calcium transients in PCB during PCA stimulation

Spicule insertion into a hermaphrodite is a task that requires a balance between sustaining and exiting repetitive intromission attempts. Upon sensing the vulva, each post cloacal sensilla (PCS) neuron, PCA, PCB and PCC, promotes spicule thrusts by inducing posterior sex-muscle contractions. Reciprocal synapses between the PCS neurons suggest that stimulation of one cell could further trigger activity in the others to amplify the circuitry's response to vulva cues (Fig. 5). However, after several minutes of un-successful penetration, this behavioral loop might become futile and further amplification should be dampened. Experimental observations suggest that this potential dampening could coincide with increased DA ray neuronal activity (Fig. 16), which is

then followed by the male terminating spicule insertion attempts and moving off the vulva. In the previous chapter I had shown that during vulva withdrawal, post-synaptic D2-like signaling dampens sex-muscles excitability to diminish unproductive spicule thrusts; however, how DA also down-modulates reciprocal signaling between the PCS neurons was not examined in detail.

Three possible mechanisms could regulate the PCS excitability that coordinates spicule thrusting with vulva cues: (1) a self-amplifying interaction established through the reciprocal excitation between the PCS neurons; (2) a directed or reciprocal down-regulating interaction between the cells; or (3) a combination of the above two hypotheses (Jarrell et al., 2012). In other words, the system might be recurrent, where the activity of one sensilla stimulates the other, but requiring extrinsic modulatory regulation; or either sensilla may be capable of directly down-modulating the other's activity, indicating that communication between them is sufficient for delimiting intromission attempts.

To distinguish between these possibilities, I assessed how single cell stimulation affects its reciprocal partner's activity. In one cell (either PCA or PCB), I stimulated the light-activated channelrhodopsin-2 (ChR2) with blue light (Nagel et al., 2005). At the same time, I measured cellular activity in the other neuron by imaging fluorescent changes of the calcium sensor GCaMP6 (Chen et al., 2013). To temporally and spatially confine the epi-fluorescent light to distinct neurons in the field of view, the male was immobilized on a microscope fitted with the Mosaic Target Illumination and Imaging System

(Andor). This illumination system targets light to one or many user-defined regions-of-interests as described previously. I expressed GCaMP or ChR2 in PCA using the glutamatergic re-uptake transporter P*eat-4* and in PCB using the synaptic vesicle acetylcholine transporter P*unc-17*. If the circuit is self-amplifying, I expected to see an increase in calcium transients in one neuron, upon stimulation of the other. However, if the stimulatory signal is unidirectional or the cells negatively regulate each other, I did not expect to see cross stimulation. I found that when I photo-stimulated PCB, PCA showed increased calcium transients (Fig. 20A). However, when PCA was stimulated, PCB did not change its activity (Fig. 20B). These results suggest PCB can stimulate PCA, but PCB's response to PCA might be non-existent, inhibitory or negatively modulated by external factors.

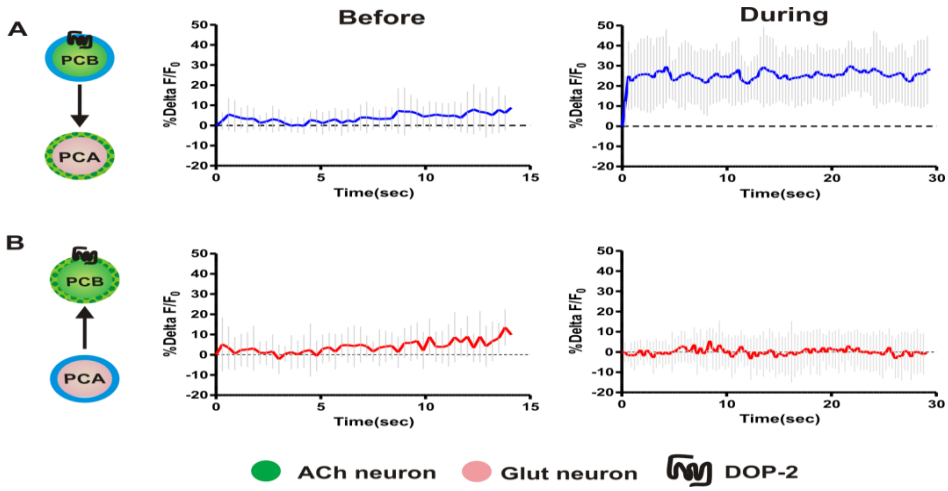

Figure 20. PCB photo-stimulation induces PCA activity but not vice versa. (A&B) PCA and PCB targeted illumination diagram. The directionality tested is described by the arrowhead. The green dotted and the blue outlines indicate selective GCaMP6 and ChR2 expression (left panels). The average %ΔF/F calcium transients determined from all tested males before (middle panel) and during photo-stimulation of the respective cell (right panel). The light gray lines represent the STDEV. (A) PCB to PCA stimulation (n=8). (B) PCA to PCB stimulation (n=10).

Since PCB expresses DOP-2 (Correa et al., 2012), I asked if DA externally down-modulates PCB activity, thus preventing the neuron from responding to PCA. Therefore, to relieve the potential DA regulation from PCB, I conducted the targeted illumination experiment with DA signaling and DOP-2-deficient males. To conduct the experiment on DA defective males I expressed the *unc-103(gf)* driven from the *dat-1* promoter, which I previously shown to behave similarly to a *cat-2(lf)* animals (Fig. 6), and to perturb D2-like signaling I used *dop-2(lf)* animals. I found that for DA-deficient and *dop-2(lf)* males, PCA stimulation resulted in increased PCB calcium transients (Fig. 20A&B). To test whether the increased PCB excitability in *dop-2* males could further potentiate the ChR2 artificial depolarization of this cell, I activated PCB in the *dop-2(lf)* background and measured PCA transients. I found that PCA transients in *dop-2(lf)* and wild type animals are similar (Fig. 20A and Fig. 21C), suggesting that cellular ChR2-activation cannot be bypassed by neuromodulatory perturbations. Taken together, these results suggest that PCA and PCB reciprocally stimulate each other; however under certain conditions (such as in the immobilized males), a D2-like pathway dampens communication in the PCA to PCB direction.

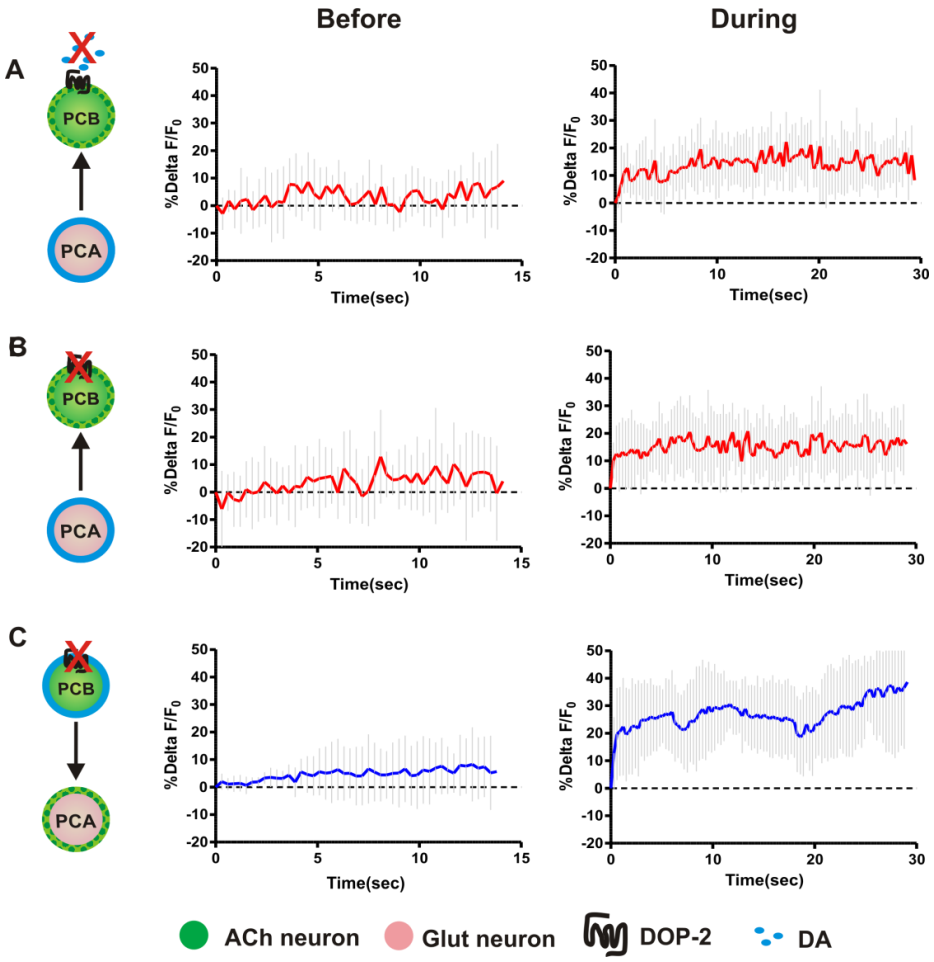

Figure 21. D2-like signaling regulates recurrency in the PCA to PCB direction. (A-C) PCA and PCB targeted illumination diagram. The directionality tested is described by the arrowhead. The green dotted and the blue outlines indicate selective GCaMP6 and ChR2 expression (left panels). The average %ΔF/F calcium transients determined from all tested males before (middle panel) and during photo-stimulation of the respective cell (right panel). The light gray lines represent the STDEV. (A) PCA to PCB stimulation in DA deficient males (n=10). (B) PCA to PCB stimulation *dop-2(lf)* males (n=10). (C) PCA to PCB stimulation in *dop-2 (lf)* males (n=8).

Chapter IV summary

In chapter IV I have demonstrated that DA signaling from ray neurons regulates the recurency amongst the post-cloaca sensilla. Through *in* copula calcium imaging I have shown that the DA ray neurons are active when males adopt arch postures during

mating. This heightened ray neuron activity occurs when arched males scan for the vulva, and majorly during arch spicule insertion attempts. I also recorded increased calcium dynamics of PCA and PCB when the male places his tail over the vulva, suggesting that the PCS is concomitantly active with DA ray neurons. Moreover, the target illumination experiment suggested that one of the DA mechanosensory rays, Rn7A, is responsive to cholinergic and/or glutamatergic signals from PCS. Therefore, the result of Rn7A activation might lead to DOP-2 stimulation in PCB. This neuronal D2-like signaling mechanism dampens the reciprocal stimulation in the PCA to PCB direction to regulate PCS excitability.

CHAPTER V

DOP-2 ATTENUATES PCS RECURRENCY VIA UNC-7*

The gap-junction UNC-7 is an effector of D2-like signaling

I next asked how the directional modulation of PCA-PCB communication is regulated by DA and DOP-2. To further identify molecular mechanisms involved in this process, I took a forward genetic approach combined with pharmacological analysis to identify molecules that are downstream of, or parallel to D2-like signaling. In brief, a mutation in *lev-11* suppresses the constitutively protracted spicules (Prc) phenotype of the *unc-103(sy557)* allele (Gruninger et al., 2008). The *unc-103; lev-11* strain was used for the EMS mutagenesis to identify mutations that restored the Prc phenotype. The pseudo-revertants were then pharmacologically tested to find lines that had increased spicule protraction when exposed to DA+ARE. I identified the *rg396* mutant strain, where a significantly higher number of males protracted their spicules in the drug bath (67% vs. 11%, *rg396 vs* controls, *p-value*<0.0001, Fig. 22A). The *rg396* strain was then outcrossed five times to repulse *unc-103* and *lev-11*. Through whole genome sequencing and classical genetic mapping, I identified the *rg396* allele as a missense mutation (A59T) located in the first exon of the gap-junction gene, *unc-7* (Fig. 22B).

---

* Portions of this chapter reprinted from Paola Correa, Todd Gruninger and L. René García (2015) DOP-2 D2-Like Receptor Regulates UNC-7 Innexins to Attenuate Recurrent Sensory Motor Neurons during *C. elegans* Copulation. *Journal of Neuroscinece* 35(27): 9990-1004 Copyright 2015 by Society for Neuroscience

The *unc-7* gene encodes two types of proteins, UNC-7 long (L) and UNC-7 short (S) isoforms. The *rg396* mutation affects the UNC-7(L) isoform, but not UNC-7(S). Both isoforms can form a heteromeric gap-junction with the UNC-9 sub-unit to electrically couple interneurons, motor neurons and muscles of several *C. elegans* sensory-motor circuits. In the locomotor circuit, these gap-junctions mediate sinusoidal movement and preferential forward locomotion (Starich et al., 1993; Starich et al., 2009; Kawano et al., 2011).

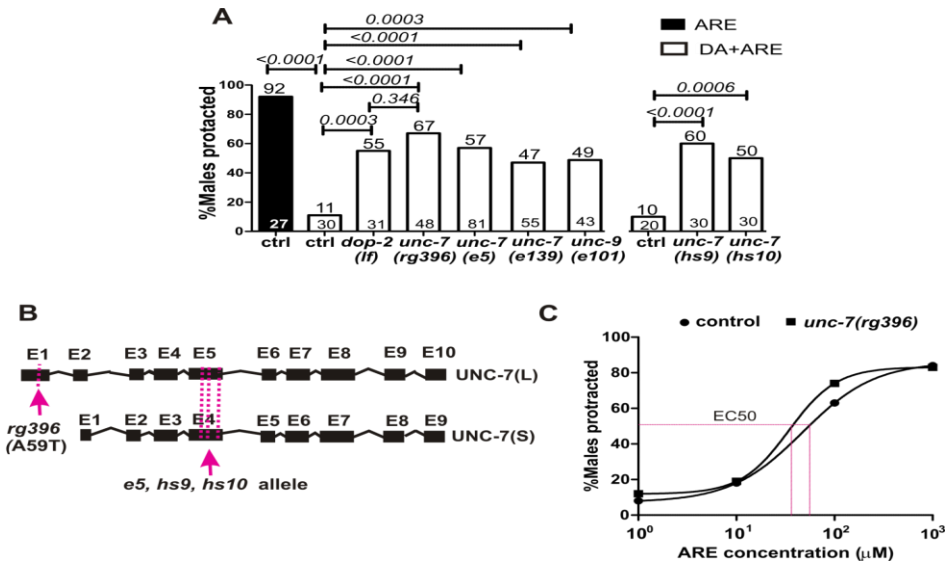

<u>Figure 22.</u> A point mutation in UNC-7 perturbs DA inhibition of ARE-induced protraction. (A) Percentage of male protraction in 20 mM DA+1 mM ARE for control and mutant males. The exact *p*-values were calculated using Fisher's exact T-test and are indicated above the black connector lines. (B) Diagram of the UNC-7 isoforms. Black boxes and lines depict predicted exons and introns in *unc-7*. Magenta arrows and dotted lines indicate the location of *unc-7* mutations. (C) Dose-response curve of ARE-induced protraction for control and *unc-7(rg396)* males. Each data point represents 20 or more males tested for the indicated concentration. The calculated EC50 is 47.4 µM and 34.2 µM for wild type and *unc-7(rg396)*, respectively.

Loss-of-function mutations in gap-junctions, such as UNC-7 and UNC-9, can affect chemical neurotransmission properties in *C.elegans* and vertebrate models (Yeh et al., 2009; Wang and Belousov, 2011). Thus, perturbing UNC-7(L) function with the A59T mutation could directly alter responses related to ACh, instead of DA signaling. To address this issue, I calculated the effective concentration at which 50% of males protract their spicules (EC50) in ARE; however, there was not a significant difference in the EC50 among *unc-7(rg396)* and control males (47.4µM and 34.2 µM, mutant versus control males, Fig. 22C). Therefore, the increased response of *unc-7(rg396)* males to ARE in the DA+ARE drug bath suggests that UNC-7 mediates DA modulation.

To ascertain if cryptic linked EMS-induced mutations in the *unc-7(rg396)* strain contribute to the DA-resistant phenotype, I tested whether other *unc-7* loss-of-function alleles also result in similar DA-signaling deficiency. These *unc-7* alleles were originally isolated due to their uncoordinated-distorted 'kinker'-like locomotion and resistance to volatile anesthetics (Brenner, 1974; Starich et al., 1993; Hecht et al., 1996; Barnes and Hekimi, 1997). I surveyed the *e5, e139, hs9* and *hs10* alleles and found that similar to *unc-7(rg396)* mutants, these mutations rendered males resistant to DA-inhibition of ARE-induced protraction (Fig. 22A), suggesting that UNC-7 gap-junctions can mediate DA-signaling. Since UNC-9 is expressed in spicule circuit neurons and muscles (Liu et al., 2011), and makes heterologous gap-junctions with UNC-7 in the locomotor circuit (Starich et al., 2009; Kawano et al., 2011) , I hypothesized that *unc-9(lf)* males might also be DA+ARE insensitive. Consistent with this idea, I found that the *unc-9(lf)* males have higher spicule protraction in this drug bath (Fig. 22A). Additionally, all *unc-7 (lf),*

unc-9(lf) and *unc-7(rg396)* mutant males displayed constitutively-protracted spicules, suggestive of heightened spicule circuit excitability in these backgrounds (Fig. 23A). Unlike the severe uncoordinated phenotype typical of *unc-7(lf)* and *unc-9(lf)* animals, the *unc-7(rg396)* males do not have gross posture or locomotion defects (Fig. 23B). However when I quantified the incidence of backward crawling in *rg396* hermaphrodites, I noticed that these animals subtly reverse more often than wild type during a 60 sec observation (22% more often versus 7%; *rg396* versus wild type, *p*-value=0.006, Fig. 23C). Taken together these results suggest that the *rg396* allele affects the mating circuit's excitability more than other circuits in the worm.

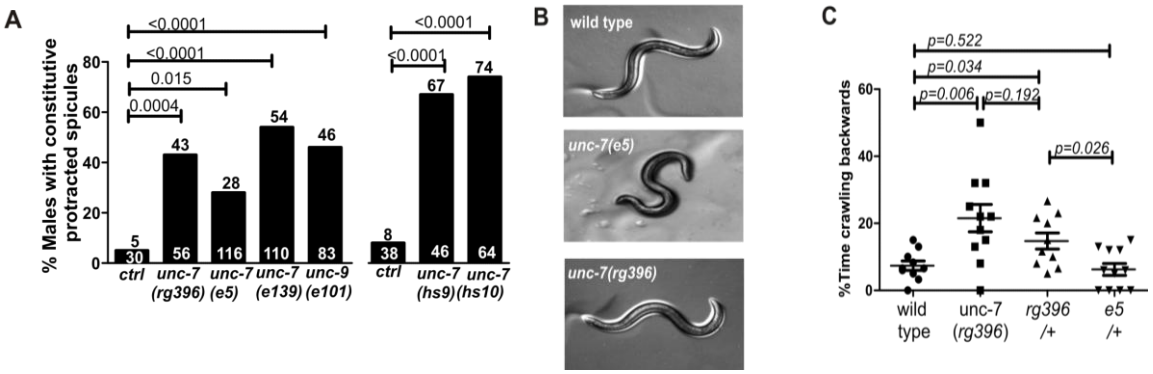

Figure 23. UNC-7 gap-junctions regulate spicule circuit excitability and locomotion directionality. (A) Percentage of males with constitutive protracted spicules for control, *unc-7* and *unc-9* mutants. Top and bottom numbers represent the percentage and number of animals tested, respectively. *p*- values indicated on the brackets according to Fisher's exact T-test (B) Images depicting representative postures of wild type (top), *unc-7(rg396)* (middle) and *unc-7(e5)* (bottom) males. (C) The percentage of time spent crawling backwards within 60sec. *p*- values indicated on the brackets according to non-parametric Mann-Whitney test.

Next I attempted to mitigate the defective drug responses in the *unc-7(rg396)* and a loss-of- function *unc-7* allele by over-expressing wild-type UNC-7. I chose to examine the

unc-7(e5) allele because the premature stop codon of this background results in an *unc-7* null (Starich et al., 1993; Starich et al., 2009). Surprisingly, I found that *unc-7(rg396)* males carrying the *unc-7*(+) transgene had similar DA+ARE sensitivity as the control strain (65% vs. 70%, respectively, Table 4); however transgenic expression restored the *unc-7(e5)* lesion drug response to wild type levels (57% vs. 18%, *p-value*<0.005, Table 4). These observations suggested that the *rg396* allele might be a dominant negative mutation. Since the *unc-7* locus is on chromosome X, and males only have one copy of this chromosome, I could not genetically test for *rg396* dominance in males. Therefore, I tested whether a single copy of this allele was sufficient to induce a locomotor deficit in the hermaphrodite, similar to the *rg396* homozygous animals. I found that heterozygous hermaphrodites had a higher incidence of crawling backwards, like the *rg396* homozygote (22% versus 15%; *rg396* versus *rg396/+*, n=11 and 10 respectively, *p*-value=0.192, Mann-Whitney non-parametric test). Due to *e5/+* animals having no locomotion deficits (6% versus 7%; *e5/+* versus wild type, n=10 and 11 respectively, *p*-value=0.522, Mann-Whitney non-parametric test), I ruled out the possibility of haploid insufficiency in the *rg396/+* background. Moreover, to confirm the *rg396* allele acts as a dominant negative in the mating circuit, I expressed the UNC-7(L)(A59T) version in wild type and found that the transgenic mutant protein expressed from its promoter induced the *rg396* phenotype and rendered males insensitive to DA inhibition (Table 4). Taken together, these results suggest that UNC-7 couples an electrical signal in the spicule circuit, and that this is potentially regulated by an upstream D2-like pathway.

Table 4. D2-like signaling inhibits ARE induced protraction via UNC-7

Genotype	DA+ARE (%Males protracted)	P-value	Compared to
control	11 (30)		
unc-7 (rg396)	65 (48)	1	*dop-2; rg396*
dop-2 (lf)	55 (31)	0.632	*dop-2; rg396*
unc-7 (rg396); dop-2	63 (43)	1, 0.632	*dop-2* OR *rg396*
unc-7 (rg396); pha-1	65(85)	1	*unc-7(rg396)*
*unc-7 (rg396);pha-1; rgEx*644 (UNC7:YFP)	70(44)	0.657	*unc7(rg396); pha-1*
unc-7(e5);pha-1	57 (81)	0.459	*unc-7(rg396)*
*unc-7(e5);pha-1;rgEx*653 (UNC7:YFP; SL2::GFP)	18 (61)	0.007	*unc-7; pha-1*
*pha-1;rgEx*653 (UNC7:YFP; SL2::GFP)	22 (91)		
*pha-1; rgEx*668 (UNC7:YFP)*	40 (59)	0.017	*pha-1;rgEx*653

*UNC7 genomic with A59T mutation

In vertebrate sensory circuits, D1- and D2-like signaling modulates gap-junction activity (Pereda et al., 1992; Kothmann et al., 2009; Kirkby and Feller, 2013); however there have been no reported genetic studies that elaborate on these interactions. Since *dop-2(lf)* and *unc-7(rg396)* males have similar drug sensitivities (Fig. 22A and Table4), these two molecules might regulate common aspects of mating circuit excitability, and thus are in the same pathway. To genetically test this hypothesis, I generated a *dop-2(lf); unc-7(rg396)* double mutant and tested whether it and *unc-7*, and *dop-2* single mutants have similar drug responses. I found that there was no change in the response to DA+ARE between the double and single mutant males (Table4), consistent with DOP-2 and UNC-7 affecting the same pathway. Furthermore, these observations suggest that DA-mediated gap-junction regulation is conserved between vertebrate and invertebrate sensory-motor circuits.

UNC-7 regulates rhythmic spicule thrusts at the vulva slit and diminishes spicule intromission attempts at non-vulva areas

In contrast to the pleotropic defects caused by the *unc-7* null allele, the restricted *unc-7(rg396)* phenotype allowed us to address how the mutant allele disrupts mating behavior. When mated to moving hermaphrodites, *unc-7(rg396*) males had a lower ability to sire cross progeny than wild type (96% *vs.* 68%, *p-value*=0.0023, Fig. 24A). To determine how *unc-7(rg396*) might disrupt mating, I digitally recorded one-day old virgin *unc-7(rg396)* and wild-type males copulating with a non-moving hermaphrodite for 120 secs or until spicule insertion. From these recordings, I measured the number and duration of male tail contacts with the vulva. Similar to the reported DA-deficient male

phenotypes (Correa et al., 2012), I found that *unc-7(rg396)* males spent on average less time in contact with the vulva than in contact with other parts of the hermaphrodite (75% *vs* 56%, *p-value*=0.03, Fig. 24B). From the recordings, I suspected that the mutants hesitate at non-vulva cuticle regions engaging in non-productive spicule insertion attempts. To quantify non-vulva spicule prodding events, I calculated a vulva index of prodding (VIP) during a 60 sec period of male tail contact with the vulva area. A VIP score of +1 indicates exclusive spicule thrusts at the vulva slit and a score of -1 indicates prodding at areas adjacent to the vulval slit. I found that *unc-7(rg396)* males had slightly lower VIP scores than wild type (0.66 *vs.* 0.88 respectively, *p-value=0.052,* Mann-Whitney non-parametric test, Fig.24C); however this difference was not significant. Nonetheless, these differences were exacerbated in UNC-7(A59T) transgenic males, where expression of the mutant molecule was restrictively driven from the *dop-2* promoter (0.35 *vs.* 0.89 respectively, *p-value=0.04,* Mann-Whitney non-parametric test, Fig.24D). These results indicate that normally wild-type UNC-7 acts to diminish PCS activity when the males are not at the vulval slit.

I additionally reported that during prodding behavior, D2-like signaling is necessary to maintain rhythmic spicule thrusts over the vulva slit. Males lacking the *dop-2* and *dop-3* D2-like receptors displayed erratic spicule prodding behavior when they attempted to breach the vulva; premature sustained thrusts were interspersed with shallow rapid spicule prods. To assess whether *unc-7(rg396)* also disrupted spicule rhythms, I recorded spicule motion during intromission behavior and measured pixel fluxes of the recordings at the area of contact between the spicule tips and the vulva slit (Correa et al., 2012). The

pixel fluxes are a proxy for the motor output magnitude; greater values indicate more exaggerated motion. As expected, I found the rhythmic spicule movements of *unc-7(rg396*) males were more vigorous (Fig.24E) and more erratic than wild type (Fig.24F). These results suggest that the male uses UNC-7, similar to D2-like receptors, for regulating the timing, rhythm and intensity of spicule insertion behavior at the vulva.

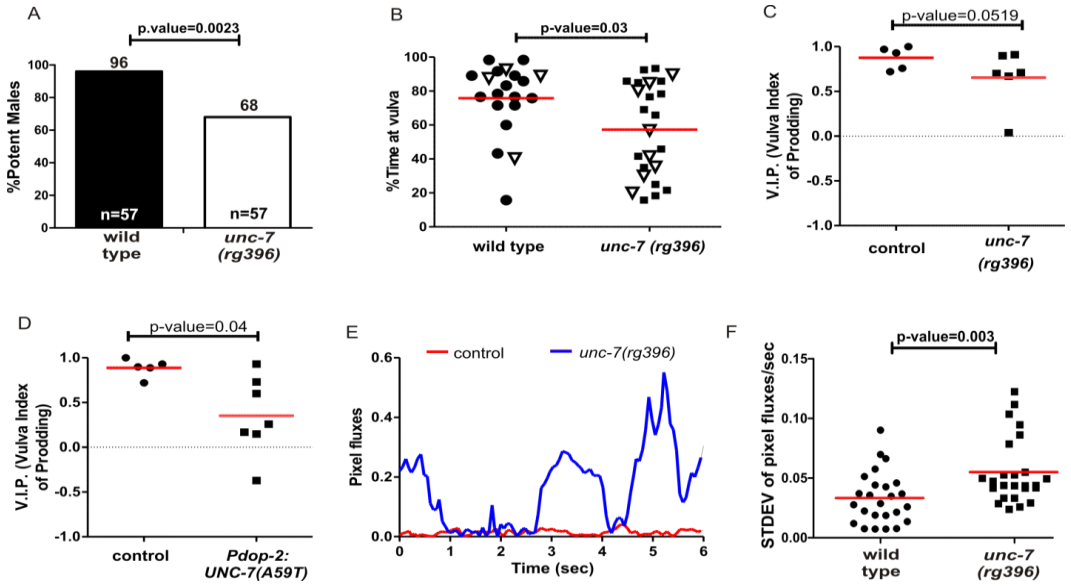

<u>Figure 24.</u> UNC-7 diminishes the magnitude of spicule insertion attempts at the vulva and restricts intromission attempts at non-vulva regions. Mating observations between wild type and *unc-7(rg396)*. (A) Mating potency for wild type and *unc-7(rg396)* with moving hermaphrodites. Numbers on top and bottom of the bars indicate percentages and number of males tested. The *P-value* was calculated using Fisher's exact T-test. (B) The percentage of time that males spent in contact with the vulva out of 120 secs. Each symbol represents an individual's male performance. Open symbols indicate a completed spicule protraction. (C & D) Vulva index of prodding (VIP) during a 60 sec of mating with non-moving hermaphrodites. (C) Comparison of wild type and *unc-7(rg396)* mutants. (D) Comparison of control and *Pdop-2*:UNC-7(L) (A59T) over-expression. (E) Representative trace of pixel fluxes during spicule insertion attempts of a wild type (red trace) and mutant male (blue trace) for 6 seconds. (F) Average standard deviation (STDEV) of pixel fluxes per second for 5 males per group. For each male, their prodding duration was broken down to five periods. Each point represents the standard deviation of pixel fluxes in a one second period. The red line represents the average value for each group. The *p-value* was calculated using the Mann-Whitney non-parametric test.

UNC-7 functions in DOP-2 expressing cells that control spicule behavior

I previously reported male specific DOP-2 expression in sex muscles and in the cholinergic neuron PCB (Fig. 10); however there are no reports of UNC-7 expression in the male tail. In the hermaphrodite, UNC-7(L) and (S) isoforms (Fig. 25) are broadly expressed in all pre-motor and motor neurons (Altun et al., 2009; Starich et al., 2009; Yeh et al., 2009; Kawano et al., 2011). Additionally, posterior body wall muscles showed UNC-7 fluorescent immunolabeling (Yeh et al., 2009; Kawano et al., 2011). To determine which tissues UNC-7 and DOP-2 overlap, I assessed the reported UNC-7(L) and (S) expression pattern in the male. The UNC-7(L) and (S) reporter constructs include ~1kb and 3.3kb upstream sequences from their respective first introns fused to YFP (Altun et al., 2009). I found no and/or very dim expression in male-specific tissues with these reporters. I reasoned that the arbitrarily chosen upstream sequences of the UNC-7 isoforms represented limited promoter regions, and therefore I constructed more comprehensive reporters. When I increased the promoter region of UNC-7(L) up to 5kb, I found expression in sex-muscles (anal depressor, gubernacular erector, gubernacular retractor and anterior oblique) (Fig. 25A). Since *unc-7* has large introns (intron 2 and 5, Fig. 22) I reasoned that there might also be enhancer elements in these regions; in addition to more upstream promoter sections. Therefore, I further extended the UNC-7(L) promoter to ~8 kb upstream of the first exon, and included the entire *unc-7* genomic region fused to YFP. In these transgenic males, I found UNC-7 expression, in addition to the mentioned sex muscles, in several mating circuit neurons (SPC, PCA, PCB, HOA, and unidentified ray neurons) (Fig. 25B-D). Similar to previous studies (Starich et al.,

2009; Yeh et al., 2009; Kawano et al., 2011), this reporter also expresses in head ganglion neurons, several ventral chord neurons, and tail neurons of the hermaphrodite; in addition to few unreported pharyngeal neurons (I5, M2,I4,M3 and I1). Therefore, this broad expression pattern indicates that UNC-7 could electrically couple sex-specific muscles and/or neurons to modulate circuitry output.

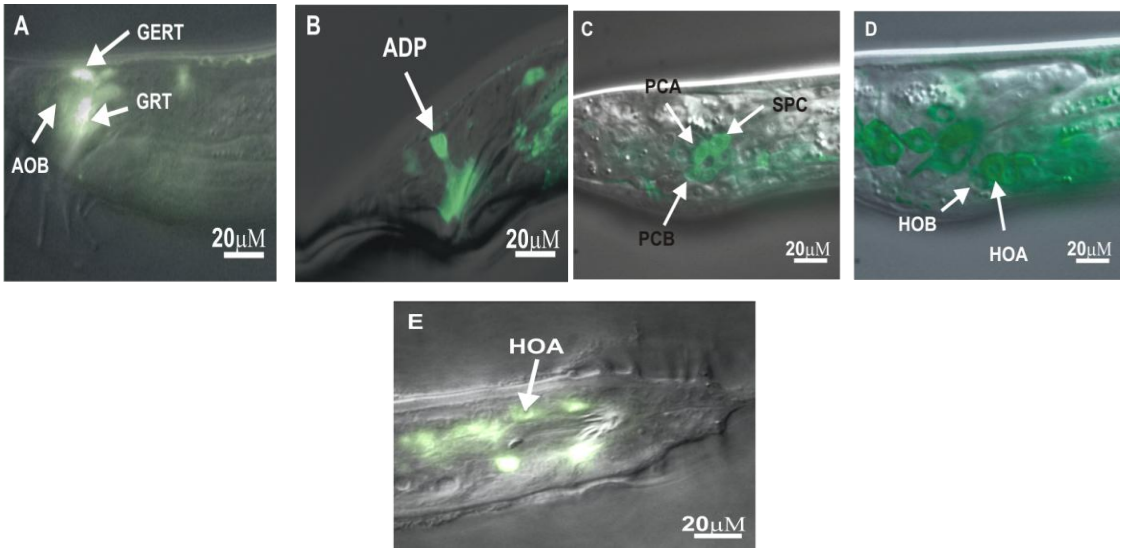

Figure 25. UNC-7 and DOP-2 expression in male-specific sensory motor neurons and copulation muscles. (A-E) Merged DIC images with YFP and/or GFP fluorescence images (A & B) Adult sex-muscle *Punc-7:YFP* expression. Gubernacular erector (GER), gubernacular retractor (GRT), anterior oblique (AOB) and anal depressor (ADP). (C&D) *Punc-7:unc-7::YFP* expression. (C) Expression in the post cloacal sensilla neurons (PCA and PCB), and SPC sensory motor neuron. (D) HOA and HOB expression in the L4 male tail. (E) *Pdop-2:GFP* expression in HOA neuron at the adult male tail.

To assess UNC-7's role in mediating DA signaling within the spicule protraction circuit, I asked where *unc-7* functions in the DA inhibition of ARE-induced responses. Since the *unc-7(rg396)* lesion is dominant, I could not use the wild-type UNC-7 transgenic. Instead, I expressed the mutant UNC-7(A59T) transgene in different cells of wild-type males, and measured the altered drug resistance. I found that UNC-7(L)(A59T)

expression from a pan-neuronal promoter (*Paex-3)* (Iwasaki et al., 1997) caused an increase in spicule protraction when males were exposed to DA+ARE (44% *vs.* 22%, transgenic males *vs.* control strain, respectively, p- value<0.005) (Table 5). In contrast, UNC-7(L)(A59T) expression from a pan-muscular promoter and sex-muscle specific promoter (*Plev-11* and *Punc-103E*, respectively) (Kagawa et al., 1995; Reiner et al., 2006a) were unable to mimic the *rg396* phenotype (17% and 28%, respectively, vs. 22% for the control strain) (Table 5). These observations indicate that expressing UNC-7(L)(A59T) in neurons mimic the *unc-7(rg396)* lesion, thus demonstrating that UNC-7 might couple neuronal activity in the mating circuit.

Table5. Tissue specific phenocopy of UNC-7(A59T)

Genotype	**DA+ARE %SpOUT(n)**	**P-value**	**Compared to**
*pha-1;rgEx*653 (UNC7:YFP; SL2::GFP)	22 (91)		
*pha-1; rgEx*668 (UNC7:YFP)*	40 (59)	0.017	*pha-1;rgEx*653
*pha-1; rgEx*672 (*Plev11:*UNC7:YFP)**	17 (69)	0.552	*pha-1;rgEx*653
*pha-1; rgEx*673 (*Paex-3:*UNC7:YFP)**	44 (81)	0.002	*pha-1;rgEx*653
*pha-1; rgEx*671 (*Punc-103E:*UNC7:YFP)**	28 (68)	0.457	*pha-1;rgEx*653
*pha-1; rgEx*674 (*Pdop-2:*UNC7:YFP)**	44(62)	0.0071	*pha-1;rgEx*653

*UNC7 genomic with A59T mutation **UNC7 (A59T) minigene

Next I asked if UNC-7 couples the electrical activity in a neuronal sub-set. Since my behavioral experiments indicate that disrupting UNC-7 in DOP-2-expressing cells induces ectopic spicule insertion attempts, I asked if UNC-7 is required directly to mediate DOP-2 inhibitory signaling in those cells. Indeed, I found that the *Pdop-2:unc-7(A59T)* transgenic males had increased number of protracted spicules in DA+ARE (44% *vs.* 22% respectively, p-value<0.05, Table 5). Thus, normal UNC-7(L) activity in DOP-2-expressing neurons is required for the DA+ARE wild-type response. I have already shown through photo-stimulation experiments that DOP-2 dampens PCB activity (Fig19), raising the question of who is PCB's gap-junction partner.

The male tail connectome indicates that HOA is a potential PCB electrical partner (Fig 3) (Jarrell et al., 2012). Previous behavioral observations indicate that the sensory hook neurons HOA and HOB not only detect the general vulva region, but also regulate rhythmic spicule thrusts. When the hook neurons are laser-ablated, the male will not only pass over the vulva many times, but will also spontaneously prod random areas of the hermaphrodite with their spicules. This phenomenon requires the PCS neurons and has been hypothesized as an adapted response of the HOA/HOB-ablated male to use its spicules for locating the vulva orifice (Liu and Sternberg, 1995; Barr and Sternberg, 1999). Since this observation suggests that the hook neurons might negatively regulate the activity of the PCS, I re-examined DOP-2 expression in the male tail and also identified it in HOA (Fig. 25). Therefore, I further examined if DOP-2 might modulate PCS activity through UNC-7 gap-junctions between PCB and HOA.

UNC-7 and HOA can inhibit PCA to PCB stimulation

Similar to how DOP-2 was determined to down-modulate PCA and PCB recurrency (Fig. 21C), I used ChR2, GCaMP6 and the Mosaic targeted illumination system to dissect how coupling between HOA and PCB affects PCS excitability. I stimulated ChR2 in PCA and measured calcium transients in PCB for intact and HOA laser-ablated males before and during blue-light PCA stimulation. As predicted, only when HOA was ablated, the PCB calcium transients increased (Fig. 26 A&B). Next, I photo-stimulated ChR2 in PCA, while simultaneously measured GCaMP6-fluorescent changes in PCB before and during PCA blue light stimulation in *unc-7(rg396)* males. Similar to the HOA-ablated male, I found that the calcium transients in PCB also increased when UNC-7 function is compromised (Fig. 26A&C). These results are consistent with the idea that HOA diminishes PCB activity through UNC-7 gap-junctions during PCS stimulation.

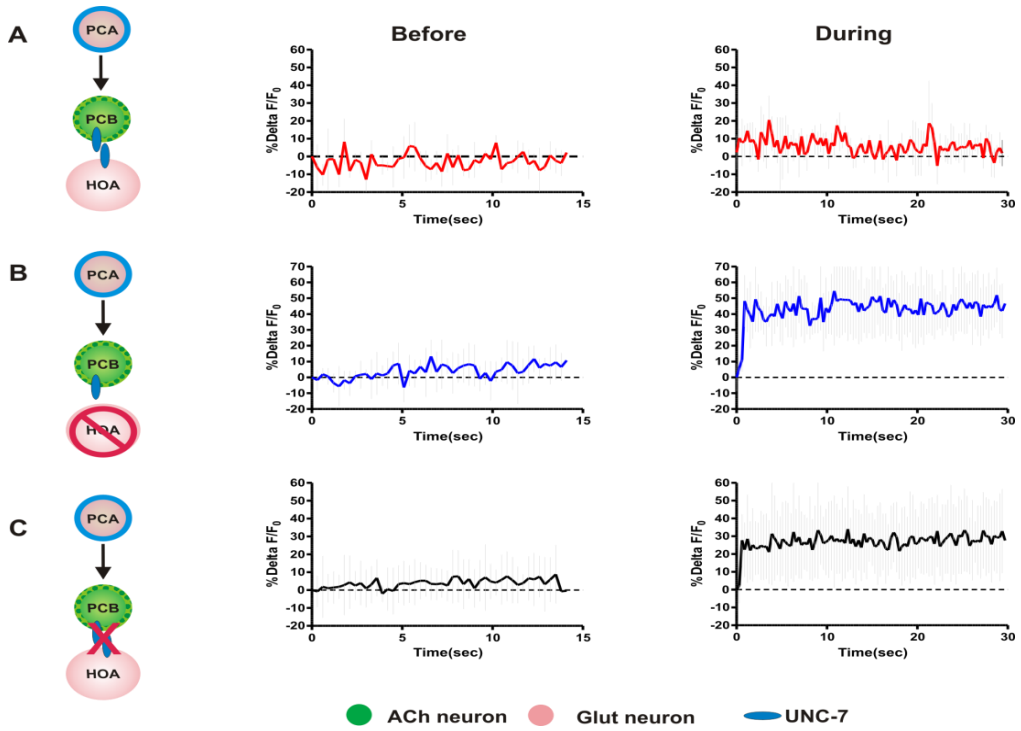

Figure 26. HOA-dependent regulation of PCS recurrency. ***A–C***, PCA to PCB targeted illumination diagrams. The directionality tested is described by the arrowhead. Green dotted and the blue outlines indicate selective GCaMP6 and ChR2 expression (left panels). The average %_F/F calcium transients determined from all tested males before (middle panels) and during PCA photostimulation(right panels). Light gray lines indicate the SD for (***A***) mock-ablated males (*n*_3), (***B***) HOA-ablated males (*n*_5), and (***C***) *unc-7(rg396*) males (*n=10)*

HOA requires AVR-14 and UNC-7 to relay hyperpolarizing signals

My findings suggest that HOA diminishes PCB excitability through UNC-7 gap junctions. This idea is consistent with reports suggesting that UNC-7 and UNC-9 gap-junction subunits can shuttle hyperpolarizing chloride (Cl^-) currents to reduce the outputs of hermaphrodite pharyngeal, egg-laying and locomotory circuits (Barnes and Hekimi, 1997; Dent et al., 2000; Altun et al., 2009). The UNC-7 and UNC-9 innexins mobilize Cl^- to mediate the inhibitory effects of the anthelmitic drugs ivermectin (IVM) and

abamectin (ABA). Both of these drugs cause general locomotory paralysis in *C. elegans*, potentially through similar signaling mechanisms (Boswell et al., 1990; Barnes and Hekimi, 1997; Ghosh et al., 2012). IVM interacts with several Cys-loop family receptors, including GABA, glutamate and nicotinic ACh receptors (Cully et al., 1994; Hernando and Bouzat, 2014). IVM binding to GABA and/or glutamate gated channels results in chloride influx, which is subsequently relayed via UNC-7 and UNC-9 to broader neuronal populations of pharyngeal and locomotory circuits (Boswell et al., 1990; Cully et al., 1994; Dent et al., 1997).

To address whether chloride down-modulation also occurs between HOA and the PCS network, I first tested if IVM and/or ABA could inhibit ARE-induced protraction, similar to DA-exposure. I found that mixing ABA with ARE was able to reduce spicule protraction by 60% (93% vs. 36% ARE vs. ABA+ARE response, p-value<0.0001, Fig. 27A); however IVM reduced spicule protraction more mildly (Fig. 27A). Therefore, I used the ABA+ARE drug bath to test whether UNC-7 was required for the ABA down-modulation. I found that both *unc-7(rg396*) and *dop-2(lf)* males were insensitive to the inhibition (Fig. 27A), suggesting an interaction between ABA-sensitive channels, DOP-2 receptors and UNC-7 gap-junctions in regulating ACh-induced spicule protraction.

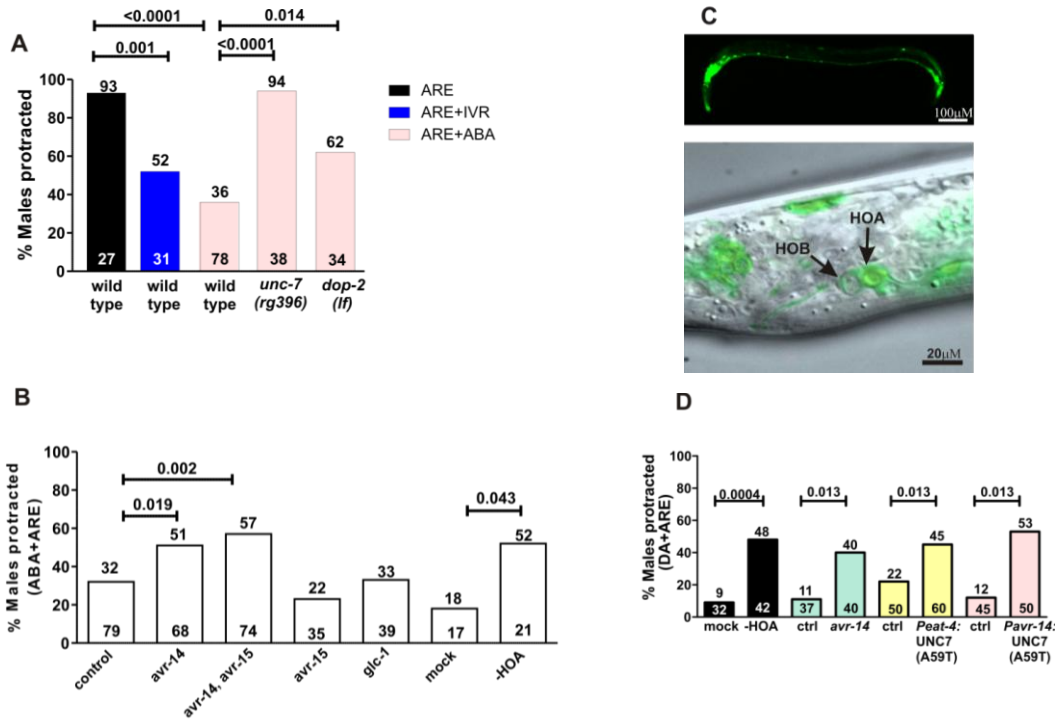

Figure 27. HOA mediates ABA inhibition of ARE-induced protraction and requires *avr-14* and *unc-7*. *A*, Percentages of wild-type and mutant males that protract their spicules in the corresponding avermectin baths. ***B***, Loss-of-function mutants for *avr-14*, *avr-15*, and *glc-1*; mock versus HOA-ablated males response to ABA_ARE. ***C***, Expression pattern of *Pavr-14:YFP* in several head, ventral chord, dorsal chord, and tail neurons (top). Overlaid DIC and confocal YFP image of *avr-14* expression in HOA (bottom). ***D***, DA _ ARE response for *avr-14*, HOA ablated males, UNC-7(A59T) tissue-specific overexpression, and respective controls.***A–D***, Top and bottom numbers indicate the percentage and number of animals tested, respectively. All *p* values were calculated using Fisher'sexact *t* test. The exact *p* values are indicated above the connector lines.

If UNC-7 relays the Cl^- current from HOA onto PCB to suppress spicule circuit excitability, then Cl^- glutamatergic and/or GABA channels should function in HOA. Since PCA chemically synapse HOA, and is likely glutamatergic (Jarrell et al., 2012; LeBoeuf et al., 2014), I addressed the possibility that glutamate chloride channels function in HOA to mediate the ABA-response. To narrow down which inhibitory

glutamate receptors function in the spicule circuit, I focused on the subset that has been shown to function in the pharynx and locomotory circuit: *avr-14; avr-15;* and *glc-1* (Dent et al., 2000; Ghosh et al., 2012). I asked which of these mutants is resistant to the ABA inhibition of ARE-induced protraction. I found that males lacking the *avr-14* gene are less-sensitive to the ABA inhibitory effect (Fig. 27B). Therefore, to confirm whether AVR-14 in HOA partially mediates inhibitory signaling, I examined the *Pavr-14*:*YFP* expression in the male. I found that this receptor is expressed in several head, ventral cord neurons and HOA (Fig. 27C). However, this decrease in sensitivity is much milder than the *unc-7(rg396)* mutant's response (Fig. 27A). The modest *avr-14* resistance to ABA might be due to receptors with redundant function. Since *C. elegans* has numerous cys-loop ionotropic receptors (Jones and Sattelle, 2008), in addition to *avr-14*, others could also be ABA-responsive. Taken together, these results suggest that chloride influx occurs in HOA at least partially through AVR-14.

To confirm the hypothesis that HOA is the neuronal substrate that mediates ABA-inhibition in the spicule circuit, I laser-ablated HOA in wild-type males and tested for their ABA+ARE response. I found that the operated males are less-sensitive to ABA-dependent inhibition when compared to mock treatments (Fig. 27B). However again, the HOA ablation was not able to account for the high level of ABA insensitivity seen in *unc-7(rg396)* mutant males, indicating that UNC-7 gap junctions must regulate spicule circuit excitability in additional sub-set of cells. Moreover, the DA+ARE resistance of *unc-7(rg396)* mutants suggests that some of the cells where UNC-7 regulates mating circuit excitability, including HOA, are under D2-like regulation. Therefore, I reasoned

that males lacking HOA and loss-of-function *avr-14* should also be resistant to DA down-modulation of ARE. I found that in both instances a higher percentage of males protract their spicules in the DA+ARE bath (Fig. 27D). Additionally, when I expressed UNC-7(A59T) in HOA, from two different promoters (*Peat-4* and *Pavr-14*), males were also insensitive to DA inhibition of ARE induced protraction (Fig. 27D). Taken together, these results are consistent with a model where activated DOP-2 results in open UNC-7 gap junctions to allow Cl^- influxes from HOA via AVR-14 to move into and reduce PCB activity (Fig. 28).

Chapter V summary

Delimiting spicule insertion attempts to the vulva is facilitated by D2-like receptor modulation of gap-junctions between PCB and the hook sensillum. Through genetic analysis I found that The UNC-7L gap-junction isoform mediates DOP-2 signaling between the cholinergic PCB neuron and its electrical partner, a hook sensillum neuron (HOA). The pharmacology indicated that the AVR-14 glutamate-gated channel partially allows chloride ions into HOA in order to promote DA downmodulation in the spicule circuit. In accordance with this idea, my circuit dissections in the *unc-7(rg396)* mutant background indicated that when DOP-2 up-regulates UNC-7 electrical communication, AVR-14-mediated inhibitory signals pass from HOA to PCB. As a consequence, the PCB and PCA recurrent communication is decreased. Behavioral observations suggest that DA dependent UNC-7 modulation dampens recursive intromission attempts when the male disengages or is dislodged from the hermaphrodite vulva.

CHAPTER VI

SUMMARY OF EXPERIMENTS AND DISCUSSION

Summary of experimental results

Male mating is one of the most complex goal-oriented behaviors in *C. elegans*, suggesting the need for modulation of temporal and spatial aspects of this stereotyped routine. My mating behavioral observations indicate that dopamine (DA) signaling diminishes ectopic spicule thrusts at non-vulva areas for efficient spicule insertion. This result suggests that DA dampens the excitability of the spicule circuit during copulation. Accordingly, pharmacogenetic analysis showed that DA down-modulates ACh-agonists induced protractions via non-redundant D2-like receptors (DOP-2 and DOP-3). Moreover, I found that this D2-like pathway transduces the DA signal to dampen sex muscle excitability through redundant G-alpha proteins, GOA-1 and GPA-7.

The pharmacogenetics showed that DOP-2 and DOP-3 reduce mating circuit excitability; thus I assessed how D2-like signaling affects spicule insertion during copulation and whether this modulation promotes mating fitness. I found that DOP-2 and DOP-3 mediate rythmicity of sex-muscle contractions to keep the male tail positioned over the vulva without startling the hermaphrodite. Nonetheless, this rhythmic regulation does not contribute to mating fitness in individual male and hermaphrodite parings. Therefore, I hypothesized that in more natural scenarios where males are surrounded by productive *versus* futile mating partners (i.e. other species and/or other males), D2-like receptors restrict mating attempts with non-receptive mates. Accordingly, I found that

D2-like signaling confines copulation with fruitful hermaphrodites, and therefore maximizes reproduction chances. This DA mediated modulation potentially not only entails sex-muscle excitability adjustments, but also PCS regulation in addition to other neuronal subsets.

To delimit spicule insertion attempts to the vulva, the PCS and DA ray neurons must interact in a time specific manner. Thus I conducted targeted optogenetic experiments to dissect the cholinergic and DA circuit crosstalk. Through calcium imaging I found that DA rays are active when males are arched prodding at the vulva, which coincides with PCA and PCB activity. Moreover, I found that one of the three DA ray neurons is stimulated by potentially PCS cholinergic signaling. These results indicate that during arched postures DOP-2 dampens PCS and/or sex-muscle excitability. Since PCA and PCB are reciprocally wired to each other, I demonstrated that DOP-2 decreases their stimulatory communication.

Finally I addressed how dampening of PCA-PCB crosstalk is regulated by DA and DOP-2. I found that the confinement of spicule insertion attempts to the vulva is facilitated by D2-like modulation of gap-junctions between PCB and the hook sensillum. I isolated a missense mutation in an isoform of the UNC-7 gap-junction, which perturbs DOP-2 signaling among PCB and its electrical partner, HOA. The glutamate-gated chloride channel AVR-14 is expressed in HOA. Moreover, analysis of the *unc-7* mutant allele indicates that when DOP-2 promotes UNC-7 electrical communication, AVR-14-mediated inhibitory signals pass from HOA to PCB. As a consequence, PCB is less receptive to be stimulated by its recurrent synaptic partner, PCA. Behavioral

observations suggest that DA neuromodulation of UNC-7 ensures attenuation of recursive intromission attempts when the male is dislodged from the hermaphrodite genitalia.

Discussion

D2-like receptors down-modulate spicule circuit excitability

Although dopamine (DA) dependent modulation of the vertebrate central nervous system (CNS) is widely accepted for regulating motor patterns (Graybiel et al., 1994; Fienberg et al., 1998), there are few in-depth analysis for how DA fine-tunes context-dependent behaviors. To address this, I analyzed how DA signaling temporally and spatially constrains specific neuromuscular outputs during *C. elegans* mating. As the wild-type male positions his tail over the vulva, he repetitively thrusts his spicules against the vulval slit. Termination of this behavior occurs after spicule penetration or loss of vulval contact. In contrast, I found that in DA-deficient *cat-2(lf)* males rhythmic spicule insertion attempts were no longer confined to the vulval region, and sometimes even initiated randomly on the hermaphrodite. This indicates that spicule motor behavior, coupled with vulva sensing is partially coordinated by DA inhibitory pathways.

Consistent with the *cat-2* male's ectopic display of motor behaviors, simultaneous application of exogenous DA with receptor-selective or nonselective acetylcholine (ACh) agonists constrains cholinergic-mediated sex-muscle contraction. Interestingly, the inhibitory effect of exogenous DA is less potent with a selective muscarinic (G-

protein coupled receptor) agonist or a muscarinic and ionotropic (ACh-gated ion channel) nonselective ACh agonist, if DA is applied first. This suggests that during mating, context-relevant DA signaling occur coincidently with ACh-mediated signaling. Moreover, since DA is less effective at down-modulating mAChR induced excitability, cholinergic GPCR signaling might make the spicule circuit refractory to non-coincident humoral DA secretions that occur elsewhere in the male potentially from non-gender specific DA neurons.

DA-dependent negative signals are partly transduced through the D2-like G-protein-coupled receptors DOP-2 and DOP-3. Even though *dop-2*; *dop-3* double mutant phenotypes are less severe than *cat-2* animals, likely because every DA receptor is affected by the *cat-2* mutation, I still found D2-like diminishes cellular excitability during copulation. My behavioral observations suggest that these receptors mediate restriction of spicule protraction behavior to the precise vulval slit area, and maintain rhythmic spicule thrusts during penetration attempts. Although previous reports demonstrate DOP-3 and GOA-1 signaling for hermaphrodite locomotion (Chase et al., 2004; Allen et al., 2011) and *in vitro* DOP-2 and GPA-14 interactions (Pandey and Harbinder, 2012), I provide genetic evidence that $G\alpha_{o/i}$ proteins, GOA-1 and GPA-7, redundantly transduce DA inhibitory signals during vulva sensing/spicule insertion behavior. These $G\alpha_{o/i}$ proteins, and their $\beta\gamma$ partners might regulate molecules such as adenylyl cyclase, L-type- voltage-gated Ca^{++} channels and K^{+} channels to decrease neuromuscular excitability (Stoof and Kebabian, 1981; Hernandez-Lopez et al., 2000; Bateup et al., 2010).

Feed-back regulation among DA ray neurons and the cloacal male specific ganglia

ACh secreted from the cloacal ganglia sustains vulval contact (Liu et al., 2011), while concurrently, the sensory rays likely provide feedback to adjust the male's movement and posture according to the hermaphrodite's position and locomotion. Each pair of bilateral ray neurons are made of two distinct sensory cells (A&B), three of the 9 ray pairs contain DA sensory neurons. When these DA male specific cells are optogenetically stimulated they induce a shallow ventral tail flexure (Koo et al., 2011). However, when artificially activated in the presence of non-selective ACh agonists endogenous DA secretion antagonizes spicule protraction. The 3 pairs of Ray-A neurons gap junction to their Ray-B counterparts, which express neuropeptides *flp-5, flp,-6,* and *flp -17 (Lints et al., 2004),* raising the possibility that stimulation of Ray-A neurons indirectly leads to neuropeptide-dependent modulation of the spicule circuit. However in the *dop-2; dop-3* double mutants, ChR2-stimulation of DA secreting cells, and possibly including the RnB neurons via gap junctions, failed to reduce simultaneous ACh agonist-evoked contractions. This suggests that DA secretions, possibly from rays 5A,7A and 9A, can attenuate the output of cholinergic signaling. Of these neurons, rays7A and rays9A make chemical synapses to cloacal-associated components (Fig. 5), suggesting that DA-ACh signals might be involved during the vulva location/spicule insertion steps.

DA signaling during scanning suggests DA interaction with general locomotor circuit

The DA ray neurons and the spicule circuit components are more dynamic during vulval contact. However, on occasion heightened ray neuronal activity is sometimes detected when the male is at non-vulval regions, suggesting that DA secretion is not tightly coupled to an explicit sensory signal. My optogenetic experiments indicate that cholinergic cloacal neuron activation stimulated Ray 7A activity. This DA-secreting cell is not post synaptic to the cholinergic cloacal neurons, indicating that DA secretion might be an indirect response to cholinergic circuit activity via humoral signaling, interneurons, or glutamatergic signal from PCA. Additionally, the Ray 5A and Ray 9A did not responded to PCB and SPC stimulation, further suggesting implications of additional internal signals from the locomotor circuit or other ray neurons.

Throughout mating, ray neurons respond with an array of different dynamics correlated with the gradual arched body posture changes, which are perhaps a read-out of DA not only modulating the PCS, but also providing feedback onto a locomotor circuit. This is a possibility since DOP-2 and DOP-3 are expressed in ventral cord neurons and body wall muscles (Chase et al., 2004), which facilitate locomotion. During non-arched postures, either scanning or at the vulva, DA ray neurons display stable activity. However, if a male develops an arched posture at the vulva, or during scanning, then the DA ray neurons dynamically up-regulate their activity, perhaps to modulate the transition of the overall motor response. During behavioral paradigms where males are paired with several non-productive partners, I have observed a similar spicule circuit independent

modulatory role for D2-like receptors. In these circumstances, reduction in D2-like signaling results in mutants engaging in prolonged backward scanning locomotion with other males and hermaphrodites of different species. Therefore, the DA-signaling mutant phenotypes, together with the expression of DA ray neuronal activity, suggest that DA refines motor outputs at the vulva and delimits them at other areas via interactions with neural-muscular networks that include the spicule protraction circuit. This ACh/DA interplay might share analogy with how the vertebrate CNS fine-tunes locomotor control.

In the vertebrate CNS, DA secretions from the substantia nigra (SN) inhibit striatal ACh interneurons, and ACh-induced DA release in these networks coordinate voluntary movements (Maurice et al., 2004; Deng et al., 2007). Although this suggests bidirectional DA/ACh signaling in the CNS, direct evidence for how these neurons shape motor outputs at the animal behavioral level is scarce, due to complex CNS connectivities (Bateup et al., 2008; Bateup et al., 2010). In the *C. elegans* male, the DA ray neurons and cholinergic cloacal ganglia interact bi-directionally to regulate sex-muscle behaviors. The optogenetic experiments suggest that cloacal ganglia neurons promote DA- ray activity and the pharmaco-genetic experiments indicate that DA attenuates the ACh spicule circuit output partly via DOP-2 and DOP-3 on PCB neurons and sex muscles. Decrease of PCB output could subsequently result in reduced DA secretion and dampening of DA and ACh circuits' interactions.

During mating, how can a male insert his spicules while attenuating DA signaling occurs? Possibly during the repetitive vulval penetration attempts, potent ACh secretions can override DA-negative signaling, due to acute vulval stimulation of the cloacal sensory-motor neurons. However, these cloacal neurons make reciprocal (recurrent) synapses with one another (Figure 5&22A). If the wild-type male moves off the vulva or if these neurons are inappropriately stimulated (on non-vulval regions, on another male, or by a mate from a different species), then a negative mechanism, such as D2-like signaling, must dampen the circuit's residual self-amplifying property. Indeed, the ectopic mating behaviors displayed by *cat-2* and *dop-2; dop-3* males give the illusion that they compulsively maintain motor behaviors (spicule prodding) in the absence or withdrawal of the appropriate stimuli. The ACh and D2-like signaling interactions in *C. elegans* are reminiscent of D2 receptor-regulated synaptic plasticity in vertebrate SN-striatal networks. In these networks, D2 receptors regulate long term synaptic depression. This form of plasticity reduces pre-existing motor memory storage and maintains a balance between old and newly encoded motor information. In DA-deficient Parkinson's disease models, dyskenisia (voluntary movement disorder) is caused by plasticity abolishment in these networks (Calabresi et al., 1992; Picconi et al., 2003; Calabresi et al., 2006; Shen et al., 2008; Bagetta et al., 2011).

D2-like dependent dampening the PCS recurrent neuronal network during spicule insertion attempts

The persistent activity in reciprocally connected neurons of animals was shown to regulate complex context-dependent behaviors. Many of these studies focused on the

recurrent neural interactions that occur in the mammalian cortex. Extensive studies showed that these cortical networks use dopamine (DA)-activated receptors to regulate their cellular firing patterns (Shepherd et al., 2005; Noudoost and Moore, 2011; Arnsten et al., 2012; Matsumoto and Takada, 2013; Happel et al., 2014). However, due to the complexity of the mammalian cortex, correlating how animal behavior is changed with DA modulation of specific recurrent networks is difficult. To identify how DA regulates persistent or repetitive behavior in a much simpler animal, I analyzed how DA dampens a recurrently wired sensory-motor network that restricts *C. elegans* male spicule thrusts to the vulva.

During copulation, the vulva mechano-chemo sensory cues stimulate the post cloacal sensilla (PCS) sensory-motor neurons, PCA, PCB and PCC. PCS activity triggers sex-muscle contractions to produce rhythmic spicule thrusts. For simplicity, I focused my attention on two of the three PCS cells. We demonstrated that not only do the PCA and PCB receive stimulatory signals from the vulva, but that they reciprocally stimulate each other when DA signaling is absent (Fig. 28A & B). This recurrent interaction potentially occurs at the initial period of spicule insertion attempts. Recurrent PCS signaling at the beginning of vulva insertion attempts might serve to reinforce the detection of vulval cues. Although the PCS neurons are functionally redundant, each of them might individually contribute to prodding through detection of distinct vulva aspects (Liu and Sternberg, 1995; Garcia et al., 2001; Liu et al., 2011). PCA is the only ciliated PCS neuron (Sulston et al., 1980), thus similar to other ciliated neurons, it might sense mechanical and/or chemical cues from the vulva. In contrast, the non-ciliated PCB and

PCC might detect other less-defined anatomical features of the vulval lips. Therefore, reciprocal communication could allow the PCS to integrate these different sensory modalities to sustain spicule thrusts.

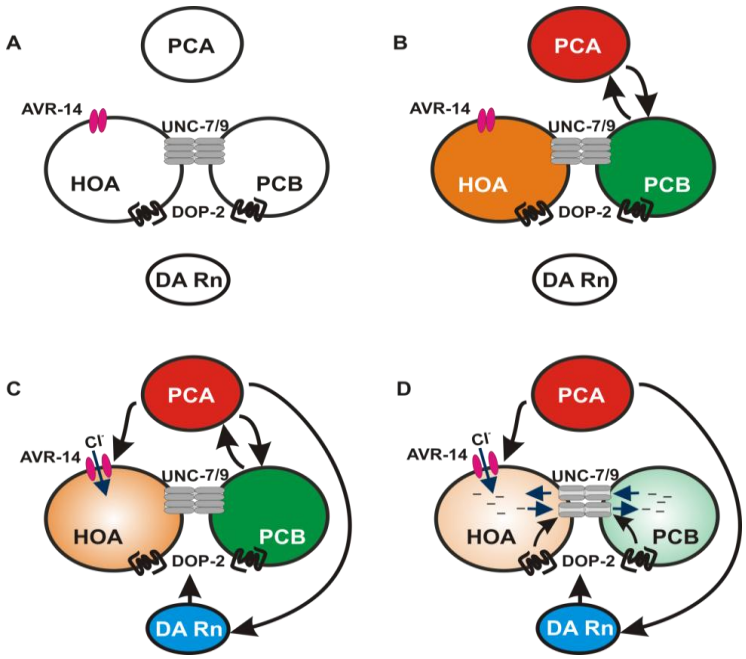

Figure 28. D2-like modulation of UNC-7 dampens PCA and PCB cross-talk. Cartoon depicting proposed PCS, HOA and ray neuron activity at different stages of spicule prodding. (A) Prior to reaching the vulva, cells are inactive due to the lack of sensory input, and therefore their interneuronal interactions are weak. (B) When at the vulva HOA, PCB and PCA are stimulated by vulva cues, triggering (C) PCA and PCB recurrency. (D) Prolonged spicule prodding results in DA ray neuron activity and consequent dampening of PCS recurrency. This occurs through opening of UNC-7/UNC-9 and relay of inhibitory signals, such as chloride (Cl^-) ions from HOA into PCB. Black arrows represent functional chemical synapses. Dotted lines and thicker lines indicate weak versus amplified cellular activity. Purple arrows represent the putative chloride hyperpolarizing current path. Shades represent cellular activity induced by stimuli and/or interneuronal communication.

Males can spend minutes displaying repetitive spicule thrusts when attempting to breach the hermaphrodite's vulva (Garcia et al., 2001). Since direct chemical and/or mechanical stimulation has been shown to stimulate *C. elegans* sensory neurons for

several seconds (Ezcurra et al., 2011; Kato et al., 2014), the recurrency could potentially sustain the PCS activity, so that they continuously stimulate the sex-muscles (Fig. 28B). However, if prodding behavior becomes prolonged, I hypothesize that DA secretion from Rn5A, 7A and 9A neurons tune down the PCS recurrency (Fig. 28D).

When the male first contacts the vulva, his body is flushed with the hermaphrodite cuticle. At the vulva, the ray neurons 5A, 7A and 9A activity is initially unchanged as compared to when the male was executing backward scanning locomotion. However, after prolonged prodding, the male adopts a ventrally arched posture, which is correlated with increased dopaminergic ray activity (Koo et al., 2011; Correa et al., 2012). I showed that direct activation of the PCS network will slowly stimulate the DA rays (Correa et al., 2012), thus I favor the hypothesis that during extended intromission attempts, the recurrent PCS activity eventually induces PCA to facilitate DA secretion from ray neurons (Fig. 28B). The DA then stimulates DOP-2 receptors to attenuate PCS neurons reciprocal signaling. From my genetic screen, I found that one target of D2-like signaling in the male tail is the UNC-7 (L) gap junction subunit. The isolated A59T missense mutation, affects the first exon of the UNC-7(L) isoform; potentially leaving UNC-7(S) intact to permeate ion passage into other cells. UNC-7(S) might also transduce DA signals in other circuits, but the expression pattern suggests that UNC-7 (L) is the predominant effector of DOP-2 for the male copulatory cells. My data indicated that during prolonged prodding, D2-like signaling via UNC-7(L) regulation can direct attenuation of PCB though one of its electrical partners, HOA (Fig. 22D).

D2-like signaling regulation of gap-junctions as a conserved mechanism

Although the PCS acts in-conjunction with the hook neurons, HOA and HOB, to initiate intromission behavior at the vulva, the two sensilla might also act together to terminate futile insertion attempts. The glutamatergic PCA makes chemical synapses to HOA, which expresses the glutamate-gated chloride channel AVR-14, in addition to DOP-2 and UNC-7 (Fig. 28). During prolonged insertion attempts, persistent PCS signaling could cause the glutamatergic PCA neurons to induce hyperpolarizing chloride influx into HOA, which can then be relayed into PCB through UNC-7 gap-junctions. My experimental observations indicate that as a consequence, the DOP-2 dependent-HOA-PCB interaction likely dampens PCB's ability to be stimulated by PCA (Fig. 28C & D), and possibly also by its other recurrent partner, PCC. The recurring amplification between the cells should be reduced, causing the primary stimulation of the circuit to shift back to the sensilla's sensory input. If the male's sensory apparatus becomes desensitized by prolonged contact with the vulva, then the reduction in PCS recurrency might allow him to move off the vulva.

The regulation of the male intromission circuit displays some parallels and differences with how DA-mediated gap junction modulation alters circuit interactions in other model systems, such as the vertebrate retina (Ribelayga et al., 2002; Ribelayga et al., 2008; Kothmann et al., 2009). The specialized rods and cones sensory neurons respond to low versus high light conditions, respectively. Studies suggest that in addition to sensory input, DA signaling can mediate preferential cone activity during bright daylight

(Ribelayga et al., 2002; Ribelayga et al., 2008). During the day, release of retinal circadian-regulated DA triggers D2-like signaling in rods and cones to dampen their electrical coupling; thus leaving cones solely responsive to light stimuli (Ribelayga et al., 2002; Ribelayga et al., 2008). In contrast, during the night, decreased DA release allows robust rods-to-cones coupling (Ribelayga et al., 2008). Although D2-like signaling dampens cell-cell interactions in both the worm and vertebrate contexts, retinal D2-like signaling diminishes gap junction-mediated stimulatory cation transport between rods and cone cells (Ribelayga et al., 2008), whereas in the worm, DOP-2 up-regulates UNC-7 to introduce inhibitory signals, possibly chloride, from HOA to PCB.

In the *C. elegans* locomotor circuit, UNC-7 and UNC-9 form heterotypic gap-junctions between cells. When UNC-7 and UNC-9 are individually expressed in the Xenopus oocytes, they can form both heterotypic and homotypic gap-junctions; interestingly, the heterotypic, but not homotypic gap-junctions show rectifying properties (Starich et al., 2009; Kawano et al., 2011). In previous work, I reported that UNC-9 is also expressed in PCB (Liu et al., 2011). Thus I do not rule out the possibility that between HOA and PCB, UNC-7 may form both heterotypic and homotypic gap junctions. If both types of gap junctions exist between PCB and HOA, then ion flow could be symmetric or asymmetric, depending on which type of junction is open via upstream neuromodulatory signaling. This type of regulation has been demonstrated in the auditory eight nerve neurons and Mauthner cell interneuron of the auditory vertebrate fish circuit. Between these cells, different connexon sub-units make up heterotypic gap-junctions (Korn and Faber, 2005; Rash et al., 2013). Since each sub-unit has slightly different gating

properties, ion passage is heightened from the Mauthner cell onto the eight nerves, resulting in asymmetric ionic distribution (Rash et al., 2013). Moreover, D1-like signaling in the Mauthner cell (Cachope et al., 2007) might contribute to specific heterotypic gap-junction subunit modification; and therefore directional gating enhancement.

Gap-junction modulation via DA in the vertebrate visual, auditory and worm copulatory circuits may also provide insight on how firing patterns are regulated in the complex mammalian cortical recurrent-neuronal networks (RNN). In the cortex, GABAergic interneurons contain reciprocal inhibitory chemical connections and are also gap-junction with each other (Galarreta and Hestrin, 1999, 2001b). When these cells receive stimulatory glutamate signals from upstream sensory systems, their inhibitory recurrency, in conjunction with gap-junctions, produce amplified oscillatory outputs that drive 30-80 Hz activity patterns in other cortical neurons. When an animal is conducting cognitive tasks, these cortical oscillations are believed to facilitate the generation of coherent environmental representations, through coordinating parallel sensory CNS processing regions (McBain and Fisahn, 2001). Since these GABAergic neurons also express D2-like receptors, the gap junctions that contribute to their synchronous oscillations could also be regulated by DA (Galarreta and Hestrin, 2001b). This idea is consistent with various studies showing that compulsive and schizophrenic individuals display abnormal DA signaling and oscillatory cortical patterns (Spencer et al., 2004; Wang et al., 2004; Furth et al., 2013; De Koning et al., 2014; Su et al., 2014).

Future experiments

My studies of D2-like signaling indicate that dampening spicule insertion circuit excitability diminishes non-productive behaviors, suggesting a favorable effect for diminishing a motor output within a motivated behavioral sub-routine. Nonetheless, there are few details left unanswered on how the *C. elegans* compact nervous system utilizes this strategy during mating. One of these aspects should address how chloride shuttling between PCB and HOA alters the excitability of these two neurons when males are attempting to insert their spicules at the vulva. Additionally, further experiments should explore which signals trigger DA ray neurons activity. I partially addressed this question and indicated that Rn7A responds to PCS stimulation; however the remaining DA cells might be stimulated by additional internal signals. Finally, future directions should elucidate how D2-like receptors regulate gap-junctions in the sex-muscles, since this slightly different mechanism would coordinate posture and spicule locomotion simultaneously.

How can the HOA and PCB circuit be studied to investigate the role of inhibitory gap-junctions modulating a motivational status?

To delimit repetitive spicule insertion attempts to vulva cues, D2-like signaling up-regulates the UNC-7 opening to mobilize chloride ions across PCB and HOA. This suggests that these gap-junctions are inhibitory and potentially transiently desynchronize mating circuit sensory neurons, when are under D2-like modulation. Recent studies indicate that in isolated cortical and cerebellar mammalian tissues, gap-junctions

distribute an after-hyperpolarization potential across cells to transiently inhibit circuitry responsiveness (Galarreta and Hestrin, 2001b, a; Vervaeke et al., 2010). These electrically wired networks also receive GABAergic inputs through GABA(A) receptors, suggesting that connexins could also shuttle chloride (Cl^-) ions. Even though Cl^- transport might affect cortical network synchronization, and therefore impinge on cognitive behaviors, there aren't any reports that explore neuronal Cl^- ion transport through gap-junctions. Thus, I propose using the model of PCB and HOA electrically wired circuit to study the temporal constrains of chloride distribution within neurons.

To circumvent technical challenges of using electrophysiology to characterize the timing of electrical signals amongst HOA and PCB, I propose using a molecularly encoded Cl^- sensor as a proxy for anion shuttling amongst these cells. This sensor simultaneously and independently measures *in vivo* Cl^- and pH changes in neuronal cell cultures (Arosio et al., 2010; Raimondo et al., 2013). The ClopHensor contains a E^2 GFP version fused to mDSred. The E^2 GFP has a highly specific anion binding site that allows for static GFP fluorescence quenching as Cl^- ions bind to it (Arosio et al., 2007). The mDSred allows for ratiometric analysis of the E^2 GFP fluorescent intensities, which can be simultaneously measured similar to the GCaMP analysis. Since this sensor hasn't being used in *C. elegans*, I would initially address whether ClopHensor can detect GABA(A) receptors induced Cl^- influx into body wall muscles, a well-characterized post-synaptic target of inhibitory GABA signaling (McIntire et al., 1993; Bamber et al., 1999). Expressing ClopHensor from a pan-muscular promoter (*lev-11)* and exposing worms to muscimol a GABA(A) receptor agonist (McIntire et al., 1993), should result in

muscular fluorescence changes. To further corroborate that these changes are due to chloride and not other anions or experimental artifacts, I would measure fluorescent changes in animals with a loss-of-function mutation in GABA(A) receptors (*unc-49* background) (Bamber et al., 1999). Since these mutants are insensitive to muscinol effects, chloride induced fluorescent changes should be abrogated. After these necessary ClopHensor calibrations, I would address whether UNC-7 chloride transport between HOA and PCB, or AVR-14 induced chloride passage into HOA can be detected.

By expressing the ClopHensor from the *dop-2* promoter I could image Cl^- fluctuations in PCB and HOA. First, I will use the ionotropic glutamate gated Cl^- channel agonist Abamectin (ABA) to assess how glutamate induced Cl^- influx travels within HOA and PCB. There are three possible outcomes from this experiment: a change only in HOA, in both HOA and PCB, or no fluctuations. A change only in HOA intracellular Cl^- increase would indicate that an additional mechanism is required to open UNC-7 and move Cl^-, such as DOP-2 signaling. Fluctuations in both cells indicate that UNC-7 on its own can conduct Cl^- and therefore DOP-2 might modulate the coupling magnitude. To further study these two possibilities I could mix ABA with DA and therefore check to see if DA signaling alters HOA and PCB fluorescent changes. The third outcome, no change in either cell, would suggest that sensor kinetics are not as fast as the electrical coupling. However, if this was done in the *unc-7(rg396)* background I could potentially see a slower chloride accumulation in HOA, corroborating my findings that UNC-7 conducts chloride among PCB and HOA.

Finally I would use the ClopHensor combined with targeted mosaic illumination to test timing differences between glutamate signaling through AVR-14 and D2-like signaling. Glutamate neurotransmission via ionotropic channels usually occurs at a faster rate than GPCR signaling (Greengard, 2001). Therefore, AVR-14 opening might happen prior to DOP-2 up-regulation of UNC-7; alternatively DA and glutamatergic signaling might co-occur. Since PCA is the potential source of glutamate signaling into HOA, and a trigger for DA ray neuron activity (Appendix) I could assess the Cl^- fluxes in HOA and PCB upon ChR2 PCA light stimulation. A concomitant signal would cause an immediate Cl^- rise in PCB and HOA; alternatively sequential Cl^- influx would result in HOA followed by PCB fluorescent changes. To corroborate that Cl^- shuttling occurs due to UNC-7, this experiment should be done in the *unc-7(rg396)* background. One of the drawbacks of this strategy is that PCA might not be the only glutamatergic signal that triggers AVR-14 opening. Nonetheless, since the ChR2 in this experiment is driven from a glutamatergic specific promoter (*eat-4*); this would allow to alternatively test if additional gluatamatergic signaling from other neurons, such as ray neurons, would induce HOA and/or PCB Cl^- fluxes.

Does the internal signal that stimulates ray neuron activity coordinates the feeding with the mating circuit?

Studies from my lab and several others suggest that the nutritional status of an animal affects goal-oriented executions (Coppola et al., 2007; Kindt et al., 2007; Gruninger et al., 2008; LeBoeuf et al., 2011; Ryan et al., 2014). Since the DA system acts either downstream or upstream of caloric intake signals in several model organisms (Krashes et

al., 2009; Tellez et al., 2013; Baimel and Borgland, 2015), DA is a potential candidate to mediate feeding and mating circuit interactions. *C. elegans* constitutively pumps their pharynx for food ingestion at approximately 5Hz (Avery and Horvitz, 1989); however when males find the vulva pharyngeal pumping rate decreases, and eventually ceases (Liu and Sternberg, 1995; Gruninger et al., 2006). These observations indicate that these two behaviors are mutually exclusive, even when plentiful food and abundant mates are present. Moreover, the neurons that diminish pumping during mating secrete serotonin, glutamate and several peptides (Gruninger et al., 2006). Since these neurons do not synapse any mating circuit cell, potentially the hormonal signals communicate to the rest of the animal the current nutritional status and potentially could set a feeding versus copulation states. Thus, I propose that the pharyngeal neuron sub-set that decreases pumping during vulva contact, in parallel up-regulates DA ray neurons via a stimulatory peptidergic signaling. Upon build up of this peptide, and consequent D2-like signaling saturation, males will withdraw from mating and resume the feeding program.

Copulation is a highly energy costly behavior (Vrablik et al., 2011; Shaw et al., 2014), thus setting feeding and copulation cycles is an excellent strategy to limit spending unnecessary energy in futile copulation attempts. The pharyngeal circuit is a good candidate network to control the length of these cycles, since this circuit increases or decreases pharyngeal pumping with high pliability and under several contexts. For instance, transient pumping suppression occurs during tail-taps and short-wavelength light exposure (Keane and Avery, 2003; Bhatla et al., 2015). In both of these

circumstances pharyngeal pumping rates are eventually reset either by pharyngeal neurons or intrinsic muscle regulations.

To identify which pharyngeal neuron initiates the communication between feeding and mating circuit, I would first focus on the established neurons that decrease pharyngeal pumping. The pharyngeal neuronal circuit is made of 20 neurons that upregulate or downmodulate pumping (Albertson and Thomson, 1976; Rogers et al., 2001; Steger and Avery, 2004). My lab found that the NSM neuron, a non-essential pumping regulator under abundant food conditions, partially diminishes pumping during mating (Gruninger et al., 2006), suggesting that additional neurons mediate pumping inhibition during copulation. Moreover, other studies suggests that I1, I2 and the non-pharyngeal neuron RIP decrease pumping rates through stimulating AVR-15, a glutamate chloride channel, in pharyngeal muscles (Keane and Avery, 2003; Bhatla et al., 2015). Since NSM secretes glutamate and serotonin (Lee et al., 1999; Hobson et al., 2006), besides several peptides, NSM glutamatergic signaling might down-modulate pumping rates in addition to I1, I2 and RIP. Therefore, I will ablate different combinations of these neurons and measure pumping rate when the male finds the vulva. To rule out that pharyngeal rate down-modulation and peptide signaling are independently coordinated by different subset of neurons, I will address if these cellular ablations result in vulva location defects similar to *dop-2* and *unc-7(rg396)*. If the cells that decrease pharyngeal pumping do not regulate any aspects of vulva location, it suggests that those neurons don not alter mating circuit excitability in parallel. Thus, separate neuronal subsets simultaneously inhibit pumping and up-regulate ray neurons. Nonetheless, if few pharyngeal neurons co-

regulate inhibition of pumping and promote ray neuron excitability, the pharyngeal neuron ablations should result in males that pump when at the vulva and cannot maintain their position over it.

Parallel to identifying which pharyngeal neuron subset establishes the communication among the pharyngeal and mating circuits, I will address which peptide signaling pathway mediates this interaction. There are approximately 103 *C. elegans* peptides, which are humorally secreted into the worm pseudosoleomic space to stimulate G-protein coupled receptors that increase or decrease cellular excitability in diverse tissues. The potential pharyngeal candidate neurons (NSM, I1, I2, RIP) secrete peptides of the neuropeptide-like (*nlp*s) and the FMRF-amide like peptides family (*flp)*, such as *nlp-3, nlp-8, nlp-13, nlp-18, nlp-19, flp-4, flp-5, flp-15* in addition to *ntc-1,* the *C. elegans* homolog for oxytocin. Moreover, unidentified relevant pharyngeal neurons might secrete additional peptides. Due to the several molecules secreted by these neurons, it might be challenging to narrow down the peptide signaling mechanism activated during mating. Thus, I propose using a forward genetic approach to identify *loss-of-function* and *gain-of-function* mutations that perturb the ligand and/or GPCRs peptide pathway involved in DA up-regulation during mating.

To find *loss-of-function* mutations in the peptide signaling pathway, I will use the *dop-2; dop-3* background to screen for animals that have increased spicule protraction incidence. I found that in the mating circuit DOP-2 and DOP-3 are non-redundant with each other, indicating that there might be another DA receptor that partially compensates

for *dop2, dop3* dysfunctions. This compensatory mechanism might include a peptide signal that up-regulates DA secretion, and therefore stimulates a third D2-like receptor downstream. Since I showed that DA deficient *cat-2* animals constitutively protract their spicules (*Prc* phenotype) and *dop-2; dop-3* animals do not (Correa et al., 2012), I will mutagenize *dop-2; dop-3* hermaphrodites and screen for the *Prc* phenotype in the F2's. Isolated lines with *Prc* males will identify mutations in the ligand, the peptidergic GPCR and/or the remaining D2-like receptor. Through classical map-by linkage, and whole genome sequencing I will then determine the molecular identity of these mutations. Moreover, I will outcross *dop-2; dop-3* to find whether the unknown induced mutation results in the *Prc* phenotype by itself, or in addition to *dop-2* and *dop-3* mutations. If the unidentified single mutation results in the *Prc* phenotype, potentially one of the perturbed genes in this background unravels an upstream DA signaling regulator, and therefore is involved in peptide signaling. Alternatively, if the mutation only produces the *Prc* phenotype in combination with *dop-2; dop-3*, it would suggest that this gene is redundant with D2-like signaling, and therefore might identify another DA receptor.

Alternatively, to find *gain-of-function* mutations in the peptide signaling I will do the screen in a background where ray neurons are hyperpolarized. I found that hyperpolarizing all DA neurons by driving *unc-103(gf)* from the DA re-uptake transporter (DAT-1) promoter results in the *Prc* animals, similar to *cat-2(lf)* males (results section). Since additional findings indicate that the source of DA that triggers D2-like signals mainly comes from DA ray neurons, I will restrict the *unc-103(gf)* expression to DA ray neurons and assess if this is sufficient to inducethe *Prc* phenotype.

To achieve this I will use the binary split Q-system, which allows for intersectional control of gene expression (Wei et al., 2012). This system separates the transcriptional activator QF into two domains, QF-Zip(-) and QF-Zip(+). The tissues that overlap expression of these two domains will bind to a QUAS sequence and drive expression of *unc-103(gf)*. For this set up I will use the *Pdat-1* and *Pmab-31* to individually drive the Zip domains, since the reported expression of these two promoters only overlaps in DA ray neurons (Jayanthi et al., 1998; Wong et al., 2010). Moreover, the *unc-103(gf)* is tagged with DsRed, which allows monitoring the specificity of this strategy. After validating that *unc-103(gf)* expression in DA ray neurons results in *Prc* males, I will integrate this extrachromosomal array and mutagenize hermaphrodites to look for lines with *Prc* phenotype revertants. These lines should identify molecules that up-regulate DA neurotransmission, and might reveal a stimulatory GPCR peptide cascade. The main caveat of this strategy is that *unc-103(gf)* hyperpolarization might not be reversible. Therefore, to malleably diminish ray neuron activity I could replace using *unc-103(gf)* and instead use an inducible histamine-gated chloride channel (HisCl1) (Pokala et al., 2014). Since histamine is not a *C. elegans* neurotransmitter, the heterologously expressed HisCl1 must be stimulated with exogenous histamine added to NGM plates. Histamine titrations make cells still amenable to endogenous regulations in some circuits (Pokala et al., 2014). Thus, selective HisCl expression in DA rays might provide an alternative background to perform the mentioned revertant *Prc* screen.

Do D2-like receptors regulate asymmetric calcium transport through gap-junctions in the sex muscles?

Recent studies in vertebrates suggest that gap-junctions can transport ions asymmetrically (Korn and Faber, 2005; Palacios-Prado and Bukauskas, 2009; Rash et al., 2013). This asymmetric gap-junction property in *C. elegans* sex-muscles might be the mechanism for delayed male arched postures during insertion attempts. The asymmetric transport occurs in heterotypic gap-junctions, where each sub-unit has slightly different gating properties, driving a directional ion passage amongst apposed cells (Palacios-Prado and Bukauskas, 2009; Rash et al., 2013). Moreover, if there is a different regulatory signaling mechanism only in one of the apposed cells, the opening of the homeotypic connexon might occur with slightly different kinetics, also driving asymmetry. In the *C. elegans* mating circuit UNC-7 and UNC-9 form heterotypic and homotypic gap-junctions, and potentially both sub-units are regulated via D2-like receptors. Thus, ion passage through these channels could occur in an asymetrical manner from heterotypic or homeotypic regulations. The UNC-7 and UNC-9 gap-junctions in the spicule circuit potentially shuttle chloride ions. In the sex muscles there is no reported chloride channel expression, indicating unlikely chloride entrance triggered by neurotransmission. Additionally, my lab found that UNC-9 potentially transports calcium across the sex-muscles (Liu et al., 2011). Thus, asymmetric calcium transport might regulate temporal aspects of sex-muscle excitability, and therefore muscle contractions patterns during mating that give rise to arch postures.

Calcium imaging analysis indicates that DA ray neurons are active during mating when males arch their posterior halve and DA cells are less dynamic when displaying a flaccid posture (Fig. 16); however whether D2-like receptors influence posture changes is unknown. Since diagonal muscle contractions potentially cause arch postures, DA signaling might alter diagonal muscle excitability. These muscles do not express DOP-2 or DOP-3, indicating indirect D2-like modulation. Moreover, the 8 diagonal muscles (DM) receive few chemical synaptic inputs, from ray neurons and a couple of sex-shared neurons (Jarrell et al., 2012). Nonetheless, the two most posterior DM7 and DM8 are heavily electrically wired to auxiliary sex-muscles, anterior oblique (AOB) and gubernacular retractors (GRT) (Jarrell et al., 2012), indicating that auxiliary sex muscles might stimulate DM contractions through gap-junctions. Upon vulva contact the PCS stimulates AOB and GRT, which relay electrical signals via UNC-9, potentially in the form of calcium, onto protractor muscles to induce spicule movement (Liu et al., 2011). However, the arched posture is not immediately adopted when the male tail sensilla contacts the vulva. Thus, I propose that during arched postures the initial calcium fluxes that went from the auxiliary sex muscles onto the protractor muscles switch directions onto the DM. Since DOP-2 is expressed in the anal depressor (AD), which is an electrical conduit onto AOB and GRT, I hypothesized that the calcium current switch is driven by DOP-2 signaling in the AD. Thus, ADP D2-like signaling promotes UNC-7/UNC-9 activity and starts tilting the calcium transport towards AOB and GRT to eventually reach the diagonals during arched postures.

To address whether the protractor muscles are active before diagonals I would assess the calcium transients of these two muscle subsets during spicule insertion attempts. For this I would express GCaMP form the *unc-103E* promoter and image these muscle groups during mating. Alternatively, since in free-moving animals focusing on these two muscle groups might be challenging, I could immobilize males and induce spicule movement via targeted illumination. Restrictive PCA stimulation via channel rhodopsin induces spicule prodding, under DA signaling regulation, this artificial setting potentially mimics the motor subroutine of spicule insertion attempts at the vulva **(**Appendix**).** Thus, I would optogenetically stimulate PCA and image calcium transients in auxiliary, diagonal and protractor sex muscles. If my hypothesis is supported, I should see calcium transients in protractors before diagonals. Alternatively, if the diagonals and protractors show simultaneous calcium transients, it would suggest that arched postures do not result from diagonal muscle contractions, but other muscle groups might contract to induce an arch, such as the body wall and/or longitudinal muscles. However, this is unlikely since body wall muscle contractions in the hermaphrodite do not induce any posture changes that are similar to the arch that males adopt during copulation.

To address if D2-like signaling redistributes calcium across sex muscles, the above calcium imaging experiments should be done in tissue specific *dop-2* and *unc-7* knock outs. As these two molecules diminish PCS and sex-muscles excitability, observations of calcium transients in the sex-muscles of *dop-2* and *unc-7* mutants might be confounding. Therefore, I would generate a muscle specific knock outs of these two genes using CRISPR-CAS9 system (Dickinson et al., 2013). Since the *dop-2(vs105)* allele is a small

deletion in the second *dop-2* exon (Chase et al., 2004), and the *unc-7(rg396)* mutation affects the first UNC-7L exon, I would use CRISPR-CAS9 mediated recombination to introduce loxP sites flanking the first and second exons of these two genes respectively. Then, extrachormosomal introduction of CRE-recombinase from the *unc-103E* promoter would recombine out these relevant exons and induce sex-muscle specific perturbations in D2-like signaling. After making these knock outs I could test whether UNC-7 and/or DOP-2 affect calcium shuttling through monitoring calcium transients in the sex muscles. Since the CRISPR-CAS9 system has variable and low efficiency depending on the gene in question (0.4%-12%) (Paix et al., 2014; Paix et al., 2015), alternatively I could use tissue specific RNAi to diminish DOP-2 or UNC-7 function in the sex muscles to further test my hypothesis.

Conclusion

In my study of the spicule intromission sub-routine I have found that D2-like signaling diminishes non-productive behavioral executions, indicating there are beneficial effects of transiently decreasing a goal-oriented sub-routine. During stimuli withdrawal, D2-like signaling dampens reciprocal circuitry activity to decrease the residual self-amplifying property of sensory/motor circuits, thus diminishing futile behavioral executions. Accordingly, mammalian studies indicate that D2-like receptors promote behavioral pliability during motivated behaviors; however, the exact cellular and molecular underpinnings of these theories remain unknown. The amenability of the *C. elegans* mating circuit allow for elucidation on the function of individual neurons contributing to

larger neural circuitry. Therefore future investigations of male copulation might also lead to understanding how the complex nematode nervous system coordinates competing goal-directed tasks.

REFERENCES

Albertson DG, Thomson JN (1976) The pharynx of Caenorhabditis elegans. Philos Trans R Soc Lond B Biol Sci 275:299-325.

Allen AT, Maher KN, Wani KA, Betts KE, Chase DL (2011) Coexpressed D1- and D2-like dopamine receptors antagonistically modulate acetylcholine release in Caenorhabditis elegans. Genetics 188:579-590.

Altun ZF, Chen B, Wang ZW, Hall DH (2009) High resolution map of *Caenorhabditis elegans* gap junction proteins. Dev Dyn 238:1936-1950.

Andersson RH, Johnston A, Herman PA, Winzer-Serhan UH, Karavanova I, Vullhorst D, Fisahn A, Buonanno A (2012) Neuregulin and dopamine modulation of hippocampal gamma oscillations is dependent on dopamine D4 receptors. Proc Natl Acad Sci U S A 109:13118-13123.

Arnsten AF, Wang MJ, Paspalas CD (2012) Neuromodulation of thought: flexibilities and vulnerabilities in prefrontal cortical network synapses. Neuron 76:223-239.

Arosio D, Ricci F, Marchetti L, Gualdani R, Albertazzi L, Beltram F (2010) Simultaneous intracellular chloride and pH measurements using a GFP-based sensor. Nat Methods 7:516-518.

Arosio D, Garau G, Ricci F, Marchetti L, Bizzarri R, Nifosi R, Beltram F (2007) Spectroscopic and structural study of proton and halide ion cooperative binding to gfp. Biophys J 93:232-244.

Arsenault JT, Rima S, Stemmann H, Vanduffel W (2014) Role of the primate ventral tegmental area in reinforcement and motivation. Curr Biol 24:1347-1353.

Avery L, Horvitz HR (1989) Pharyngeal pumping continues after laser killing of the pharyngeal nervous system of C. elegans. Neuron 3:473-485.

Bagetta V, Picconi B, Marinucci S, Sgobio C, Pendolino V, Ghiglieri V, Fusco FR, Giampa C, Calabresi P (2011) Dopamine-dependent long-term depression is expressed in striatal spiny neurons of both direct and indirect pathways: implications for Parkinson's disease. J Neurosci 31:12513-12522.

Baik JH (2013) Dopamine signaling in reward-related behaviors. Front Neural Circuits 7:152.

Baimel C, Borgland SL (2015) Orexin Signaling in the VTA Gates Morphine-Induced Synaptic Plasticity. J Neurosci 35:7295-7303.

Baker DA, Fuchs RA, Specio SE, Khroyan TV, Neisewander JL (1998) Effects of intraaccumbens administration of SCH-23390 on cocaine-induced locomotion and conditioned place preference. Synapse 30:181-193.

Bamber BA, Beg AA, Twyman RE, Jorgensen EM (1999) The Caenorhabditis elegans unc-49 locus encodes multiple subunits of a heteromultimeric GABA receptor. J Neurosci 19:5348-5359.

Barnes TM, Hekimi S (1997) The Caenorhabditis elegans avermectin resistance and anesthetic response gene unc-9 encodes a member of a protein family implicated in electrical coupling of excitable cells. J Neurochem 69:2251-2260.

Barr MM, Sternberg PW (1999) A polycystic kidney-disease gene homologue required for male mating behaviour in *C. elegans*. Nature 401:386-389.

Barrios A, Nurrish S, Emmons SW (2008) Sensory regulation of C. elegans male mate-searching behavior. Curr Biol 18:1865-1871.

Bateup HS, Svenningsson P, Kuroiwa M, Gong S, Nishi A, Heintz N, Greengard P (2008) Cell type-specific regulation of DARPP-32 phosphorylation by psychostimulant and antipsychotic drugs. Nat Neurosci 11:932-939.

Bateup HS, Santini E, Shen W, Birnbaum S, Valjent E, Surmeier DJ, Fisone G, Nestler EJ, Greengard P (2010) Distinct subclasses of medium spiny neurons differentially regulate striatal motor behaviors. Proc Natl Acad Sci U S A 107:14845-14850.

Beaulieu JM, Gainetdinov RR (2011) The Physiology, Signaling, and Pharmacology of Dopamine Receptors. Pharmacological Reviews 63:182-217.

Beaulieu JM, Sotnikova TD, Marion S, Lefkowitz RJ, Gainetdinov RR, Caron MG (2005) An Akt/beta-arrestin 2/PP2A signaling complex mediates dopaminergic neurotransmission and behavior. Cell 122:261-273.

Beaulieu JM, Sotnikova TD, Yao WD, Kockeritz L, Woodgett JR, Gainetdinov RR, Caron MG (2004) Lithium antagonizes dopamine-dependent behaviors mediated by an AKT/glycogen synthase kinase 3 signaling cascade. Proc Natl Acad Sci U S A 101:5099-5104.

Bhatla N, Droste R, Sando SR, Huang A, Horvitz HR (2015) Distinct Neural Circuits Control Rhythm Inhibition and Spitting by the Myogenic Pharynx of C. elegans. Curr Biol 25:2075-2089.

Bhattacharya R, Touroutine D, Barbagallo B, Climer J, Lambert CM, Clark CM, Alkema MJ, Francis MM (2014) A conserved dopamine-cholecystokinin signaling pathway shapes context-dependent Caenorhabditis elegans behavior. PLoS Genet 10:e1004584.

Bjorklund A, Dunnett SB (2007) Dopamine neuron systems in the brain: an update. Trends Neurosci 30:194-202.

Bloomfield SA, Volgyi B (2009) The diverse functional roles and regulation of neuronal gap junctions in the retina. Nat Rev Neurosci 10:495-506.

Bock R, Shin JH, Kaplan AR, Dobi A, Markey E, Kramer PF, Gremel CM, Christensen CH, Adrover MF, Alvarez VA (2013) Strengthening the accumbal indirect pathway promotes resilience to compulsive cocaine use. Nat Neurosci 16:632-638.

Boswell MV, Morgan PG, Sedensky MM (1990) Interaction of GABA and volatile anesthetics in the nematode *Caenorhabditis elegans*. FASEB J 4:2506-2510.

Brenner S (1974) The genetics of *Caenorhabditis elegans*. Genetics 77:71-94.

Brozoski TJ, Brown RM, Rosvold HE, Goldman PS (1979) Cognitive deficit caused by regional depletion of dopamine in prefrontal cortex of rhesus monkey. Science 205:929-932.

Cachope R, Mackie K, Triller A, O'Brien J, Pereda AE (2007) Potentiation of electrical and chemical synaptic transmission mediated by endocannabinoids. Neuron 56:1034-1047.

Calabresi P, Maj R, Mercuri NB, Bernardi G (1992) Coactivation of D1 and D2 dopamine receptors is required for long-term synaptic depression in the striatum. Neurosci Lett 142:95-99.

Calabresi P, Picconi B, Parnetti L, Di Filippo M (2006) A convergent model for cognitive dysfunctions in Parkinson's disease: the critical dopamine-acetylcholine synaptic balance. Lancet Neurol 5:974-983.

Cervo L, Samanin R (1995) Effects of dopaminergic and glutamatergic receptor antagonists on the acquisition and expression of cocaine conditioning place preference. Brain Res 673:242-250.

Chase DL, Pepper JS, Koelle MR (2004) Mechanism of extrasynaptic dopamine signaling in *Caenorhabditis elegans*. Nat Neurosci 7:1096-1103.

Chen TW, Wardill TJ, Sun Y, Pulver SR, Renninger SL, Baohan A, Schreiter ER, Kerr RA, Orger MB, Jayaraman V, Looger LL, Svoboda K, Kim DS (2013) Ultrasensitive fluorescent proteins for imaging neuronal activity. Nature 499:295-300.

Choi KH, Edwards S, Graham DL, Larson EB, Whisler KN, Simmons D, Friedman AK, Walsh JJ, Rahman Z, Monteggia LM, Eisch AJ, Neve RL, Nestler EJ, Han MH, Self

DW (2011) Reinforcement-related regulation of AMPA glutamate receptor subunits in the ventral tegmental area enhances motivation for cocaine. J Neurosci 31:7927-7937.

Coppola A, Liu ZW, Andrews ZB, Paradis E, Roy MC, Friedman JM, Ricquier D, Richard D, Horvath TL, Gao XB, Diano S (2007) A central thermogenic-like mechanism in feeding regulation: an interplay between arcuate nucleus T3 and UCP2. Cell Metab 5:21-33.

Correa P, LeBoeuf B, Garcia LR (2012) *C. elegans* dopaminergic D2-like receptors delimit recurrent cholinergic-mediated motor programs during a goal-oriented behavior. PLoS Genet 8:e1003015.

Creese I, Burt DR, Snyder SH (1976) Dopamine receptor binding predicts clinical and pharmacological potencies of antischizophrenic drugs. Science 192:481-483.

Cully DF, Vassilatis DK, Liu KK, Paress PS, Van der Ploeg LH, Schaeffer JM, Arena JP (1994) Cloning of an avermectin-sensitive glutamate-gated chloride channel from *Caenorhabditis elegans*. Nature 371:707-711.

D'Ardenne K, Eshel N, Luka J, Lenartowicz A, Nystrom LE, Cohen JD (2012) Role of prefrontal cortex and the midbrain dopamine system in working memory updating. Proc Natl Acad Sci U S A 109:19900-19909.

De Koning MB, Bloemen OJ, Van Duin ED, Booij J, Abel KM, De Haan L, Linszen DH, Van Amelsvoort TA (2014) Pre-pulse inhibition and striatal dopamine in subjects at an ultra-high risk for psychosis. J Psychopharmacol 28:553-560.

Deng P, Zhang Y, Xu ZC (2007) Involvement of I(h) in dopamine modulation of tonic firing in striatal cholinergic interneurons. J Neurosci 27:3148-3156.

Dent JA, Davis MW, Avery L (1997) *avr-15* encodes a chloride channel subunit that mediates inhibitory glutamatergic neurotransmission and ivermectin sensitivity in *Caenorhabditis elegans*. EMBO J 16:5867-5879.

Dent JA, Smith MM, Vassilatis DK, Avery L (2000) The genetics of ivermectin resistance in *Caenorhabditis elegans*. Proc Natl Acad Sci U S A 97:2674-2679.

Dickinson DJ, Ward JD, Reiner DJ, Goldstein B (2013) Engineering the Caenorhabditis elegans genome using Cas9-triggered homologous recombination. Nat Methods 10:1028-1034.

Ding J, Guzman JN, Tkatch T, Chen S, Goldberg JA, Ebert PJ, Levitt P, Wilson CJ, Hamm HE, Surmeier DJ (2006) RGS4-dependent attenuation of M4 autoreceptor function in striatal cholinergic interneurons following dopamine depletion. Nat Neurosci 9:832-842.

Edwards SL, Charlie NK, Milfort MC, Brown BS, Gravlin CN, Knecht JE, Miller KG (2008) A novel molecular solution for ultraviolet light detection in *Caenorhabditis elegans*. PLoS Biol 6:e198.

Ezak MJ, Ferkey DM (2010) The C. elegans D2-like dopamine receptor DOP-3 decreases behavioral sensitivity to the olfactory stimulus 1-octanol. PLoS One 5:e9487.

Ezcurra M, Tanizawa Y, Swoboda P, Schafer WR (2011) Food sensitizes C. elegans avoidance behaviours through acute dopamine signalling. EMBO J 30:1110-1122.

Ferkey DM, Hyde R, Haspel G, Dionne HM, Hess HA, Suzuki H, Schafer WR, Koelle MR, Hart AC (2007) C. elegans G protein regulator RGS-3 controls sensitivity to sensory stimuli. Neuron 53:39-52.

Fienberg AA et al. (1998) DARPP-32: regulator of the efficacy of dopaminergic neurotransmission. Science 281:838-842.

Flavell SW, Pokala N, Macosko EZ, Albrecht DR, Larsch J, Bargmann CI (2013) Serotonin and the neuropeptide PDF initiate and extend opposing behavioral states in *C. elegans*. Cell 154:1023-1035.

Ford CP (2014) The role of D2-autoreceptors in regulating dopamine neuron activity and transmission. Neuroscience 282C:13-22.

Furth KE, Mastwal S, Wang KH, Buonanno A, Vullhorst D (2013) Dopamine, cognitive function, and gamma oscillations: role of D4 receptors. Front Cell Neurosci 7:102.

Galarreta M, Hestrin S (1999) A network of fast-spiking cells in the neocortex connected by electrical synapses. Nature 402:72-75.

Galarreta M, Hestrin S (2001a) Electrical synapses between GABA-releasing interneurons. Nat Rev Neurosci 2:425-433.

Galarreta M, Hestrin S (2001b) Spike transmission and synchrony detection in networks of GABAergic interneurons. Science 292:2295-2299.

Garcia LR, Sternberg PW (2003) Caenorhabditis elegans UNC-103 ERG-like potassium channel regulates contractile behaviors of sex muscles in males before and during mating. J Neurosci 23:2696-2705.

Garcia LR, Mehta P, Sternberg PW (2001) Regulation of distinct muscle behaviors controls the *C. elegans* male's copulatory spicules during mating. Cell 107:777-788.

Ghosh R, Andersen EC, Shapiro JA, Gerke JP, Kruglyak L (2012) Natural variation in a chloride channel subunit confers avermectin resistance in *C. elegans*. Science 335:574-578.

Giros B, Jaber M, Jones SR, Wightman RM, Caron MG (1996) Hyperlocomotion and indifference to cocaine and amphetamine in mice lacking the dopamine transporter. Nature 379:606-612.

Goldman-Rakic PS, Leranth C, Williams SM, Mons N, Geffard M (1989) Dopamine synaptic complex with pyramidal neurons in primate cerebral cortex. Proc Natl Acad Sci U S A 86:9015-9019.

Gore BB, Zweifel LS (2013) Genetic reconstruction of dopamine D1 receptor signaling in the nucleus accumbens facilitates natural and drug reward responses. J Neurosci 33:8640-8649.

Graybiel AM, Aosaki T, Flaherty AW, Kimura M (1994) The basal ganglia and adaptive motor control. Science 265:1826-1831.

Greengard P (2001) The neurobiology of slow synaptic transmission. Science 294:1024-1030.

Gruninger TR, Gualberto DG, Garcia LR (2008) Sensory perception of food and insulin-like signals influence seizure susceptibility. PLoS Genet 4:e1000117.

Gruninger TR, Gualberto DG, LeBoeuf B, Garcia LR (2006) Integration of male mating and feeding behaviors in Caenorhabditis elegans. J Neurosci 26:169-179.

Guo X, Navetta A, Gualberto DG, Garcia LR (2012) Behavioral decay in aging male C. elegans correlates with increased cell excitability. Neurobiol Aging.

Guo ZV, Hart AC, Ramanathan S (2009) Optical interrogation of neural circuits in Caenorhabditis elegans. Nat Methods 6:891-896.

Happel MF, Deliano M, Handschuh J, Ohl FW (2014) Dopamine-modulated recurrent corticoefferent feedback in primary sensory cortex promotes detection of behaviorally relevant stimuli. J Neurosci 34:1234-1247.

Hearing M, Kotecki L, Marron Fernandez de Velasco E, Fajardo-Serrano A, Chung HJ, Lujan R, Wickman K (2013) Repeated cocaine weakens GABA(B)-Girk signaling in layer 5/6 pyramidal neurons in the prelimbic cortex. Neuron 80:159-170.

Hecht RM, Norman MA, Vu T, Jones W (1996) A novel set of uncoordinated mutants in Caenorhabditis elegans uncovered by cold-sensitive mutations. Genome 39:459-464.

Hernandez-Lopez S, Tkatch T, Perez-Garci E, Galarraga E, Bargas J, Hamm H, Surmeier DJ (2000) D2 dopamine receptors in striatal medium spiny neurons reduce L-

type Ca2+ currents and excitability via a novel PLC[beta]1-IP3-calcineurin-signaling cascade. J Neurosci 20:8987-8995.

Hernando G, Bouzat C (2014) *Caenorhabditis elegans* neuromuscular junction: GABA receptors and ivermectin action. PLoS One 9:e95072.

Hills T, Brockie PJ, Maricq AV (2004) Dopamine and glutamate control area-restricted search behavior in Caenorhabditis elegans. J Neurosci 24:1217-1225.

Hobson RJ, Hapiak VM, Xiao H, Buehrer KL, Komuniecki PR, Komuniecki RW (2006) SER-7, a Caenorhabditis elegans 5-HT7-like receptor, is essential for the 5-HT stimulation of pharyngeal pumping and egg laying. Genetics 172:159-169.

Hodgkin J, Horvitz HR, Brenner S (1979) Nondisjunction mutants of the nematode *Caenorhabditis elegans*. Genetics 91:67-94.

Hu Z, Vashlishan-Murray AB, Kaplan JM (2015) NLP-12 engages different UNC-13 proteins to potentiate tonic and evoked release. J Neurosci 35:1038-1042.

Iwasaki K, Staunton J, Saifee O, Nonet M, Thomas JH (1997) *aex-3* encodes a novel regulator of presynaptic activity in *C. elegans*. Neuron 18:613-622.

Jansen G, Thijssen KL, Werner P, van der Horst M, Hazendonk E, Plasterk RH (1999) The complete family of genes encoding G proteins of Caenorhabditis elegans. Nat Genet 21:414-419.

Jarrell TA, Wang Y, Bloniarz AE, Brittin CA, Xu M, Thomson JN, Albertson DG, Hall DH, Emmons SW (2012) The connectome of a decision-making neural network. Science 337:437-444.

Jayanthi LD, Apparsundaram S, Malone MD, Ward E, Miller DM, Eppler M, Blakely RD (1998) The Caenorhabditis elegans gene T23G5.5 encodes an antidepressant- and cocaine-sensitive dopamine transporter. Mol Pharmacol 54:601-609.

Jones AK, Sattelle DB (2008) The cys-loop ligand-gated ion channel gene superfamily of the nematode, *Caenorhabditis elegans*. Invert Neurosci 8:41-47.

Joshua M, Adler A, Mitelman R, Vaadia E, Bergman H (2008) Midbrain dopaminergic neurons and striatal cholinergic interneurons encode the difference between reward and aversive events at different epochs of probabilistic classical conditioning trials. J Neurosci 28:11673-11684.

Kagawa H, Sugimoto K, Matsumoto H, Inoue T, Imadzu H, Takuwa K, Sakube Y (1995) Genome structure, mapping and expression of the tropomyosin gene *tmy-1* of C*aenorhabditis elegans*. J Mol Biol 251:603-613.

Kamath RS, Martinez-Campos M, Zipperlen P, Fraser AG, Ahringer J (2001) Effectiveness of specific RNA-mediated interference through ingested double-stranded RNA in Caenorhabditis elegans. Genome Biol 2:RESEARCH0002.

Kaplan JM, Horvitz HR (1993) A dual mechanosensory and chemosensory neuron in Caenorhabditis elegans. Proc Natl Acad Sci U S A 90:2227-2231.

Kato S, Xu Y, Cho CE, Abbott LF, Bargmann CI (2014) Temporal responses of *C. elegans* chemosensory neurons are preserved in behavioral dynamics. Neuron 81:616-628.

Kawano T, Po MD, Gao S, Leung G, Ryu WS, Zhen M (2011) An imbalancing act: gap junctions reduce the backward motor circuit activity to bias *C. elegans* for forward locomotion. Neuron 72:572-586.

Keane J, Avery L (2003) Mechanosensory inputs influence Caenorhabditis elegans pharyngeal activity via ivermectin sensitivity genes. Genetics 164:153-162.

Keeler JF, Pretsell DO, Robbins TW (2014) Functional implications of dopamine D1 vs. D2 receptors: A 'prepare and select' model of the striatal direct vs. indirect pathways. Neuroscience 282C:156-175.

Kindt KS, Quast KB, Giles AC, De S, Hendrey D, Nicastro I, Rankin CH, Schafer WR (2007) Dopamine mediates context-dependent modulation of sensory plasticity in C. elegans. Neuron 55:662-676.

Kirkby LA, Feller MB (2013) Intrinsically photosensitive ganglion cells contribute to plasticity in retinal wave circuits. Proc Natl Acad Sci U S A 110:12090-12095.

Koo PK, Bian X, Sherlekar AL, Bunkers MR, Lints R (2011) The robustness of *Caenorhabditis elegans* male mating behavior depends on the distributed properties of ray sensory neurons and their output through core and male-specific targets. J Neurosci 31:7497-7510.

Korn H, Faber DS (2005) The Mauthner cell half a century later: a neurobiological model for decision-making? Neuron 47:13-28.

Kothmann WW, Massey SC, O'Brien J (2009) Dopamine-stimulated dephosphorylation of connexin 36 mediates AII amacrine cell uncoupling. J Neurosci 29:14903-14911.

Krashes MJ, DasGupta S, Vreede A, White B, Armstrong JD, Waddell S (2009) A neural circuit mechanism integrating motivational state with memory expression in Drosophila. Cell 139:416-427.

LeBoeuf B, Gruninger TR, Garcia LR (2007) Food deprivation attenuates seizures through CaMKII and EAG K+ channels. PLoS Genet 3:1622-1632.

LeBoeuf B, Guo X, Garcia LR (2011) The effects of transient starvation persist through direct interactions between CaMKII and ether-a-go-go K+ channels in C. elegans males. Neuroscience 175:1-17.

LeBoeuf B, Correa P, Jee C, Garcia LR (2014) *Caenorhabditis elegans* male sensory-motor neurons and dopaminergic support cells couple ejaculation and post-ejaculatory behaviors. Elife 3.

Lee RY, Sawin ER, Chalfie M, Horvitz HR, Avery L (1999) EAT-4, a homolog of a mammalian sodium-dependent inorganic phosphate cotransporter, is necessary for glutamatergic neurotransmission in caenorhabditis elegans. J Neurosci 19:159-167.

Lee SM, Yang Y, Mailman RB (2014) Dopamine D1 receptor signaling: does GalphaQ-phospholipase C actually play a role? J Pharmacol Exp Ther 351:9-17.

Lewis JA, Wu CH, Berg H, Levine JH (1980) The genetics of levamisole resistance in the nematode Caenorhabditis elegans. Genetics 95:905-928.

Li W, Feng Z, Sternberg PW, Xu XZ (2006) A C. elegans stretch receptor neuron revealed by a mechanosensitive TRP channel homologue. Nature 440:684-687.

Lints R, Emmons SW (1999) Patterning of dopaminergic neurotransmitter identity among Caenorhabditis elegans ray sensory neurons by a TGFbeta family signaling pathway and a Hox gene. Development 126:5819-5831.

Lints R, Jia L, Kim K, Li C, Emmons SW (2004) Axial patterning of *C. elegans* male sensilla identities by selector genes. Dev Biol 269:137-151.

Liu J, Wang F, Huang C, Long LH, Wu WN, Cai F, Wang JH, Ma LQ, Chen JG (2009) Activation of phosphatidylinositol-linked novel D1 dopamine receptor contributes to the calcium mobilization in cultured rat prefrontal cortical astrocytes. Cell Mol Neurobiol 29:317-328.

Liu KS, Sternberg PW (1995) Sensory regulation of male mating behavior in *Caenorhabditis elegans*. Neuron 14:79-89.

Liu T, Kim K, Li C, Barr MM (2007a) FMRFamide-like neuropeptides and mechanosensory touch receptor neurons regulate male sexual turning behavior in Caenorhabditis elegans. J Neurosci 27:7174-7182.

Liu Y, LeBoeuf B, Garcia LR (2007b) G alpha(q)-coupled muscarinic acetylcholine receptors enhance nicotinic acetylcholine receptor signaling in Caenorhabditis elegans mating behavior. J Neurosci 27:1411-1421.

Liu Y, Lebeouf B, Guo X, Correa PA, Gualberto DG, Lints R, Garcia LR (2011) A Cholinergic-Regulated Circuit Coordinates the Maintenance and Bi-Stable States of a Sensory-Motor Behavior during Caenorhabditis elegans Male Copulation. PLoS Genet 7:e1001326.

Lobo MK, Covington HE, 3rd, Chaudhury D, Friedman AK, Sun H, Damez-Werno D, Dietz DM, Zaman S, Koo JW, Kennedy PJ, Mouzon E, Mogri M, Neve RL, Deisseroth K, Han MH, Nestler EJ (2010) Cell type-specific loss of BDNF signaling mimics optogenetic control of cocaine reward. Science 330:385-390.

Loer CM, Kenyon CJ (1993) Serotonin-deficient mutants and male mating behavior in the nematode Caenorhabditis elegans. J Neurosci 13:5407-5417.

Martinowich K, Cardinale KM, Schloesser RJ, Hsu M, Greig NH, Manji HK (2012) Acetylcholinesterase inhibition ameliorates deficits in motivational drive. Behav Brain Funct 8:15.

Matsumoto M, Hikosaka O (2009) Two types of dopamine neuron distinctly convey positive and negative motivational signals. Nature 459:837-841.

Matsumoto M, Takada M (2013) Distinct representations of cognitive and motivational signals in midbrain dopamine neurons. Neuron 79:1011-1024.

Maurice N, Mercer J, Chan CS, Hernandez-Lopez S, Held J, Tkatch T, Surmeier DJ (2004) D2 dopamine receptor-mediated modulation of voltage-dependent Na+ channels reduces autonomous activity in striatal cholinergic interneurons. J Neurosci 24:10289-10301.

McBain CJ, Fisahn A (2001) Interneurons unbound. Nat Rev Neurosci 2:11-23.

McDonald PW, Hardie SL, Jessen TN, Carvelli L, Matthies DS, Blakely RD (2007) Vigorous motor activity in Caenorhabditis elegans requires efficient clearance of dopamine mediated by synaptic localization of the dopamine transporter DAT-1. J Neurosci 27:14216-14227.

McIntire SL, Jorgensen E, Horvitz HR (1993) Genes required for GABA function in Caenorhabditis elegans. Nature 364:334-337.

Mendel JE, Korswagen HC, Liu KS, Hajdu-Cronin YM, Simon MI, Plasterk RH, Sternberg PW (1995) Participation of the protein Go in multiple aspects of behavior in C. elegans. Science 267:1652-1655.

Morris G, Arkadir D, Nevet A, Vaadia E, Bergman H (2004) Coincident but distinct messages of midbrain dopamine and striatal tonically active neurons. Neuron 43:133-143.

Nagel G, Brauner M, Liewald JF, Adeishvili N, Bamberg E, Gottschalk A (2005) Light activation of channelrhodopsin-2 in excitable cells of *Caenorhabditis elegans* triggers rapid behavioral responses. Curr Biol 15:2279-2284.

Noudoost B, Moore T (2011) Control of visual cortical signals by prefrontal dopamine. Nature 474:372-375.

Nurrish S, Segalat L, Kaplan JM (1999) Serotonin inhibition of synaptic transmission: Galpha(0) decreases the abundance of UNC-13 at release sites. Neuron 24:231-242.

O'Hagan R, Piasecki BP, Silva M, Phirke P, Nguyen KC, Hall DH, Swoboda P, Barr MM (2011) The tubulin deglutamylase CCPP-1 regulates the function and stability of sensory cilia in C. elegans. Curr Biol 21:1685-1694.

Paix A, Folkmann A, Rasoloson D, Seydoux G (2015) High Efficiency, Homology-Directed Genome Editing in Caenorhabditis elegans Using CRISPR/Cas9 Ribonucleoprotein Complexes. Genetics.

Paix A, Wang Y, Smith HE, Lee CY, Calidas D, Lu T, Smith J, Schmidt H, Krause MW, Seydoux G (2014) Scalable and versatile genome editing using linear DNAs with microhomology to Cas9 Sites in Caenorhabditis elegans. Genetics 198:1347-1356.

Palacios-Prado N, Bukauskas FF (2009) Heterotypic gap junction channels as voltage-sensitive valves for intercellular signaling. Proc Natl Acad Sci U S A 106:14855-14860.

Pandey P, Harbinder S (2012) The Caenorhabditis elegans D2-like dopamine receptor DOP-2 physically interacts with GPA-14, a G-alpha-i subunit. J Mol Signal 7:3.

Pereda A, Triller A, Korn H, Faber DS (1992) Dopamine enhances both electrotonic coupling and chemical excitatory postsynaptic potentials at mixed synapses. Proc Natl Acad Sci U S A 89:12088-12092.

Petersen CI, McFarland TR, Stepanovic SZ, Yang P, Reiner DJ, Hayashi K, George AL, Roden DM, Thomas JH, Balser JR (2004) In vivo identification of genes that modify ether-a-go-go-related gene activity in Caenorhabditis elegans may also affect human cardiac arrhythmia. Proc Natl Acad Sci U S A 101:11773-11778.

Picconi B, Centonze D, Hakansson K, Bernardi G, Greengard P, Fisone G, Cenci MA, Calabresi P (2003) Loss of bidirectional striatal synaptic plasticity in L-DOPA-induced dyskinesia. Nat Neurosci 6:501-506.

Pisani A, Bernardi G, Ding J, Surmeier DJ (2007) Re-emergence of striatal cholinergic interneurons in movement disorders. Trends Neurosci 30:545-553.

Pisani A, Bonsi P, Centonze D, Calabresi P, Bernardi G (2000) Activation of D2-like dopamine receptors reduces synaptic inputs to striatal cholinergic interneurons. J Neurosci 20:RC69.

Pokala N, Liu Q, Gordus A, Bargmann CI (2014) Inducible and titratable silencing of Caenorhabditis elegans neurons in vivo with histamine-gated chloride channels. Proc Natl Acad Sci U S A 111:2770-2775.

Pope P, Wing AM, Praamstra P, Miall RC (2005) Force related activations in rhythmic sequence production. Neuroimage 27:909-918.

Puig MV, Rose J, Schmidt R, Freund N (2014) Dopamine modulation of learning and memory in the prefrontal cortex: insights from studies in primates, rodents, and birds. Front Neural Circuits 8:93.

Raimondo JV, Joyce B, Kay L, Schlagheck T, Newey SE, Srinivas S, Akerman CJ (2013) A genetically-encoded chloride and pH sensor for dissociating ion dynamics in the nervous system. Front Cell Neurosci 7:202.

Rash JE, Curti S, Vanderpool KG, Kamasawa N, Nannapaneni S, Palacios-Prado N, Flores CE, Yasumura T, O'Brien J, Lynn BD, Bukauskas FF, Nagy JI, Pereda AE (2013) Molecular and functional asymmetry at a vertebrate electrical synapse. Neuron 79:957-969.

Raz A, Frechter-Mazar V, Feingold A, Abeles M, Vaadia E, Bergman H (2001) Activity of pallidal and striatal tonically active neurons is correlated in mptp-treated monkeys but not in normal monkeys. J Neurosci 21:RC128.

Reiner DJ, Weinshenker D, Tian H, Thomas JH, Nishiwaki K, Miwa J, Gruninger T, Leboeuf B, Garcia LR (2006a) Behavioral genetics of *Caenorhabditis elegans*-encoded erg-like K(+) channel. J Neurogenet 20:41-66.

Reiner DJ, Weinshenker D, Tian H, Thomas JH, Nishiwaki K, Miwa J, Gruninger T, Leboeuf B, Garcia LR (2006b) Behavioral genetics of caenorhabditis elegans unc-103-encoded erg-like K(+) channel. J Neurogenet 20:41-66.

Ribelayga C, Wang Y, Mangel SC (2002) Dopamine mediates circadian clock regulation of rod and cone input to fish retinal horizontal cells. J Physiol 544:801-816.

Ribelayga C, Cao Y, Mangel SC (2008) The circadian clock in the retina controls rod-cone coupling. Neuron 59:790-801.

Rogers CM, Franks CJ, Walker RJ, Burke JF, Holden-Dye L (2001) Regulation of the pharynx of Caenorhabditis elegans by 5-HT, octopamine, and FMRFamide-like neuropeptides. J Neurobiol 49:235-244.

Rose JK, Rankin CH (2001) Analyses of habituation in Caenorhabditis elegans. Learn Mem 8:63-69.

Ryan DA, Miller RM, Lee K, Neal SJ, Fagan KA, Sengupta P, Portman DS (2014) Sex, age, and hunger regulate behavioral prioritization through dynamic modulation of chemoreceptor expression. Curr Biol 24:2509-2517.

Salamone JD, Correa M (2012) The mysterious motivational functions of mesolimbic dopamine. Neuron 76:470-485.

Sanyal S, Wintle RF, Kindt KS, Nuttley WM, Arvan R, Fitzmaurice P, Bigras E, Merz DC, Hebert TE, van der Kooy D, Schafer WR, Culotti JG, Van Tol HH (2004) Dopamine modulates the plasticity of mechanosensory responses in Caenorhabditis elegans. EMBO J 23:473-482.

Sawin ER, Ranganathan R, Horvitz HR (2000) *C. elegans* locomotory rate is modulated by the environment through a dopaminergic pathway and by experience through a serotonergic pathway. Neuron 26:619-631.

Schafer WR, Kenyon CJ (1995) A calcium-channel homologue required for adaptation to dopamine and serotonin in Caenorhabditis elegans. Nature 375:73-78.

Schindelman G, Whittaker AJ, Thum JY, Gharib S, Sternberg PW (2006) Initiation of male sperm-transfer behavior in Caenorhabditis elegans requires input from the ventral nerve cord. BMC Biol 4:26.

Schnabel H, Schnabel R (1990) An organ-specific differentiation gene, *pha-1*, from *Caenorhabditis elegans*. Science 250:686-688.

Segalat L, Elkes DA, Kaplan JM (1995) Modulation of serotonin-controlled behaviors by Go in Caenorhabditis elegans. Science 267:1648-1651.

Shao YR, Isett BR, Miyashita T, Chung J, Pourzia O, Gasperini RJ, Feldman DE (2013) Plasticity of recurrent l2/3 inhibition and gamma oscillations by whisker experience. Neuron 80:210-222.

Shaw WR, Teodori E, Mitchell SN, Baldini F, Gabrieli P, Rogers DW, Catteruccia F (2014) Mating activates the heme peroxidase HPX15 in the sperm storage organ to ensure fertility in Anopheles gambiae. Proc Natl Acad Sci U S A 111:5854-5859.

Shen W, Flajolet M, Greengard P, Surmeier DJ (2008) Dichotomous dopaminergic control of striatal synaptic plasticity. Science 321:848-851.

Shepherd GM, Stepanyants A, Bureau I, Chklovskii D, Svoboda K (2005) Geometric and functional organization of cortical circuits. Nat Neurosci 8:782-790.

Smith Y, Bevan MD, Shink E, Bolam JP (1998) Microcircuitry of the direct and indirect pathways of the basal ganglia. Neuroscience 86:353-387.

Spencer KM, Nestor PG, Perlmutter R, Niznikiewicz MA, Klump MC, Frumin M, Shenton ME, McCarley RW (2004) Neural synchrony indexes disordered perception and cognition in schizophrenia. Proc Natl Acad Sci U S A 101:17288-17293.

Srinivasan J, Kaplan F, Ajredini R, Zachariah C, Alborn HT, Teal PE, Malik RU, Edison AS, Sternberg PW, Schroeder FC (2008) A blend of small molecules regulates both mating and development in Caenorhabditis elegans. Nature 454:1115-1118.

St Peters M, Demeter E, Lustig C, Bruno JP, Sarter M (2011) Enhanced control of attention by stimulating mesolimbic-corticopetal cholinergic circuitry. J Neurosci 31:9760-9771.

Starich TA, Herman RK, Shaw JE (1993) Molecular and genetic analysis of *unc-7*, a *Caenorhabditis elegans* gene required for coordinated locomotion. Genetics 133:527-541.

Starich TA, Xu J, Skerrett IM, Nicholson BJ, Shaw JE (2009) Interactions between innexins UNC-7 and UNC-9 mediate electrical synapse specificity in the *Caenorhabditis elegans* locomotory nervous system. Neural Dev 4:16.

Steger KA, Avery L (2004) The GAR-3 muscarinic receptor cooperates with calcium signals to regulate muscle contraction in the Caenorhabditis elegans pharynx. Genetics 167:633-643.

Stoof JC, Kebabian JW (1981) Opposing roles for D-1 and D-2 dopamine receptors in efflux of cyclic AMP from rat neostriatum. Nature 294:366-368.

Su P, Li S, Chen S, Lipina TV, Wang M, Lai TK, Lee FH, Zhang H, Zhai D, Ferguson SS, Nobrega JN, Wong AH, Roder JC, Fletcher PJ, Liu F (2014) A dopamine D2 receptor-DISC1 protein complex may contribute to antipsychotic-like effects. Neuron 84:1302-1316.

Sugiura M, Fuke S, Suo S, Sasagawa N, Van Tol HH, Ishiura S (2005) Characterization of a novel D2-like dopamine receptor with a truncated splice variant and a D1-like dopamine receptor unique to invertebrates from C*aenorhabditis elegans*. J Neurochem 94:1146-1157.

Sulston J, Dew M, Brenner S (1975) Dopaminergic neurons in the nematode Caenorhabditis elegans. J Comp Neurol 163:215-226.

Sulston JE, Albertson DG, Thomson JN (1980) The Caenorhabditis elegans male: postembryonic development of nongonadal structures. Dev Biol 78:542-576.

Suo S, Sasagawa N, Ishiura S (2002) Identification of a dopamine receptor from Caenorhabditis elegans. Neurosci Lett 319:13-16.

Suo S, Sasagawa N, Ishiura S (2003) Cloning and characterization of a Caenorhabditis elegans D2-like dopamine receptor. J Neurochem 86:869-878.

Tellez LA, Medina S, Han W, Ferreira JG, Licona-Limon P, Ren X, Lam TT, Schwartz GJ, de Araujo IE (2013) A gut lipid messenger links excess dietary fat to dopamine deficiency. Science 341:800-802.

Tian L, Hires SA, Mao T, Huber D, Chiappe ME, Chalasani SH, Petreanu L, Akerboom J, McKinney SA, Schreiter ER, Bargmann CI, Jayaraman V, Svoboda K, Looger LL (2009) Imaging neural activity in worms, flies and mice with improved GCaMP calcium indicators. Nat Methods 6:875-881.

Tsai HC, Zhang F, Adamantidis A, Stuber GD, Bonci A, de Lecea L, Deisseroth K (2009) Phasic firing in dopaminergic neurons is sufficient for behavioral conditioning. Science 324:1080-1084.

Vaillancourt DE, Yu H, Mayka MA, Corcos DM (2007) Role of the basal ganglia and frontal cortex in selecting and producing internally guided force pulses. Neuroimage 36:793-803.

Vassilatis DK, Arena JP, Plasterk RH, Wilkinson HA, Schaeffer JM, Cully DF, Van der Ploeg LH (1997) Genetic and biochemical evidence for a novel avermectin-sensitive chloride channel in *Caenorhabditis elegans*. Isolation and characterization. J Biol Chem 272:33167-33174.

Vervaeke K, Lorincz A, Gleeson P, Farinella M, Nusser Z, Silver RA (2010) Rapid desynchronization of an electrically coupled interneuron network with sparse excitatory synaptic input. Neuron 67:435-451.

Vidal-Gadea A, Topper S, Young L, Crisp A, Kressin L, Elbel E, Maples T, Brauner M, Erbguth K, Axelrod A, Gottschalk A, Siegel D, Pierce-Shimomura JT (2011) Caenorhabditis elegans selects distinct crawling and swimming gaits via dopamine and serotonin. Proc Natl Acad Sci U S A 108:17504-17509.

Vijayraghavan S, Wang M, Birnbaum SG, Williams GV, Arnsten AF (2007) Inverted-U dopamine D1 receptor actions on prefrontal neurons engaged in working memory. Nat Neurosci 10:376-384.

Vrablik TL, Wang W, Upadhyay A, Hanna-Rose W (2011) Muscle type-specific responses to NAD+ salvage biosynthesis promote muscle function in Caenorhabditis elegans. Dev Biol 349:387-394.

Wang M, Vijayraghavan S, Goldman-Rakic PS (2004) Selective D2 receptor actions on the functional circuitry of working memory. Science 303:853-856.

Wang Y, Goldman-Rakic PS (2004) D2 receptor regulation of synaptic burst firing in prefrontal cortical pyramidal neurons. Proc Natl Acad Sci U S A 101:5093-5098.

Wang Y, Belousov AB (2011) Deletion of neuronal gap junction protein connexin 36 impairs hippocampal LTP. Neurosci Lett 502:30-32.

Wang Z, Kai L, Day M, Ronesi J, Yin HH, Ding J, Tkatch T, Lovinger DM, Surmeier DJ (2006) Dopaminergic control of corticostriatal long-term synaptic depression in medium spiny neurons is mediated by cholinergic interneurons. Neuron 50:443-452.

Wani KA, Catanese M, Normantowicz R, Herd M, Maher KN, Chase DL (2012) D1 dopamine receptor signaling is modulated by the R7 RGS protein EAT-16 and the R7 binding protein RSBP-1 in Caenoerhabditis elegans motor neurons. PLoS One 7:e37831.

Wei X, Potter CJ, Luo L, Shen K (2012) Controlling gene expression with the Q repressible binary expression system in *Caenorhabditis elegans*. Nat Methods 9:391-395.

Weinshenker D, Garriga G, Thomas JH (1995) Genetic and pharmacological analysis of neurotransmitters controlling egg laying in C. elegans. J Neurosci 15:6975-6985.

Weinshenker D, Wei A, Salkoff L, Thomas JH (1999) Block of an ether-a-go-go-like K(+) channel by imipramine rescues egl-2 excitation defects in Caenorhabditis elegans. J Neurosci 19:9831-9840.

White JG, Southgate E, Thomson JN, Brenner S (1986) The structure of the nervous system of the nematode Caenorhabditis elegans. Philos Trans R Soc Lond B Biol Sci 314:1-340.

White JQ, Nicholas TJ, Gritton J, Truong L, Davidson ER, Jorgensen EM (2007) The sensory circuitry for sexual attraction in C. elegans males. Curr Biol 17:1847-1857.

Whittaker AJ, Sternberg PW (2009) Coordination of opposing sex-specific and core muscle groups regulates male tail posture during Caenorhabditis elegans male mating behavior. BMC Biol 7:33.

Wise RA (2004) Dopamine, learning and motivation. Nat Rev Neurosci 5:483-494.

Wong YF, Sheng Q, Chung JW, Chan JK, Chow KL (2010) mab-31 and the TGF-beta pathway act in the ray lineage to pattern C. elegans male sensory rays. BMC Dev Biol 10:82.

Yan Z, Hsieh-Wilson L, Feng J, Tomizawa K, Allen PB, Fienberg AA, Nairn AC, Greengard P (1999) Protein phosphatase 1 modulation of neostriatal AMPA channels: regulation by DARPP-32 and spinophilin. Nat Neurosci 2:13-17.

Yeh E, Kawano T, Ng S, Fetter R, Hung W, Wang Y, Zhen M (2009) *Caenorhabditis elegans* innexins regulate active zone differentiation. J Neurosci 29:5207-5217.

Zaldivar D, Rauch A, Whittingstall K, Logothetis NK, Goense J (2014) Dopamine-induced dissociation of BOLD and neural activity in macaque visual cortex. Curr Biol 24:2805-2811.

APPENDIX A

PRIMERS USED IN THIS STUDY

Table1S. Sequence of primers used in this study

Primer name	Sequence
DOP3geneF	gcgcccggatccatgttggctggacaacaccacgttacagac
DOP3geneR	gcgcccaccggttctttttttgaatatcccgcatgataaaatgttccggaag
dop3(vs106)F	cgaaattcaaatcttcttccatcttcttgc
dop3(vs106)R	gtctataaaaagcgatgtgggcac
FDop2	atggaggccggagagacatgg
Dop2R	atggcataactatgatggccac
ATTB1Dop2pr	ggggacaagtttgtacaaaaaagcaggctccgatttgtgctcacactcgtcgagtaccc
Attb2Dop2pr	ggggaccactttgtacaagaaagctgggtgtctctccggcctccagtttttggagttgg
RNAigpa16	ggggacaagtttgtacaaaaaagcaggctcccgtgcaccaaggataatttatttgggcgc
Pgpa16Rv2	ggg gaccactttgtacaagaaagctggtactcttcagtcgtatatccgacgtcgtg
Pgpa16Fv2	ggggaccactttgtacaagaaagctgggtactcttcagtcgtatatccgacgtcgtg
gpa7pk610indelR	ctagaaaatatggatagctccgttgactatgc
dop4(tm1392)F	ttggcttacgggtctgatccgaacg
dop4(tm1392)R	gcagaccaattttgtccaaccaccatcc
attb1DOP2F	ggggacaagtttgtacaaaaaagcaggctatggaggccggagagacatgga
attb2DOP2R	ggggaccactttgtacaagaaagctgggtttagacatgcgcctgcttgttactgaaatgg
gpa7pk610F	gatgttggatcggttgcttttagcctgtc
gpa7pk610R	aagcgaatgatatcacttaccaccggg
gpa14pk347F	cttggaggacctttaagtggaaagagtac
gpa14pk347R	gctttaaatacactttccatgcaggcgcg
gpa14pkindelF	acgtgggtggtcaaagatcggaacgaa
Pgpa-7F	ggggacaagtttgtacaaaaaagcaggctccgacaactttctgccggacactgaccgttt
Pgpa-7R	ggggaccactttgtacaagaaagctgggtgatgatccgaagactcatcgattgatccttc
attb1Pavr-14F	ggggacaagtttgtacaaaaaagcaggctcc ctgccccgagaacctaaacaacattgaat
attb1Pavr-14R	*ggggaccacttgtacaagaaagc tgg gta cgtcagtcgataatgccacatctgaaagt*
Punc7(8kb)F:	ggggacaagtttgtacaaaaaagcaggctcc tatcgcaagttcacctcatctgtgccttc
Punc7(8/9)R:	ggg gac cac ttt gta caa gaa agc tgg gta acatccgtctaaacttgcacgttgaggcg
attb1Punc7F:	ggggacaagtttgtacaaaaaagcaggctcc *cccatagagagtgatgggcccaacctttc*
UNC-7(gene)attb1:	ggggacaagtttgtacaaaaaagcaggctcc atgctcggctcctccagcaatcct
UNC-7(gene)attb2:	ggg gac cac ttt gta caa gaa agc tgg gta cggtctatcgtcccttgaccgtgttc

APPENDIX B

ADDITIONAL CALCIUM IMAGING

To address if ray neurons respond to glutamatergic signals from PCA GCaMP6 was expressed in the DA ray neurons and the *eat-4P* drove expression ChR2 to activate PCA and simultaneously image ray neurons transients (Fig. 1S). Additionally, I also measured the magnitude of spicule movement upon blue light stimulation PCA in control and males with decreased DA (Fig. 2S).

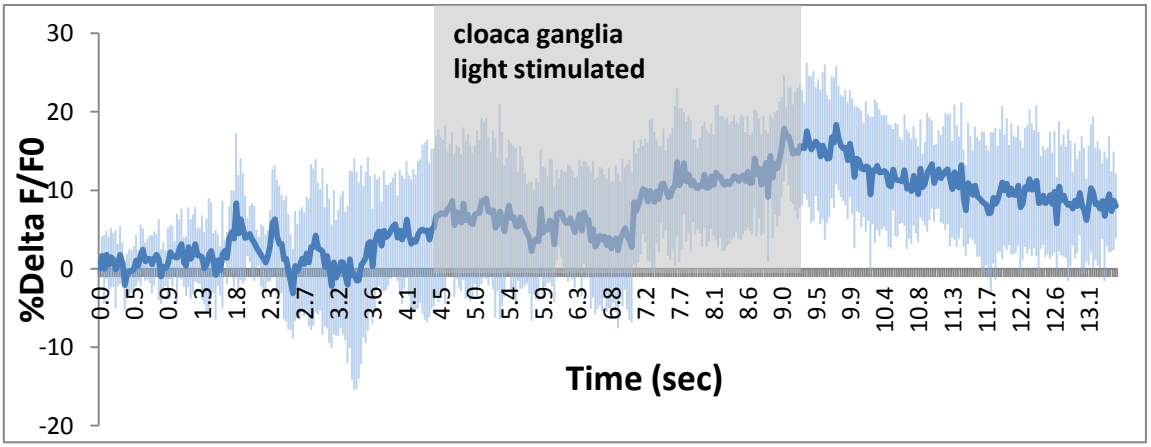

Figure 1S. Calcium transients in DA ray neurons while shinning blue light on PCA (shaded area). A total of seven males were assessed after exposing them to retinol.

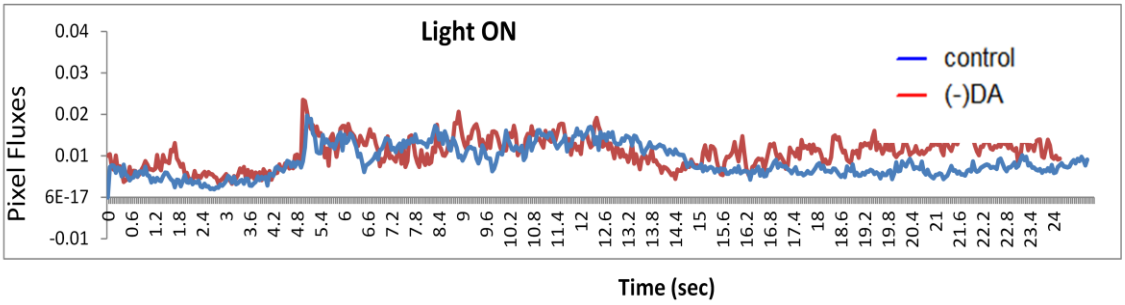

Figure 2S. PCA was turned on between 4.5 until 13 secs while the pixel fluxes were measured as a proxy for spicule movement.